**Title**
Modeling and Analysis of a Mobility Portfolio Framework for Shared-Autonomous Transportation Systems



**Author**
AN, SUNGHI

**Publication Date**
2022

Peer reviewed|Thesis/dissertation

UNIVERSITY OF CALIFORNIA,
IRVINE

# Modeling and Analysis of a Mobility Portfolio Framework for Shared-Autonomous Transportation Systems

DISSERTATION

submitted in partial satisfaction of the requirements
for the degree of

DOCTOR OF PHILOSOPHY

in Civil and Environmental Engineering

by

Sunghi An

Dissertation Committee:
Professor R. Jayakrishnan, Chair
Assistant Professor Michael Hyland
Professor Will Recker
Professor John Turner

2022

# DEDICATION

To

my parents

Sangyoung An and Jiwon Yim

and

my sister

Sungwon An

# TABLE OF CONTENTS

# LIST OF FIGURES

# LIST OF TABLES

# ACKNOWLEDGEMENTS

I would like to express my sincere gratitude to my thesis committee, Prof. R. Jayakrishnan, Prof. Will Recker, Prof. Michael Hyland, and Prof. John Turner, for their support, insightful comments, and priceless feedback throughout my doctoral candidacy.

I am especially grateful to my PhD advisor, Prof. Jayakrishnan, for his invaluable guidance, supervision, mentorship, and ceaseless encouragement. It has been an honor and privilege to work with him during my PhD journey. Prof. Jayakrishnan always encouraged me to broaden my intellectual horizons and made time to talk and brainstorm with me whenever I found myself stuck on a problem.

I would like to express my deep appreciation to professors in ITS, Prof. Stephen Ritchie, Prof. Jen-Daniel Saphores, Prof. Wenlong Jin, Prof. Michael McNally, who not only taught the lecturers that motivated my research, but also had their kindness and helpful nature.

I am also indebted to thank the other member of the transportation faculty at Myongji University, Dr. Hyunmyung Kim who introduced me to academic research and encouraged me to pursue a PhD with invaluable support.

In addition, I want to thank my colleagues Dr. Daisik Nam, Dr. and Dr. Riju Lavanya. A special word of gratitude is due to Daisik Nam for showing confidence in my work and for his help in developing my research ideas. I am also grateful to Riju for his kind review and comments on my work.

I owe a debt of gratitude to my research team Dr. Neda Masoud, Dr. Dingtong Yang, Dr. Jianbo (Gabriel) Yu, Marjan Mosslemi, Negin Shariat, Eduardo Marino, and Pengyuan Sun. I would like to thank my colleagues, Dr. Youngeun Bae, Dr. Kyung Hyun, Dr. Kyungsoo Jeong, Dr. Jun Hyeong Park, Younghun Bahk, Bumsub Park, Koti Reddy Allu, Naila Sharmeen, Xuting Wang, Felipe Augusto de Souza, Navjyoth Sarma JS, Khalid Abdulghanim, Yiqiao Li, Lu Xu, and Irene Martinez Josemaria, to making the last six years in ITS memorable.

Finally, I would like to acknowledge with immense gratitude, the love and support of my family. I am grateful to my parents, Sangyong and Jiwon for their continuous support and for giving me encouragement and love, and to my sister Sungwon who always made me smile. They all kept me going and this dissertation would not have been possible without them.

I must acknowledge that the contents of chapter 3 of this dissertation is a reprint of the material as it appears in MDPI. This thesis research was partially funded by the U.S. Department of Transportation and the California Department of Transportation through the University of California Center on Economic Competitiveness in Transportation (DOT/UCCONNECT) and the Pacific Southwest Research University Transportation Center (DOT/PSR-UTC). I also want to thank the Department of Civil and Environmental Engineering, and the Institute of Transportation Studies at University of California, Irvine for supporting this research.

*“The shortest answer is doing the thing.”*

Ernest Hemingway

# VITA

Sunghi An

## EDUCATION

**Doctor of Philosophy in Civil Engineering** **2022**
University of California, Irvine *Irvine, CA*

**Master of Science in Transportation Planning** **2012**
Myongji University *Yongin, Korea*

**Bachelor of Science in Transportation Engineering** **2008**
Myongji University *Yongin, Korea*

# ABSTRACT OF THE DISSERTATION

Modeling and Analysis of a Mobility Portfolio Framework for Shared-Autonomous Transportation Systems

by

Sunghi An

Doctor of Philosophy in Civil and Environmental Engineering

University of California, Irvine, 2022

Professor R. Jayakrishnan, Chair

The emerging and rapidly changing landscape of autonomous vehicles and shared mobility technologies bring up possibilities for a paradigm shift in how we model and analyze mobility. Transportation and mobility systems can now be connected continuously and seamlessly, which can make them more flexible and shareable. What can make this possible? Put simply, it would require integrating various mobility options so that travelers can freely hop among them. The demarcation lines among modes can then become increasingly hazy, as every individual trip may include multiple modes to various degrees. This implies that the paradigm shift is in how we view the travel modes. What were traditionally considered as limited discrete mode options, need to be seen as part of a continuum. In turn, we should focus more on mode combinations rather than individual travel modes. In this dissertation, we propose shifting the focus to the new idea of a mode option pool with an associated structure. The option pool would include every type of travel option in a continuous spectrum. This observation motivates the phrase 'travel-option chain (TOC)' mode proposed in this dissertation as a combination of travel options in a continuous spectrum.

Shared use of vehicles – either time-shared, or seat-shared – expands the travel option pool. Autonomous vehicle technology makes even more time-shared use of vehicles possible, as the driver constraint is also removed, and thus further expands the travel mode option pool. Then the question is on how to make such a larger option pool available for a large number of users, to improve their level of mobility and the productivity of the vehicles as well as the associated infrastructure. One aspect that needs to be addressed is that people cannot be individually owning the vehicles and infrastructure involved in all of the mobility options they use from the pool. Different people may partially or fully own different components such as, for instance, vehicles or spaces where they are parked. Some ownership may be time-shared as well. Publicly provided transit systems with purchased tickets will naturally be part of many TOC modes. Subscription-type ownership is a possibility, if mobility service providers offer the options for purchase, and they can be bundled options as well, similar to phone plans. This fits within Mobility-as-a-Service (MaaS) platforms that have been proposed in recent years. In this dissertation, a powerful user-side concept, 'mobility portfolios' is proposed that encompasses MaaS platforms, subscriptions, ownership, bundled plans and selection of optimal TOCs from a continuum spectrum of modes.

The question then ensues on how we can find the optimal TOC modes. From an analytical standpoint, this can be solved with a ridematching problem formulation of matching paths in a time-expanded multimodal network. A more vexing problem is how people can travel on these TOC modes unless they have paid for it in a certain way. The mobility portfolio scheme proposed in this dissertation is geared to make it possible for them to pay for it in an efficient way and in a shareable manner with enough flexibility. This dissertation defines mobility portfolio as a "grouping of the number of hours/cost/resources that can be spent on each distinct travel options, so as to fit within a time/cost/resource constraint specified for a given time period". The portfolio approach compartmentalizes the travel options that are chained, and allocates appropriate "quantities" of them, when we view them as consumable travel commodities and resources. The portfolio scheme incorporates pricing for the commodities and are expected to bring in efficiency and cost savings while increasing shared mobility participation. This is a good approach for controlling TOC mode change travel behaviors and it subsumes currently envisaged ideas such as MaaS mobility bundles in a smart and shared mobility system with subscription options.

The focus of this dissertation is on the user level decisions on selecting the TOC modes from their mobility portfolios scheme. Innovative options such as users offering their own resources (e.g., owned vehicles) and their own services (e.g., potential driving for shared rides) are incorporated in the portfolios. We develop an iterative framework which is rooted on a learning-based travel cost perception update model, so as to model the users being provided with the best travel options as well as the best usage plan for mobility portfolios. Performing simulated case studies on a real network, we confirm that the proposed framework converges to the optimum mobility portfolio state for system participants and improves the performance of the system by inducing people to use shared mobility options more.

# Chapter 1

# Motivation

Traffic congestion is one of the major problems in cities all over the world, with solo drivers in privately-owned vehicles being a significant component of it. The latest data from the 2017 National Household Travel Survey reveal some startling figures: almost 88% of commuters make their trip in a private vehicle, and work-related trips have a vehicle occupancy of merely 1.18 persons per vehicle. Moreover, the duration of an average car trip in the United States is approximately 27 minutes. We can, therefore, reasonably conclude that a typical car is in use only for a small fraction of time during the day and is parked for the overwhelming majority of the time. If vehicle occupancy is converted from persons per vehicle to a dynamic metric such as seat-hours used, the operational efficiency of a typical car is less than 5%. These traditional trip patterns have serious, long-term implications. As vehicle trips of low operational efficiency continue to be a large fraction of overall traffic, congestion is expected to worsen, leading to unacceptably high levels of greenhouse gas emissions. Over the last decade, the concept of ridesharing has received attention from academia, planning agencies, and private companies because of its potential to reduce individual car ownership, decreasing the number of cars on the road, thereby mitigating traffic congestion and lowering overall emissions. Studies show that each car-sharing vehicle in use results in 9 to 13 fewer cars on the road (Shaheen and Chan, 2015). Closely related to ridesharing is the concept of carsharing that has also gained popularity over the past several years.

The sharing economy in transportation, housing, and other sectors has become an integral part of our lives. People are increasingly receptive to the idea that empty vehicle seats can be shared, and the number of participants in shared mobility systems continues to increase. In tandem, real-time communication and information technologies (CIT) have contributed to the popularity of shared mobility frameworks, as they enable drivers and riders to be matched on-demand and provide a convenient payment system. Furthermore, innovations in autonomous vehicle (AV) technologies broaden the horizons of shared mobility with possibilities such as on-demand shared AV fleets, peer-to-peer AV fleets, AV carsharing, etc.

## 1.1 Overview of Multimodal Ridesharing systems

Multimodal ridesharing systems (RSS) is a broad umbrella term that describes many mobility services. A common misconception is that ridesharing is synonymous with carpooling. Perhaps the most well-known mechanism for carpooling is to match drivers and riders that have the same origin and destination (which usually limits the matching rate). Multimodal ridesharing systems extend the concept of carpooling to include multiple modal connections. In such a system, riders and drivers provide their origin/destination and desired departure/arrival time. The system can match a rider to multiple drivers to increase the matching rate and to provide a faster path. It should be noted that the term “driver” can conceptually include virtual “drivers” representing other modes of transport, such as transit or bikes. Rudnicki et al. (2008) studied ridesharing with walking, where the roles of drivers and passengers were known and each driver was assigned to passengers with the same destination (Rudnicki et al., 2008; Czioska et al., 2017). Other studies (Gruebele, 2008; Aydin et al., 2020) have proposed route/hop planning schemes, such as: (a) car -> car -> car; (b) car; (c) car -> airplane -> bus; (d) foot -> car -> car -> car; (e) car -> subway -> bus; (f) bicycle -> car -> bicycle; (g) foot; (h) bicycle; (i) foot -> bus -> foot. In previous studies conducted at UC Irvine (Masoud et al., 2017; Masoud and Jayakrishnan, 2017a), a multimodal ridesharing system was proposed to enhance the use of the LA Metro Red Line (a subway), allowing transfers between shared-ride cars and the LA Metro. One of the highlights of these studies is that a sizable fraction of travelers in drive-alone vehicles switched to transit (Masoud et al., 2017). Figure 1.1 illustrates the concept of multimodal RSS.

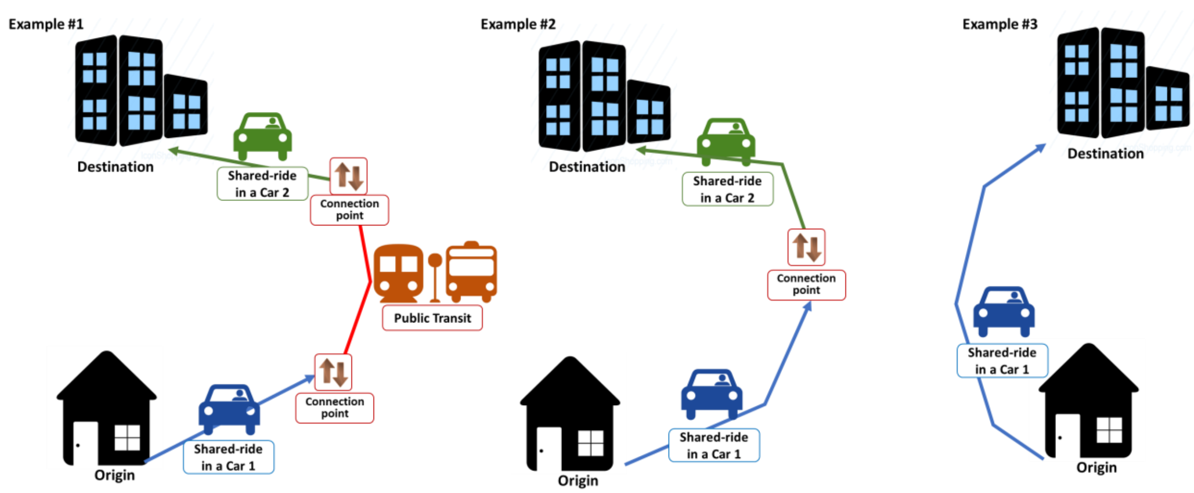


Figure 1.1 Multimodal ridesharing system concepts.

## 1.2 Need for Innovations in Trip Modeling

There is a broad consensus in academia and in the private sector that the ongoing revolution in transportation systems will bring about changes in car-ownership and has the potential to make transportation networks more efficient. Several interesting questions emerge: How will transportation systems change in the short term and long term as shared and autonomous systems become more prevalent? How do we model people's movements and travel mode choice behavior in the context of shared mobility systems?

Autonomous vehicle technologies can make transportation and mobility systems more flexible and shareable by connecting them continuously and seamlessly. Before that happens, we need a paradigm shift in how we model and analyze mobility in the first place. One promising avenue of inquiry is to integrate several mobility options so that travelers can freely hop among them. The boundaries that demarcate different modes can then become increasingly fluid, as every individual trip may include multiple modes to various degrees. This implies that the paradigm shift is in how we view travel modes. What were traditionally considered discrete mode options now need to be seen as part of a continuum. Therefore, an analysis of mode combinations rather than isolated travel modes becomes necessary.

Let us, for instance, envision a ridesharing scenario in which a person A who wants to be served for her trip is picked up by driver B who drops her off at an intermediate point, waiting to be picked up by another driver to drop her off to her final destination. The driver B proceeds to a different route to serve another user. Therefore, driver B's travel mode is a combination of travel mode options such as drive-alone, drive yourself and ridesharing. Finally, another driver C (who is driving alone) picks up person A and drops her off at her destination. Three participants in this example shift their travel mode options seamlessly and keep moving continuously until finishing their journey (Figure 1.2).

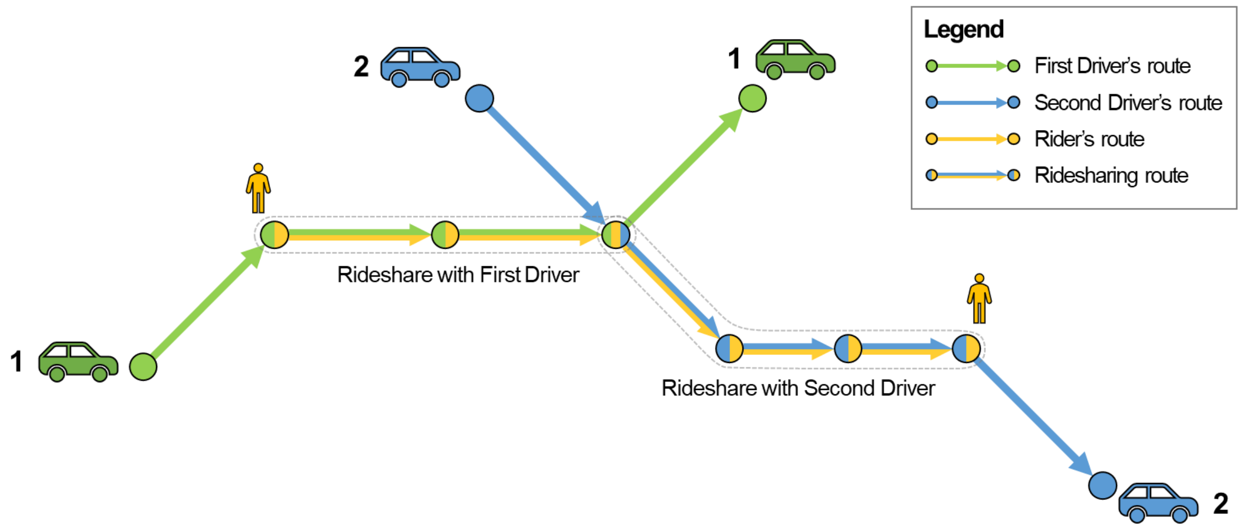


Figure 1.2 Travel mode example

This example, though simple, illustrates the challenge in modeling the participants' travel-mode sharing behavior in a discrete manner, as is common in traditional transportation planning system contexts.

## 1.3 Goals of the Dissertation

In this dissertation, we propose and develop the idea of a "mode option pool" to model individual trips. The mode option pool is defined as a set of all available travel options to a user with each travel option having its own characteristics (e.g., drive yourself option, shared-seat option, public option, bike, vehicle ownership option, etc.). This observation motivates the term 'travel-option chain (TOC)' mode proposed in this dissertation as a combination of travel options in a continuous spectrum. The advantage of this model is that it can generate a “mode” for individuals by combining any characteristics of mode options. For instance, a ridesharing driver’s TOC mode can be defined as: [drive yourself option(1), vehicle-ownership option(1), shared-seat option(1)]. The term M(x) denotes a binary variable which is 1 if a person experiences the designated option M, otherwise it is 0. As another example, a ridesharing rider’s TOC mode can be defined with a chain [drive yourself option(0), vehicle-ownership option(0), shared-seat option(1)]. Finally, a carsharing user’s TOC mode can be defined as [drive yourself option(1), vehicle-ownership option(0)].

Shared use of vehicles – either time-shared, or seat-shared – expands the travel option pool. Incorporating Autonomous Vehicle technology in this scenario further expands the travel mode option pool, since the driver constraint is also removed. An immediate observation is that this system needs to have a large option pool available for a large number of users to be efficient in terms of user mobility and the productivity of the vehicles and their associated infrastructure. One aspect that needs to be addressed is that it is infeasible for any individual to own all mobility options and infrastructure involved in all of the mobility options available in the travel option pool. Different people may partially or fully own different components such as vehicles or the spaces where they are parked. They may also have purchased the right to temprarily “own” a seat in a transit vehicle for some trips with a transit pass. Our proposed system allows for the possibility of time-shared ownership of all or most system components as well. Publicly provided transit systems with purchased tickets will naturally be part of many TOC modes. Subscription-type ownership is a possibility if a particular mobility service provider offers the option for purchase. Mobility service providers can offer bundled options as well, similar to phone plans. This fits within

Mobility-as-a-Service (MaaS) platforms that have been proposed in recent years. In this dissertation, we propose a powerful user-side concept called "mobility portfolio" that encompasses MaaS platforms, subscriptions, ownership options, bundled plans and selection of optimal TOCs from a continuum of modes.

The focus of this dissertation is on the user level decisions of selecting the TOC modes in the mode option pool from their mobility portfolios scheme. Innovative options such as users offering their own resources (e.g., owned vehicles) and their own services (e.g., potential driving for shared rides) are incorporated in the portfolios. We implement this paradigm by developing an agent-based platform for various geographical networks, travelers, and mobility service supply side details. Our developed platform has the ability to model an integrated shared transportation system which encompasses a wide range of mobility services such as peer-to-peer ridesharing, shared autonomous fleets, and peer-to-peer carsharing. We propose an iterative framework which is rooted in a learning-based travel cost perception update model, to model the provision (assumed to be by user apps) of optimal mobility portfolio solutions to individuals. The objective of the mathematical formulation attempts to minimize the total travel expenditure of users during mobility portfolio periods, which could be several days, weeks, or months. The TOC modes in the proposed mobility portfolio model are obtained from the results of a ride matching problem applied at the individual level for each trip. We extended Masoud and Jayakrishnan (2017a)'s dynamic programming (DP) algorithm to find the minimum cost itinerary for riders in an expanded travel option pool throughout the week, month, and season. This modification with the proposed iterative method allows individuals to dynamically shift their travel status (i.e., to be a ridesharing driver or a rider) within the period, if necessary.

## 1.4 Dissertation Outline

This dissertation is organized as follows. In chapter 2, we present a literature review of research on shared transportation concepts. Chapter 3 contains a description of the modeling details of the proposed continuous-mode and shared transportation system platform. Chapter 4 introduces the mobility portfolio framework and its component modules. We present the mathematical formulation of the mobility portfolio problem along with its variants, including bundling mechanisms, and their associated solution methodologies. We design numerical experiments and discuss the results obtained in chapter 5. We formulate and solve a multi-hop ridematching optimization problem which lies at the core of the proposed mobility portfolio framework in chapter 6. We provide a conjoint analysis of factors that influence travelers' decisions to adopt multimodal rideshare systems like ours in chapter 7. Finally, chapter 8 provides a summary of the conclusions and directions for future research.

# Chapter 2

# Literature Review

The value of the global sharing economy has continued to rise and is predicted to increase to more than 300 billion dollars in 2025, from just 15 billion dollars in 2014. This phenomenon has been accompanied by technological advances in the transportation field, leading to increased efficiency of transportation services. Shared transportation systems allow users to access those services more easily and provide system-wide benefits. Therefore, optimizing such systems will remain a focus of transportation researchers, state agencies and commercial interests in the foreseeable future. In this chapter, we present a literature review of various paradigms and methodologies that are related to the concept of shared transportation services.

## 2.1 Mobility-as-a-Service (MaaS)

As vehicles are increasingly viewed not only as personal possessions but as shareable goods, the concept of Mobility as a Service (MaaS) has emerged and evolved into various types of subscription-based services such as ride-hailing, car-sharing, peer-to-peer ridesharing, and bike-sharing. The popularity of MaaS in the commercial world has sparked interest in academia as well. There exists a significant body of literature related to MaaS. MaaS has a wide range of sustainability objectives such as reducing vehicle miles/hours traveled, green-house-gas emissions, private car ownership, and transportation iniquity. Also, as research on autonomous vehicles has accelerated radically over the past decade, shared autonomous fleet vehicles are being increasingly viewed as a new form of MaaS with the overall goal of sustainable development. In this section we focus on four specific areas where this development is taking place. We describe them in more detail in the following sub-sections. Note that all or most MaaS systems that currently exist or are proposed have a limited and discrete view of the modes that become part of it, while this dissertation considers the TPC option space to be essentially a continuous spectrum. In that sense, the work in dissertation is a much more generalized framework that subsumes current definitions of MaaS systems

### 2.1.1 Ridesharing System and Matching Problem

Ridesharing is not a new concept. Through the 1960s and into the mid-1970s in the United States, carpooling to work was a popular choice among commuters. In the subsequent decades, however, use of this mode declined as a result of increasing car ownership rates. The remarkable development in information and communication technologies (ICT) and the emergence of the sharing economy in recent years have revived the idea of ridesharing systems.

A key aspect of any shared mobility system is the ride matching process between the mobility service provider and the "mobility recipient". A higher match rate results in a more efficient and profitable rideshare system, which is why it has been the focus of research in both academia and industry.

The first efforts to solve the ridesharing matching problem focused on pairing a single rider with a single driver (Agatz et al., 2010; Agatz et al., 2011; Furuhata et al., 2013; Herbawi and Weber, 2012). Albeit simple, it continues to be the most popular ridesharing matching method in the absence of sophisticated technologies and routing algorithms. Its matching rate, however, is not satisfactory because an underlying requirement of this system is that the origin and destination point of a rider needs to be identical to that of the driver. One way to improve the matching rate is to allow the driver to transfer between drivers so that a single rider could potentially be serviced by multiple drivers (Agatz et al., 2010; Herbawi and Weber, 2011a; Herbawi and Weber, 2011b). Yet another improvement is to give enough time flexibility to a driver so that she could serve multiple riders before finishing her own trip (Agatz et al., 2010; Furuhata et al., 2013). Eventually, a many-to-many ridesharing approach was suggested (Agatz et al., 2010; Masoud and Jayakrishnan, 2017a; Masoud and Jayakrishnan, 2017b), along with the concept of meeting points which allow riders to transfer between drivers (Agatz et al., 2010; Masoud and Jayakrishnan, 2017a; Stiglica et al., 2015; Li et al., 2018). With the aim of providing a flexible P2P ridesharing system in real-time and improving computational efficiency, Masoud and Jayakrishnan (2017a) introduced the Ellipsoid Spatiotemporal Accessibility Method (ESTAM) to create a reduced network for each individual. They used to Dynamic Programming (DP) algorithm to solve the ride-matching problem optimally.

One highly useful feature of a ridesharing system is that it is relatively flexible and can integrate with an existing rigid traditional transportation system. As the ridesharing pool is increased by incorporating sharable vehicles (which can include private vehicles) with other travel modes (e.g., public transit system, walk, and so on), ridesharing participants who are willing to be shared riders (SRs) can take advantage of a more diverse and customized set of travel options. Under a multimodal ridesharing system, these systems can be used as public transit feeders that deliver travelers to public transit stations that have fixed schedules and routes (Agatz et al., 2010; Masoud and Jayakrishnan, 2017a; Masoud and Jayakrishnan, 2017b; Varone and Aissat, 2015; Fahnenschreiber et al., 2013; Faroqi and Sadeghi-Niaraki., 2015; Masoud et al., 2017; Ma et al., 2018; Stiglica et al., 2018). Considering 'walking' as one type of ridesharing mode, Lin et al., (2016) proposed a ridesharing-by-virtual-pools (RSVP) system and tested this system at transportation hubs. A real-time ridesharing service system can be considered as an alternative public transportation mode as well (Aissat and Varone, 2015; Xing et al., 2009; Ma, 2017). By allowing transfer between different types of travel modes, Masoud and Jayakrishnan (2017b) formulated a binary optimization problem in a time-expanded network for the multi-hop peer-to-peer (P2P) ride-matching problem. In their study, a decomposition algorithm was adopted to reduce the size of the problem and to accelerate the ride-matching problem solution via solving multiple smaller problems. Wang (2013) considers metrics such as systemwide travel and travel cost to formulate and solve a dynamic ridesharing matching problem. Herbawi and Weber (2011) also formulate a dynamic ride-matching problem by minimizing the total travel time of both drivers and riders.

### 2.1.2 Carsharing System and Car Ownership

Carsharing is another critical component of shared mobility systems. The key aspects of carsharing are (a) a car is a sharable good when it is idle and (b) people join the service to rent vehicles for a short-term period. Early carsharing systems were primarily business-to-consumer (B2C) services with vehicles provided at fixed spots. Therefore, determining the optimal location of the carsharing vehicles was an important research topic (Herbawi et al., 2016; Bsaybes et al., 2015; Nourinejad et al., 2015; Jorge et al., 2014; Wagner et al., 2015; Huang et al., 2018). When electric vehicles are used for carsharing, the carsharing location problem is combined with the electric vehicle charging location problem (Bruglieri et al., 2017; Bruglieri et al., 2018a; Bruglieri et al., 2018b).

Several studies have documented the effects of carsharing on private vehicle ownership. Shaheen et al., (2018) document the trends in carsharing and vehicle ownership in North America. They report that the number of users of carsharing markets has gradually increased, while the growth in private vehicle ownership has decreased over the same time period. Glotz-Richter (2012) report the effects of replacing car ownership with carsharing: almost 90% of carsharing users said car-sharing completely replaced a car in their household (i.e., the household did not have a private vehicle anymore), and 32% of carsharing users stopped using their private car entirely. Glotz-Richter's findings lend support to the notion that people are enthusiastic towards the idea of carsharing, especially when it is cost-efficient. With the help of ICTs, carsharing systems could be reshaped as peer-to-peer (p2p) mobility services. In p2p carsharing systems, participants can rent other vehicles and at the same time rent their own vehicles to other people in the system. By providing a vehicle with low costs (by covering the costs of insurance, for example) and high accessibility and flexibility, more and more people can join p2p carsharing systems. This can create strong network effects that encourage more people to join the system, thereby achieving economies of scale. Shaheen et al., (2015) conducted a survey to examine users' awareness and perception of P2P carsharing in relation to vehicle ownership and travel behavior in San Francisco and Oakland. Despite the economic and demographic discrepancies between respondents from those cities, on an average 35% of respondents whose travel type was a 'vehicle owner' reported that they would consider using p2p carsharing or renting out their own vehicle through a p2p operator. In a subsequent study, Shaheen et al., (2018) found that there exists a small proportion of the population who would be amenable to giving up car ownership entirely and would prefer a rented car from p2p carshaing system. Ballús-Armet et al., (2015) found that the group who had the most openness towards p2p carsharing system was the group who did not own their car and wanted to increase their mobility availability. However, those who have a fixed daily commute trip preferred to continue to use their current travel mode.

### 2.1.3 Autonomous Vehicles and Their Implications

The availability and deployment of autonomous vehicles, especially fully autonomous vehicles (AVs) will lead to various changes in our society in the coming decades. Therefore, it is crucial to design mobility systems that fully leverage the potential of these vehicles. As this new travel mode emerges, research efforts have been undertaken to integrate it with shared transportation systems. New forms of shared mobility such as free-floating carsharing service with autonomous vehicle fleets can be a sustainable and road-friendly transportation alternative that increases overall network capacities and performance (Zhang et al, 2015). A single AV can be accessible to many more people than currently served by personal autos. Thus, they reduce ownership costs for users. In certain scenarios, shared autonomous vehicles (SAV) show potential to become high-occupancy vehicles which can replace several single-driver vehicles (Fagnant et al., 2015; Segal and Kockelman, 2016; Gurumurthy and Kockelman, 2018). Schoettle and Sivak (2015) show that in extreme cases, car ownership rate could drop by around 43%, from an average of 2.1 vehicles to 1.2 vehicles per household, providing more opportunities for a single mode to be accessible to multiple people. Hyland and Mahmassani (2018) suggest optimization strategies to operate autonomous vehicle fleets dynamically to improve SAVs' performance efficiency in reducing empty miles and traveler wait times. When AVs are used in a fleet such as commute shuttle buses or reserved mass transit (Gucwa, 2014; Fagnant et al., 2015), the optimization problem becomes matching users' accessibility characteristics to AVs schedule/routing constraints, analogous to ridesharing accessibility problem formulations.

### 2.1.4 Travel Behavior Change in Shared Mobility systems

Transformations in mobility services effected by means of newly applied travel modes (e.g., P2P ridesharing, P2P carsharing, etc.) and realizable mode (e.g., AV fleets) are expected to cause changes in travel behavior. The most popular methods to forecast travel mode choice behavior is the well-known discrete choice modeling approach. Priatama et al., (2018) used a binary logit model to develop a mode choice model, considering a ridesharing service in DKI Jakarta. In their study, ridesharing service's fare per km and waiting time for the service were selected as model parameters. Moeckel et al., (2013) proposed a nested multinomial logit mode choice model by integrating not only drive-alone and shared-ride modal options but also public side travel options (e.g., bus, rail and air). Zhao and Kockelman (2018) used a multinomial logit model to investigate the impact of connected autonomous vehicles (CAVs) and shared autonomous vehicles (SAVs) and applied their developed model to the existing travel demand model for the Austin, Texas, region. In their study, SAV was considered a carsharing (renting) mode.) To satisfy the independence of irrelevant alternative (IIA) axiom, in their study, SAVs and CAVs were distinct travel modes compared to Auto and Bus modes. Considering several factors such as VOTT, personal vehicle operation cost, parking, and toll costs, which may affect the travel mode choice behavior, they found that more people are willing to shift their travel mode if Avs are more cost effective.

## 2.2 Transformation in Transportation Services

The shared mobility options described in the previous section can operate inside a comprehensive mobility service platform. A well-designed platform can perform several functions, such as planning a journey, book trips with various mobility operators, handle payments, and transporting passengers. Such a platform could also leverage the massive real-time data available to it to make travel-related recommendations to users, based on their experiences. These recommendations can include bundled mobility services that contain tailor-made combinations of shared mobility option and credits for each option, just like in a mobile plan. In this section we focus on two specific areas: recommender systems with MaaS and MaaS bundle design.

### 2.2.1 MaaS Recommender System

In general, recommender systems are widely accepted in content delivery services as news magazines, academic articles, advertisements, and various other products. The aim is to maximize recommendation acceptance rate, user satisfactions, or corporate profits (Adomavicius and Tuzhilin, 2005). These systems have gained popularity as smartphones have become ubiquitous, which allows companies to provide real-time information that users need or may be interested in via apps. By integrating recommender systems and smartphone applications, various recommendation services in the domains of health, tourism, and education have become common. In addition, using GPS trajectories, check-in data from social networks and points of interest is available to platform owners, allowing them to recommend location to their users context (Wang et al., 2013; Yin and Lee, 2010; Berjani and Strufe, 2011; Levandoski et al., 2012). It is, therefore, only a matter of time that recommender systems would be used in transportation systems of the future.

In the transportation context, users can be recommended trip activity locations, routes, departure time and pickup locations. The success of recommender systems depends on how well it predicts people’s behavior and preferences. To this end, various techniques based on learning have been conducted. One such technique is the Multi-Armed bandit (MAB) algorithm (Chu et al., 2010, and Zhou and Chow, 2019). Using this technique, Chow and Liu (2012) proposed recommendation for points of interest based on routing costs and activity benefits. Zhou et al., (2019) suggest a system which can provide departure time and path selection by considering on-time arrival reliability. Yoon et al., (2020) provided a destination recommender system for mobility-on-demand (MOD) services. They proposed a platform that provides MOD vehicles that are equipped with various destination information. The platform computes routes and destinations for new requests from existing passengers' pickup and drop-off points. Li et al. (2015) proposed a recommendation mechanism for taxi drivers to reduce the number of vehicles on the roads and the cost of trips. Their recommender system has been integrated with a real-world fleet management system. Xu et al., (2020) developed a recommender systems framework to balance mobility supply and demand in e-hailing platforms. Their study aimed to reposition drivers, generating possible destinations by considering point of interests (POIs) with the highest number of passenger requests in historical data. They applied the proposed framework to the online system of Chinese ride-hailing company DiDi Chuxing and reported that it enhanced driver experience and led to a modest increase in their incomes.

In addition to recommender systems for mobility suppliers, research has been devoted to recommender systems at the individual level. Gustowski et al., (2017) proposed a conceptual framework that builds contexts for individuals that based on their profile, activity, and environment (spatiotemporal information, and climatic information). By leveraging this information, they developed recommendation systems for personalized context-aware services to mobile users in smart cities. By collecting people's historical location information, activity duration information, and demographic information such age, gender majority and main languages, they predicted feasible locations to access services, and to recommend precise routes to get there. Song (2018) developed a model that provides personalized urban mobility solutions. Their recommendations were delivered using an app-based service with menus containing contains route and mode combinations. They computed optimal menu options for users by using historical and current information about their acceptance or rejection behavior.

### 2.2.1 MaaS Bundling Design

Along with MaaS-related services and studies, MaaS bundling design problems have been formulated by researchers to study shared-mobility systems. Bundling is a widely accepted concept in marketing and economics. Despite the fact that the original purpose of bundling schemes in economics is to maximize profits, in transportation, bundling scheme is devised to encourage people to use more sustainable travel modes. From this perspective, the bundling idea has developed into a form of a combined ticket that contains several public transportation choices such as metro, bus, taxi, etc.

We propose a generalized comprehensive framework of grouping mobility options with the associated bundled payment plans for subscription-based mobility in our research, which we term “mobility portfolios” (Jayakrishnan et al., 2019). As for relevant previous work in this direction, Matyas and Kamargianni (2019) independently conducted an initial study on a concept of designing MaaS bundles to support shared modes and proposed it as a monthly subscription plan, similar to mobile phone plans. The options included were few and conceptually discrete in their concept. In their study, they offer three MaaS bundle plans with different combinations of mobility options (e.g., public transport, bike sharing, car sharing, and taxi). To attract people to MaaS bundles more actively, incentive-based schemes are applied for each option *(*Ho et al., 2018; Ho et al., 2021a; Ho et al., 2021b). Furthermore, each plan has limited credits in the form of fixed bundle cost per month. Similar to the other MaaS mobile applications, a MaaS bundle also can be delivered via a mobile application with a mobile payment system. Ho et al. (2021a) build a digital MaaS trial platform with a booking and payment integration system, and aggregate five existing private-sector MaaS services (ride-share, public transit, taxi, car-sharing, car-rental) as mobility bundle options.

Most MaaS bundling design problems are based on survey methods to drive the properties of bundle options and offer bundle choice models to estimate the interest in MaaS subscription bundles. Ho et al. (2021b) propose a mixed multinomial logit model and find that subscribers' travel activity and cost savings from discounted fares on options are factors that influence their mode choices.

## 2.3 Discussion

We review two streams of literature in this chapter: literature on MaaS and shared mobility services, and literature on transformation in transportation services strategy. Earlier works on MaaS and shared mobility services aimed to increase the matching ratio between the potential shared-mobility users and the shared-mobility providers. We examined the existing literature related to AV and AV fleets and vehicle ownership changes and find that shared mobility services combined with MaaS lead to a change in people's mode choice behaviors. While studies related to shared mobility services studies have been conducted only for each specific mobility service, MaaS bundling design methodologies focus on overall strategies to provide an all-encompassing shared mobility bundle for users. Recommender systems with MaaS systems can bring more personalized services and provide optimal mobility solution according to individual tastes.

# Chapter 3

# A Study of the Factors Affecting Multimodal Ridesharing with Choice-based Conjoint Analysis

## 3.1 Motivation

The research in this dissertation started with an early study on the user-acceptance of multi-modal shared mobility systems, as it is the primary component of the proposed mobility portfolios based on a comprehensive continuous-spectrum of TOC “modes”. Before embarking on developing a full-fledged model framework with portfolio schemes, it is important to identify the key factors that could affect the success of the framework from a user standpoint, even if such a study wold naturally involved only a somewhat-limited form of multi-modal ridesharing. Thus the study in this chapter is a based on a user-survey that involved only the currently proposed ride-sharing systems without the significant enhancements that will be brought by the mobility portfolio schemes discussed in the subsequent chapters.

Multimodal ridesharing systems (RSS), where multiple transportation modes fulfil rider trip demands, have been the focus of recent studies seeking to improve the matching rate and connectivity across travel modes, with the aim of providing increased mobility (Rudnicki et al., 2008; Masoud et al., 2017; Masoud and Jayakrishnan, 2017b). Multimodal RSS, however, have several key issues that must be addressed before they can be viable: (a) do RSS provide reasonable travel times (Gruebele, 2008; Korea Railroad Research Institute, 2016; Agatz et al., 2011; Wang, 2013; Bilali et al., 2019)?; (b) do RSS properly price their services (Gruebele, 2008; Agatz et al., 2011; Wang, 2013; Agatz et al., 2012; Ginaviciene and Sprogyu, 2020)?; (c) can RSS ensure a reasonable number of transfers (Masoud and Jayakrishnan, 2017b; Wang, 2013)?; (d) do RSS provide sufficient ridesharing incentives to encourage their use (Gruebele, 2008;Brownstone and Golob, 1992)?

These are the most significant issues influencing a potential user's inclination towards multimodal RSS. By adopting multimodal RSS services, users could have their time and travel costs lowered, compared to their current travel options. At the same time, even people willing to use multimodal RSS services might not accept this option if they end up paying more for it. Similarly, even with lower travel cost and travel time, a user may only be willing to accept a transfer inconvenience if there is a sufficient incentive, such as a subsidy.

Therefore, with any type of multimodal ridesharing system, it is necessary to analyze how travelers respond to the set of attributes characterizing the system. Capturing the implicit determinants of individual preferences is also important. Factor analysis and conjoint analysis are commonly used as multivariate statistical techniques to gain insights regarding consumer behavior through empirical or quantitative measurements (Korea Railroad Research Institute, 2016; Kim et al., 2015). Kim et al. (2015) analyzed the potential factors affecting the attitudes of participants towards car ownership and program participation in electric vehicle sharing programs (EVSPs). Unlike factor analysis, which is used to examine how underlying constructs influence responses on a number of measured variables, a conjoint analysis is used in market research to determine how people value different features that constitute an individual product or service. A conjoint analysis examines which combination of a limited number of attributes is most influential on an individual's decision making. This analysis also makes it possible to evaluate the relative importance of a set of attributes. While common in marketing research, conjoint analysis has not been widely used in transportation systems research, although it can be useful in providing insights into user acceptance of newly proposed systems and designs. In this dissertation, we employ a choice-based conjoint analysis method. Data were collected using a web-based survey system, targeting people who live in Southern California (e.g., Los Angeles, Irvine, San Diego, and Santa Barbara).

The remainder of the chapter is structured as follows. In the next section, we briefly introduce the concept of multimodal ridesharing. Section 3.3 outlines the technical approach that was used for the conjoint survey design. We describe the data that were collected and present the conjoint analysis with a multinomial logit model in section 3.4. We follow this with a discussion of the impact factor results and conclude the chapter with a discussion on future research opportunities.

## 3.2 Choice-based Conjoint Survey Design

As part of this study, a choice-based conjoint survey was designed and conducted in the Southern California region, comprising the cities of Los Angeles, San Diego, Santa Barbara, and Irvine. The sample size of the survey was 4,254 choices obtained from 401 participants. The web-based survey was chosen because it can minimize missing data by advising respondents to respond to all questions. In addition, a well-designed survey website can help respondents to understand the purpose of the survey and, thus, can increase their participation (Ginaviciene and Sprogyu, 2020).

### 3.2.1 Conjoint Survey Design

Conjoint analysis is a marketing research technique used to assess the weight individuals place on different features of a given product or service. Products are represented by their attributes and respondents provide data about their preferences for hypothetical products that are defined by combinations of attributes. A range of new models and techniques for the estimation of part-worth functions have been developed. While several conjoint methods exist, two primary alternatives are the ratings-based (RB) and choice-based (CB) conjoint analyses. A significant systematic difference between these two analysis options is the compatibility effect. For example, some attributes (such as brand name) tend to be more critical in RB models, whereas some comparable attributes (such as price) are likely to be more important in CB models (Karniouchina et al., 2009). Choice-based conjoint analysis has become perhaps the most widely used conjoint technique in marketing research. Rao (2013) described the major steps in a conjoint study. These include problem selection of attributes and design of profiles (i.e., the set of at-tribute levels describing a system design alternative), choice set and analysis methods, and, finally, utilization of results (see Figure 3.1a). To analyze the impact factors of the multimodal ridesharing system, we designed a survey questionnaire by applying choice-based conjoint analysis shown in Figure 3.1b.

The selection of attributes and the design of choice sets is critical in conjoint studies because each attribute combination for hypothetical products influences the choice of an alternative.

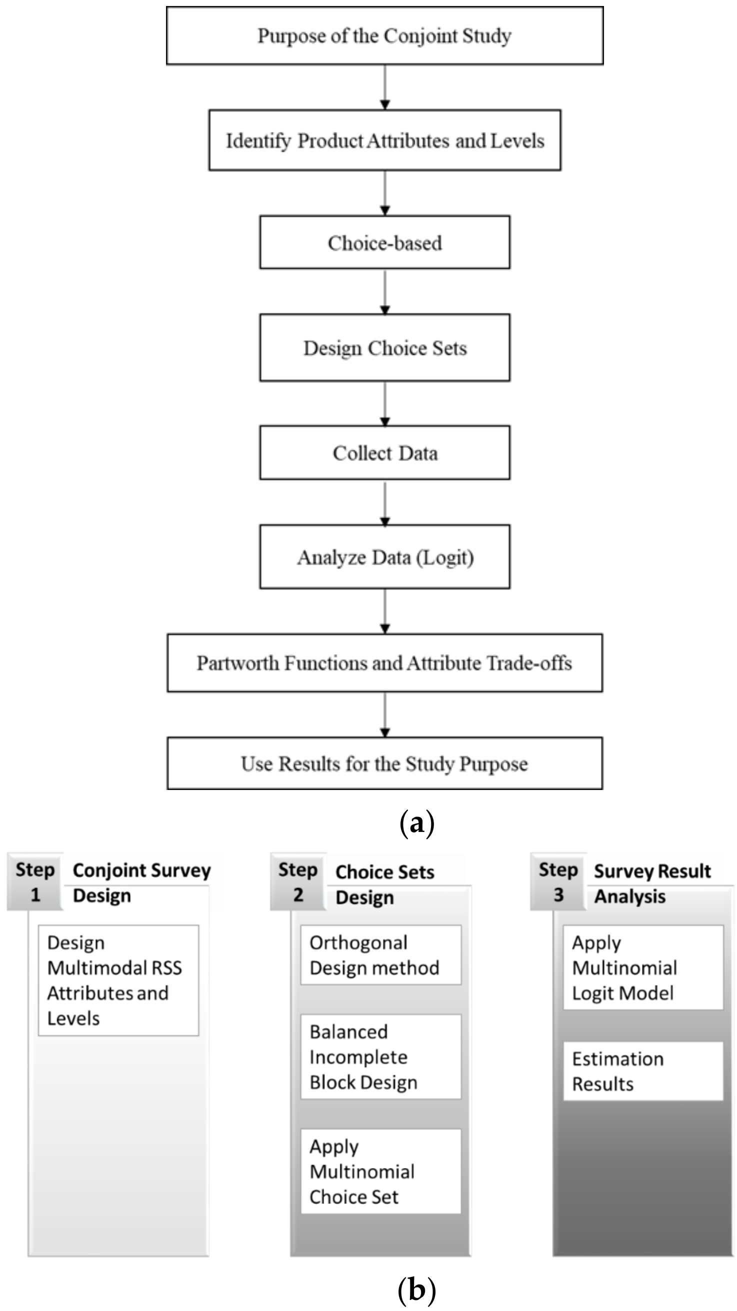


Figure 3.1 Overview of conjoint analysis design: (a) major steps in conjoint study; (b) conjoint analysis steps for multimodal RSS impact factor analysis.

Hypothetical alternatives are presented as profiles, which is defined as a set of attribute levels that describes the hypothetical system design alternative. In general, the number of levels is restricted to a relatively small number for any attribute, from as few as 2 to no more than 5 or 6, to ensure that fewer profiles are generated for data collection. Next, we describe some relevant studies that influenced our selection of attributes.

Various metrics can be considered to evaluate the utility of a travel mode. Wang (2013) considered system-wide travel and travel cost to optimize a dynamic ridesharing matching problem. Herbawi and Weber (2012) formulated a dynamic ride-matching problem by minimizing the total travel time of both the driver and riders. Ko et al. (2017) considered EVSP renting and returning hours as the survey components for an electric vehicle sharing program.

A survey conducted by the Korea Railroad Research Institute (2016) considered travel time and travel cost to be the representative attributes for the proposed rail alternatives. Accordingly, travel time and travel cost were considered important factors that affect the choice of transport mode (Furuhata et al., 2013; Stiglic et al., 2016).

Multimodal ridesharing systems (RSS) technically include transferring between travel modes, and the number of transfers may be a critical factor affecting the preferences of potential multimodal RSS users. Masoud et al. (2017) considered LA Metro Red Line stations as transfer points to provide a connection point between travel modes. Wang (2013) stated that consistent, seamless, and efficient mode transfers will only be possible with effective optimization technologies. Furuhata et al. (2013) addressed the necessity for transfer points to support high-dimensional ride-matching algorithms.

It is also possible to encourage people to use multimodal RSS by providing sustainable transportation incentives. Brownstone and Golob (1992) studied the effects of incentives that are designed to promote carpool ridesharing on work trips to reduce congestion and air pollution. They proposed ordered-probit discrete choice models to estimate the commuting mode choice of full-time workers in the Los Angeles area. Three kinds of incentives to control transportation demand were investigated: (a) reserved or other preferential parking for ride-sharers; (b) direct carpooling and/or vanpooling cost subsides by employers; (c) guaranteed rides home for ride-sharers. They found that providing all workers with these incentives would reduce drive-alone commuting by 11 to 18 percent. The effectiveness of high-occupancy vehicle (HOV) lanes in promoting ridesharing on Southern California freeways was also considered as a rideshare incentive (Brownstone and Golob, 1992; Lloret-Batlle et al., 2017).

Two recent programs offered some insight into the design of our survey. San Luis Obispo (California) Council of Governments (SLOCOG) launched the county-wide SLO Regional Rideshare program[1] to reduce the reliance on driving alone and to improve mobility. SLO Regional Rideshare provides the "iRideshare" service, which is a free online ride-matching system with online trip logging for rewards and prizes. Back 'N' Forth Club Rewards is a free program in the region that is offered to businesses and organizations that encourage employees to use sustainable transportation when commuting. Employees record their trips made by bike, carpool, vanpool, bus, telecommute, or on foot into their personal calendars at iRideshare.org and then redeem points for

[1] SLO Rideshare System, https://www.slocog.org/programs/system-efficiency/slo-regional-rideshare

gift cards. This system provides carpooling reimbursements to drivers and offers discounted pricing to riders. The riders cover a share of driver costs, ranging from approximately USD 2 to USD 10, and the drivers receive reimbursements ranging from USD 3 to USD 9 per passenger per trip. Another such program is a sustainable transportation incentive program at Santa Monica College (California) that is designed to reduce the use of single-occupancy vehicles. The college provided monthly incentives per usage of sustainable transportation alternatives, such as biking, walking, and carpooling. To ensure incentive compatibility, the program offers three options of ridesharing incentives, namely, USD 150, USD 200, and USD 250 per month. Based on these findings, in this dissertation, ridesharing travel time changes (compared to the user's current travel time), ridesharing travel cost changes (compared to the user's current travel cost), the number of transfers, and the monetary incentives for ridesharing (as an annual reward) are considered as attributes of the multimodal RSS survey. Table 3.1 shows the attributes of the multimodal RSS and the option levels. Once the attributes and levels are chosen, the next step is to generate the stimulus set of hypothetical profiles to be evaluated by respondents. The procedure for constructing stimulus profiles is intertwined with the particular conjoint approach used (Rao, 2013). Well-known statistical techniques such the full cards method and fractional factorial design are used to generate profiles. In the full cards method, the profiles are generated by a full factorial design, including all combinations of the attribute levels. However, these designs are not practical when the total number of combinations is large (Rao, 2013). With this method, our study would generate 81 profiles, which is too large for respondents to evaluate.

This problem can be resolved by using a fractional factorial design, which reduces the number of profiles using an orthogonal design, and which offers several advantages. First, these designs are concise yet convey all the information needed to the responder to make their choices. Second, they enable the estimation of all of the main effects of attributes in a conjoint study. These designs can be restricted to blocks so that each individual receives a balanced subset of profiles (Rao, 2013).

Table 3.1 Multimodal RSS attributes and levels

| Attribute | | Sub-attribute | Level |
|---|---|---|---|
| Efficiency | Number of transfers | 2 times or more | 1 |
| | | 1 time | 2 |
| | | No transfer | 3 |
| Mobility | Ridesharing travel time compared to your current travel time | Up to 10 min. longer | 1 |
| | | Up to 5 min. longer | 2 |
| | | Equal or less | 3 |
| Economic Feasibility | Ridesharing travel cost compared to your current travel cost | Up to 10% higher | 1 |
| | | Up to 5% higher | 2 |
| | | Equal or less | 3 |
| | Ridesharing incentives | Up to USD 150 annual refund | 1 |
| | | Up to USD 200 annual refund | 2 |
| | | Up to USD 250 annual refund | 3 |

The condition for a design to be orthogonal (which is called symmetric if each attribute in the design has the same number of levels) is that each level of one factor appears with each level of another factor with proportional frequencies. In a symmetric orthogonal design, every level of a factor occurs an equal number of times with every level of another factor. Orthogonal arrays can either be balanced or imbalanced in terms of the levels of attributes. The property of level balance implies that every level occurs the same number of times within each attribute in the design. An imbalanced design allows for larger standard errors in the parameter (part-worth) estimates. Therefore, to reduce errors, the orthogonal design method was adopted with the balanced incomplete block design process. Details of the process can be found in Rao (2013).

### 3.2.2 Conjoint Choice Set Design

In general, there are two types of choice-based conjoint schemes that are studied: (1) binary choice experiments where the response is binary to a stimulus profile; (2) multinomial choice experiments where the responses are to a set of three or more alternatives, including a "no choice" option, which can make a decision more realistic (Rao, 2013; Lloret-Batlle et al., 2017) A binary choice experiment is used when each profile is presented to the respondent seeking a response of yes or no. We designed a multinomial choice experiment to determine the relative importance of each multimodal RSS attribute. We chose the process suggested by Rao (2013) to design our multinomial choice experiments. The first step is to design the profiles of alternatives, using the attributes and their levels. The second step of the process is to scheme choice sets, with each set consisting of a subset of these profiled alternatives. Choice sets can be created manually (using a shifting method), which develops an ordered combination of attribute levels. The shifted-design choice set is shown in Table 3.2, where 27 profiles emerge for different sets of attribute levels. A sample from the conjoint questionnaire is shown in Table 3.3.

Table 3.2 Shifted design for nine choice sets of three for four attributes, each at three levels

| **Choice set** | **Profile** | **Attribute 1** | **Attribute 2** | **Attribute 3** | **Attribute 4** |
|---|---|---|---|---|---|
| 1 | 1 | 1 | 1 | 3 | 1 |
| | 2 | 2 | 2 | 2 | 2 |
| | 3 | 3 | 3 | 1 | 3 |
| 2 | 4 | 1 | 2 | 2 | 3 |
| | 5 | 2 | 3 | 1 | 1 |
| | 6 | 3 | 1 | 3 | 2 |
| 3 | 7 | 1 | 3 | 1 | 2 |
| | 8 | 2 | 1 | 3 | 3 |

| | | | | | |
|---|---|---|---|---|---|
| | 9 | 3 | 2 | 2 | 1 |
| 4 | 10 | 2 | 1 | 2 | 2 |
| | 11 | 3 | 2 | 1 | 3 |
| | 12 | 1 | 3 | 3 | 1 |
| 5 | 13 | 2 | 2 | 1 | 1 |
| | 14 | 3 | 3 | 3 | 2 |
| | 15 | 1 | 1 | 2 | 3 |
| 6 | 16 | 2 | 3 | 3 | 3 |
| | 17 | 3 | 1 | 2 | 1 |
| | 18 | 1 | 2 | 1 | 2 |
| 7 | 19 | 3 | 1 | 1 | 3 |
| | 20 | 1 | 2 | 3 | 1 |
| | 21 | 2 | 3 | 2 | 2 |
| 8 | 22 | 3 | 2 | 3 | 2 |
| | 23 | 1 | 3 | 2 | 3 |
| | 24 | 2 | 1 | 1 | 1 |
| 9 | 25 | 3 | 3 | 2 | 1 |
| | 26 | 1 | 1 | 1 | 2 |
| | 27 | 2 | 2 | 3 | 3 |

Table 3.3 A sample choice attributes and option levels from the conjoint questionnaire

| **Choice Set** | **Attribute** | **Option 1** | **Option 2** | **Option 3** | |
|---|---|---|---|---|---|
| 1 | Number of transfers | 2 times or more | 1 time | No transfer | None of these options |
| | Ridesharing travel time compared to user's current travel time | Up to 10 min. longer | Up to 5 min. longer | Equal or less | |
| | Ridesharing travel cost compared to user's current travel cost | Up to 10% higher | Up to 5% higher | Equal or less | |
| | Ridesharing incentives | Up to USD 150 annual reward | Up to USD 200 annual reward | Up to USD 250 annual reward | |
| Select | | ☐ | ☐ | ☐ | ☐ |

### 3.2.3 Sociodemographic and Trip Characteristics Factor

In the survey, respondents were asked about their sociodemographic factors, such as employment status, age, gender, and household income and trip characteristics, such as primary trip purpose, trip frequency, primary trip mode, travel time, travel distance, and the number of transfers. Their willingness to use multimodal RSS was also considered.

### 3.2.4 Characteristics of Respondents

Table 3.4 displays the sociodemographic and travel characteristics of respondents to the web-based survey.

As indicated in Table 3.4, most respondents were female (61.3%), full-time employed (46.6%), and within the 35-44 age group (53.9%). Concerning the primary travel mode, 78.8% of the respondents preferred to use personal vehicles when they made their most frequent trip (i.e., to/from work: 43.1%). Due to the high proportion of private vehicle users, almost 70 percent of respondents made zero transfers. An interesting observation is that 83.5% of respondents answered that they were willing to use a multimodal ridesharing system. This reveals that most people are willing to change their travel mode when they are offered a multimodal ridesharing system, as long as it satisfies their preferences.

Both travel time and trip distance appear to be evenly distributed. Respondents' household incomes were also evenly distributed, with the median group of between USD 50,000 and USD 75,000 (25.2% of respondents). The most common trip frequency was found to more than once per week but not every day was reported by almost half (48.8%) of the respondents.

Table 3.4 Sociodemographic and trip characteristics of the participants survey respondents

| | | **Sociodemographic characteristics** | | |
|---|---|---|---|---|
| Sociodemo-graphic Characteristics | Variable | Description | Sociodemographic Characteristics | Variable |
| | Employment Status | Employed full-time | 187 | Employment Status |
| | | Employed part-time | 68 | 17.0 |
| | | Homemaker | 35 | 8.7 |
| | | Student | 41 | 10.2 |
| | | Retired | 34 | 8.5 |
| | | Unemployed | 36 | 9.0 |
| | Age | Under 16 years old | 1 | Age |
| | | 16-24 years old | 60 | 15.0 |
| | | 25-34 years old | 131 | 32.7 |
| | | 35-44 years old | 85 | 21.2 |
| | | 45-54 years old | 50 | 12.5 |
| | | 55-64 years old | 51 | 12.7 |
| | | 65 years old or older | 22 | 5.5 |
| | | Prefer not to answer | 1 | 0.2 |
| | Gender | Female | 246 | Gender |
| | | Male | 151 | 37.7 |
| | | Prefer not to answer | 3 | 0.7 |
| | | Other | 1 | 0.2 |
| | Household Income | Less than USD 15,000 | 27 | Household Income |
| | | USD 15,000 to USD 25,000 | 30 | 7.5 |
| | | USD 25,000 to USD 35,000 | 25 | 6.2 |
| | | USD 35,000 to USD 50,000 | 52 | 13.0 |
| | | USD 50,000 to USD 75,000 | 101 | 25.2 |
| | | USD 75,000 to USD 100,000 | 60 | 15.0 |
| | | USD 100,000 to USD 150,000 | 45 | 11.2 |
| | | More than USD 150,000 | 36 | 9.0 |
| | | Prefer not to answer | 25 | 6.2 |
| Trip Characteristics | Most Frequent Trip | To/from work | Trip Characteristics | Most Frequent Trip |

| | | | | |
|---|---|---|---|---|
| | | School | 42 | 10.5 |
| | | Shopping | 71 | 17.7 |
| | | Personal business | 79 | 19.7 |
| | | Social and recreation | 30 | 7.5 |
| | | Other | 6 | 1.5 |
| | Trip Frequency | Less than once per week | 32 | Trip Frequency |
| | | More than once per week, but not every day | 193 | 48.1 |
| | | Once every day | 124 | 30.9 |
| | | More than once every day | 52 | 13.0 |
| | Primary Travel Mode | Personal vehicle (car, truck, van, motorcycle, etc.) | 316 | Primary Travel Mode |
| | | Rail (Subway, light rail, commuter rail, etc.) | 8 | 2.0 |
| | | Bus | 27 | 6.7 |
| | | Bicycle | 10 | 2.5 |
| | | Walk | 8 | 2.0 |
| | | Uber/Lyft/taxi/shuttle | 13 | 3.2 |
| | | Carpool, vanpool | 15 | 3.7 |
| | | Other | 4 | 1.0 |
| | Average Travel Time | Less than 5 minutes | 15 | Average Travel Time |
| | | 6 ~ 10 minutes | 60 | 15.0 |
| | | 11 ~ 15 minutes | 87 | 21.7 |
| | | 16 ~ 20 minutes | 68 | 17.0 |
| | | 21 ~ 30 minutes | 75 | 18.7 |
| | | 31 ~ 45 minutes | 49 | 12.2 |
| | | 45 ~ 60 minutes | 20 | 5.0 |
| | | More than 60 minutes | 27 | 6.7 |
| | Average Trip Distance | Less than 5 miles | 70 | Average Trip Distance |
| | | 6 ~ 10 miles | 119 | 29.7 |
| | | 11 ~ 20 miles | 103 | 25.7 |
| | | 21 ~ 30 miles | 62 | 15.5 |
| | | 31 ~ 40 miles | 28 | 7.0 |
| | | 41 ~ 50 miles | 9 | 2.2 |
| | | more than 50 miles | 10 | 2.5 |

| | | | | |
|---|---|---|---|---|
| | Number of Transfers | 0 | 279 | Number of Transfers |
| | | 1 | 86 | 21.4 |
| | | 2 or more | 36 | 9.0 |
| | Willingness to use multimodal RSS | Yes, I would definitely try | 149 | Willingness to use multimodal RSS |
| | | Maybe, I would consider trying | 186 | 46.4 |
| | | No, I would definitely not try | 66 | 16.5 |

## 3.4 Choice-based Conjoint Analysis: Mathematical Formulation

Conjoint analysis is a commonly applied multivariate statistical technique that is used to gain understanding of how people make distinctions between products or services, so as to design new products or services that incorporate the most valued aspects. There are only a small number of transportation-related studies that use choice-based conjoint analysis based on surveys (Kofteci et al., 2010; Jianrong et al., 2011; Seok et al., 2016). This dissertation utilized a multinomial logit (MNL) model to estimate behavior based on choice-based conjoint data, which provides the preferences for each attribute of a product or service.

In conjoint analysis, each respondent must choose one alternative from each of several choice sets. These choice sets are constructed by dividing the total set of profiles across K choice sets. In this dissertation, each choice set contained the same number of alternatives without loss of generality. The utility of alternative m in choice set $s$ for individual $i$ is de-fined as equation (3.1):

$$u_{ism} = X_{sm}\beta + e_{ism} \tag{3.1}$$

where $X_{sm}$ is a $(1 \times S)$ vector of variables representing the characteristics of the $m^{th}$ choice alternative in choice set s, $\beta$ is an $(S \times 1)$ vector of unknown parameters, and $e_{ism}$ is an error term. The MNL model treats each observation from the same respondent as an independent observation, which falls within the standard random utility approach (Haaijer, 1999). Under this criterion, the MNL model for 400 respondents choosing from 15 choice sets is computationally equivalent to 6,000 respondents choosing from one choice set.

The choice probabilities in the conjoint MNL approach can be obtained by using the straightforward generalization of equation (3.2). The probability that alternative $m$ is chosen from set $s$ is:

$$P_{sm} = \frac{\exp\,(X_{sm}\beta)}{\sum_{n-1}^{M} \exp\,(X_{sm}\beta)} \tag{3.2}$$

The maximum likelihood technique is most suitable to estimate the logit model using data at the individual level. Assuming that choices are available for I individuals, let the choice for the $i^{th}$person be denoted by $\left(y_{i1}, \dots, y_{iS_i}\right)$, where $S_i$ is the choice set of the $i^{th}$ person and each y is equal to 0 or 1, depending on whether the corresponding alternative is chosen or not (Rao, 2013).

Maximum likelihood estimation determines the values of parameters so as to maximize the probability (or likelihood) of matching the observed data. For the $i^{th}$individual with choice set $S = \{1,2, \dots, s_i\}$, the likelihood of observing the choices $\{y_{i1}, \dots, y_{iS_i}\}$ is:

$$L_i = \prod_{s=1}^{S} \prod_{m=1}^{M} P_{sm}^{y_{ism}} \tag{3.3}$$

The joint likelihood for the sample as a whole is $L = \prod_{i=1}^{N} L_i$ . Here, L is a function of the unknown parameters, $\beta$. The $\beta$ values are determined by maximizing $L$ with respect to the $\beta$'s using standard optimization methods. As is common, equation (3.3) is replaced in the formulation by a log function, as in Equation (3.4), which simplifies the optimization process:

$$l = \sum_{i-1}^{I} \sum_{s-1}^{S} \sum_{m-1}^{M} y_{ism} \ln{(p_{sm})} \tag{3.4}$$

Our application used optimization algorithms in XLSTAT (19.4 Version).

## 3.5 Results

### 3.5.1 Model Fitness

The statistical significance test results for choice-based conjoint analysis with the MNL model is presented in Table 3.5. If the p-value is low (defined here as a value less than 0.05), the model is said to be statistically significant. As shown in Table 3.5, with 95% confidence, the p-value of the choice-based conjoint model that drew from 4,254 observations is less than 0.0001, implying that this model is statistically significant.

Table 3.5 Statistical significance test results

| Content | Statistic |
|---|---|
| Observations | 4,254.0 |
| Likelihood value | 484.8 |
| Score | 473.5 |
| Wald | 43.7 |
| p-value | < 0.0001 |

The statistical significance test was also conducted for the four defined impact factors for a multimodal ridesharing system. The p-values for the number of transfers, ridesharing travel time, and ridesharing travel cost are less than 0.0001. The ridesharing incentive factor has a p-value of 0.148, as shown in Table 3.6.

Table 3.6 Statistical significance test results of multimodal ridesharing system attributes

| Attribute | Chi-square (Wald) | Pr > Wald | Chi-square (LR) | Pr > Wald |
|---|---|---|---|---|
| Number of transfers | 305.3 | < 0.0001 | 328.4 | < 0.0001 |
| Ridesharing travel time compared to your current travel time | 25.7 | < 0.0001 | 25.7 | < 0.0001 |
| Ridesharing travel cost compared to your current travel cost | 40.3 | < 0.0001 | 39.8 | < 0.0001 |
| Ridesharing incentive | 3.8 | 0.148 | 3.8 | 0.150 |

### 3.5.2 Conjoint Analysis Results

To analyze the influence of the factors on the choice between alternatives within the multimodal ridesharing system, a numerical part-worth utility value was computed for each level of each attribute. Considering ridesharing travel cost as a quantitative attribute, the estimated parameters for each level of the other three attributes were computed. As shown in Table 3.7, the importance between attributes can be confirmed by the Wald value. Transfer level 3 has the largest Wald value, making it the most important explanatory variable, while ridesharing incentive shows the lowest importance. The reason for the negative estimated coefficient for ridesharing travel cost is that, as travel cost increases, it has a negative effect on the selection. From this table, our results reveal that the fewer the number of transfers, the shorter the travel time, and the more the incentive, the more positive the effect is on the multimodal ridesharing system.

Table 3.7 Statistical impact factor parameter estimates for multimodal ridesharing systems

| **Attribute** | **Level** | **Estimated coefficient** | **Wald Chi-Square** | **Pr > Chi2** |
|---|---|---|---|---|
| Ridesharing travel cost compared to the current travel cost | - | -0.234*** | 28.9 | < 0.0001 |
| Number of transfers | 2 | 0.524*** | 32.9 | < 0.0001 |
| | 3 | 1.511*** | 294.3 | < 0.0001 |
| Ridesharing travel time compared to the current travel time | 2 | 0.194** | 4.9 | 0.026 |
| | 3 | 0.434*** | 25.6 | < 0.0001 |
| Ridesharing incentive | 2 | -0.037 | 0.2 | 0.664 |
| | 3 | 0.152* | 3.1 | 0.077 |

1 * 0.10 level, ** 0.05 level, *** 0.01 level.

### 3.5.3 Willingness to Pay for the Multimodal Ridesharing Service

In economics terms, willingness to pay (WTP) is the amount an individual would be willing to spend to receive a good or to avoid an undesirable outcome. Thus, a transaction occurs when an individual's WTP equals or exceeds an offered price. This principle holds for the participants in the multimodal RSS being studied.

As shown in Table 3.8, the choice-based conjoint model suggests that people are likely to pay USD 2.24 and USD 6.45 when a multimodal RSS provides one transfer and zero transfers, compared to two or more transfers, respectively. This result reveals that a "no transfer" option is the most preferred factor for a multimodal ridesharing system.

Table 3.8 Willingness to pay for each attribute

| Attribute | Level | Willingness to Pay (USD) |
|---|---|---|
| Number of transfers | 2 | 2.24 |
| | 3 | 6.45 |
| Ridesharing travel time compared to the current travel time | 2 | 0.83 |
| | 3 | 1.85 |
| Ridesharing incentive | 2 | -0.16 |
| | 3 | 0.65 |

Based on the WTP values, the second most important factor is ridesharing travel time. The WTP value of each ridesharing travel time level was calculated based on the first level of ridesharing travel time, which is "up to 10 minutes longer travel time compared to the participant's current travel time". For level two and level three of the ridesharing travel time attribute, the participants were more likely to pay USD 0.83 and USD 1.85, respectively.

Compared to the first level of ridesharing incentive, USD 150, participants were willing to pay USD 0.65 when receiving USD 250 as a ridesharing incentive. However, the results indicate that participants are not likely to pay when the incentive is only USD 200. It could be interpreted that the USD 50 variance between ridesharing incentive levels is not significant enough, meaning the p-value of “ridesharing incentive: level 2” in Table 3.7 is not significant. This could be addressed by increasing the variance between incentive levels. It is also possible that our design used incentive levels that were too low. It is, of course, conceivable that a sufficiently high level of monetary incentive would make any option fully attractive, and that we only used conservative amounts in this study. Based on a complete cost–benefit analysis of such RSS options, one can calculate the plausible maximum amounts of incentives and use that in future studies.

In summary, the analysis results validate our hypotheses and behavior expectations that a multimodal ridesharing system with fewer transfers, shorter travel times, and more usage incentives will have a higher level of participation. Based on their willingness to pay, potential users value fewer transfers the most.

## 3.6 Discussion

In this chapter, as a starting point of further research that propose mobility portfolio schemes, we first assessed individual choice behaviors for currently proposed multimodal ridesharing systems (RSS) which are not portfolio-based but have several characteristics of the travel options that will be included in mobility portfolio systems. A web-based survey provided the data to examine the relevant impact factors with conjoint analysis and discrete choice modeling. The results demonstrate the relative magnitude of multimodal RSS’ factors and reveal which factors better encourage the use of such ridesharing systems. The results reinforce the importance and viability of factor estimation modeling, and the significance of the "number of transfers" factor in how people choose to make their trips. Future research can improve the reliability of survey-based factorial analysis by incorporating current multimodal RSS factors, and by developing more specific attitudinal statements to expand latent factor analysis, such as safety factors. Particularly, considering the ongoing impact of COVID-19, users might place more weight on safety while using different ridesharing modes. By conducting further studies, it is expected that insights will be gained regarding the changes in the perception of ridesharing. Improving these models will promote better planning, engineering, and operations in many regions and communities across the United States, which have not yet been well studied regarding the potential of multimodal ridesharing systems.

The research in this chapter yielded insights on user-side acceptance of currently proposed shared mobility options, with an emphasis on the primary factors of significance to user-side choices in using such systems. The chapters thus provided valuable input in developing the comprehensive mobility portfolio model and optimization framework described in the remaining chapters of this dissertation.

# Chapter 4

# New Concept of Travel Modes

## 4.1 Definition of research terms

Advances in the field of transportation, developments in ICT technologies, and the rise of the sharing economy have led to development of the well-known concept of Smart City. In smart cities, people can utilize an integrated shared transportation system which encompass a wide range of seamlessly connected mobility services. In this chapter, we offer a new strategy to model individuals' movements in the system by splitting a travel mode into a combination of travel options originating from what we define as a travel option pool.

People in an integrated shared transportation system need to have the ability to hop among different travel modes freely, making their travel mode a chain of multiple travel modes. Furthermore, we can envision a system where people can provide accessibility to their vehicles by giving temporal ownership to other people. We postulate that these are basic properties that any transportation system of the future would need to have. This also implies that people in such system have more complicated travel modes compared to the discrete modes in traditional systems. Therefore, the travel modes in highly integrated and shared transportation systems of the future need to be modeled differently. To illustrate travel modes that are possible in such systems, we define several novel concepts and research terms in this dissertation.

### 4.1.1 Travel option chain mode

In this dissertation, we firstly define the concept of 'travel option chain (TOC) mode' that is a combination of various travel options which generate from the continuous spectrum of the travel mode option pool. The following explanation shows in more detail why TOC mode is needed.

> In conventional travel analysis, an individual can use a 'car' for his trip. Within the umbrella of shared transportation, a travel mode is a commodity which is not only what one consumes, but also what one can share (e.g., ridesharing driver – drive yourself and sharing empty seat, carsharing, ridesharing rider – not driving your car but riding other's vehicle, etc.). Therefore, in a seamlessly shared transportation system, she can still use a 'car' for a trip, but he/she can also utilize her car while doing ridesharing, carsharing, and so on. So, the travel mode is decided by usage where these travel options come from.

The benefit of modeling trips in a TOC mode is that the current rigid transportation system (with discrete travel mode such as vehicle, public transit, bike, etc.) can be transformed into a more flexible and shareable system for more efficient travel. 'Travel option' is a cross-linkable resource that a person can use that makes up the TOC mode. We consider that each travel option has its own set of characteristics, each with its own properties that we term as "levels." Table 4.1 shows an example of the characteristics of a travel option and its associated levels.

Table 4.1 Characteristics of a Travel Option

| **Characteristics of Travel Option** | **Level** |
|---|---|
| Driving Mode | 0 (Drive yourself) |
| | 1 (Autonomous) |
| | 2 (Not Drive) |
| Number of Connection | 0 (No Transfer) |
| | 1 (Need Transfer) |
| Parking Space | 0 (Need) |
| | 1 (No Need) |
| Willing to use empty seats | 0 (Yes) |
| | 1 (No) |
| Punctuality | 0 (High) |
| | 1 (Low) |
| Travel time | 0 (No Delay) |
| | 1 (Up to 5-min. Delay) |
| | 2 (Up to 10-min. Delay) |
| Public transit | 0 (Not Use) |
| | 1 (Use) |
| Walk | 0 (Not Use) |
| | 1 (Use) |
| Ownership | 0 (Own – Not Share) |
| | 1 (Own – Share) |
| | 2 (Not Own – Share) |
| Vehicle type | 0 (Luxury) |
| | 1 (SUV) |
| | 2 (Sedan) |
| | … |
| | N -2 (Bus) |
| | N-1 (Metro) |
| | N (Walk) |
| | … |
| … | … |

Having defined the characteristics and levels of a mode, various TOC modes can now be described.

We denote the term $X(y)$ to represent a travel option $X$ and its level $y$. For example, an SUV solo driver can be illustrated by combining ‘driving mode (0)’, ‘willing to use empty seats (1)’, and vehicle type (1). Similarly, a sedan ridesharing driver can be described as a combination of ‘driver mode (0)’, ‘willing to use empty seats (0)’, and ‘vehicle type (2)’. In the same vein, a ridesharing rider mode can be captured by combining ‘driving mode (2)’, ‘willing to use empty seats (0)’ and ‘vehicle type ($\alpha$)’. It is worth mentioning here that a vehicle type for ridesharing riders is dependent on served drivers’ vehicle type. Thus, we illustrate ridesharing riders’ vehicle type as $\alpha$.

For a more nuanced analysis, we categorize a travel mode’s characteristics into three groups: travel efficiency (default), travel convenience, and travel sustainability. Each group contains different travel mode options. Travel efficiency group contains travel time, parking hours, parking space, walking time, waiting time, punctuality and so on. In terms of traveling convenience, drive-yourself, number of transfers, and Wi-Fi availability could be potential characteristics. Finally, fraction of seats used, fraction of personal vehicle operational time used, and public transit usage could be considered as sustainability factors.

### 4.1.2 Travel mode option pool

‘Travel mode option pool’ is a set of travel options which is available for a user’s entire trip. The travel option pool comprises various kinds of travel options with their defined characteristics, so that various TOC modes can be generated from a continuous spectrum by combining any travel options. The major advantage of defining the mode option pool is flexibility. Depending on the number of travel option groups and travel options in each group, the travel mode option pool can create an endless variety of TOC modes. Therefore, any time a new kind of mobility service is introduced in the future (such as autonomous vehicle (AV) or AV fleet), our proposed model can seamlessly incorporate it in its formulation by simply adding that service's characteristics into the pool.

### 4.1.3 Mobility Portfolio

As described earlier, a Mobility Portfolio is a grouping of the number of hours/cost/resources that can be spent on each distinct travel options, so as to fit within a time/cost/resource constraint specified for a given time period. Mobility portfolio is a key contribution of this dissertation. The portfolio approach compartmentalizes the travel options that are chained, models them as consumable travel commodities and resources, and, finally, includes appropriate quantities of them with their own prices that determine the payment the users make for purchasing the portfolio. The portfolio scheme incorporates pricing for the commodities and is expected to bring in efficiency and cost savings while increasing shared mobility participation, because a lot more travel options can then be paid for and combined for multi-modal travel. Existing literature and various case studies have shown it to be a promising approach for promoting beneficial changes in travel behavior. The mobility portfolio framework subsumes currently envisaged ideas such as MaaS mobility bundles in a smart and shared mobility system with subscription options.

As the development of the portfolio scheme is intricately connected to the platform built to study it, the agent-based study platform itself is described first in the chapter, as that makes the conceptual explanations in the remainder of the chapter easier.

## 4.2 Conceptual Simulation Platform for Mobility Portfolio

The main idea underlying mobility portfolios is that all travel options are available and by paying for an option people can receive temporal ownership of it. In order to materialize the mobility portfolio, various agents such as the transportation network, payment system, and ridesharing system are required to cooperate. Using agent-based modeling techniques, we build a simulation platform to illustrate how our proposed concepts of travel mode and the mobility portfolio can be deployed in practice.

### 4.2.1 Agent-based modeling

An agent-based model (ABM) is a technique to simulate various agents and analyze the interaction between these agents. In the context of agent-based transportation modeling, agents refer to any autonomous entities within a system. At the individual level, an agent can be a traveler, such as private driver, or a truck driver. At the collective level, examples of agents are traffic operators, adaptive traffic control devices, shippers, and public agencies (which are themselves composed of agents such as urban planners, committee members, and elected officials), consultants, and connected/autonomous vehicles. In this dissertation we design a multi-agent, shared and automated transportation system using a simulation framework with three agent groups: a transportation network agent, a mobility portfolio agent, and a peer-to-peer ridesharing agent. This platform can incorporate any number of additional agents as long as their properties can be mathematically described. Examples include network traffic control agents, fare control agents, etc. Figure 4.1 illustrates the overview of the proposed agent-based conceptual mobility portfolio platform.

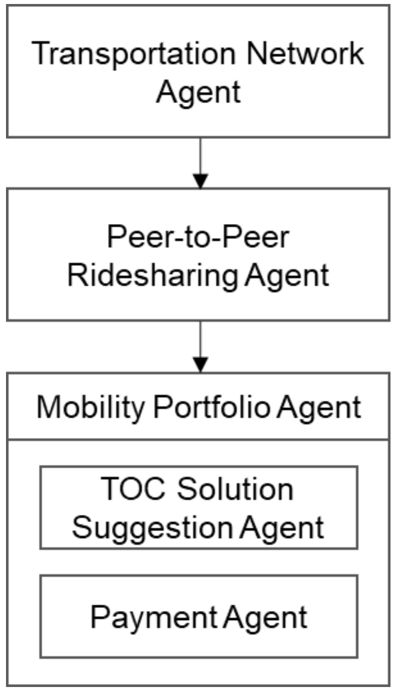

Figure 4.1 Overview of the conceptual mobility portfolio platform

### 4.2.2 Transportation Network Agent

The main purpose of this dissertation is to provide a framework for a single transportation platform which can operate different types of transportation services. Connecting various transportation modes and aggregating those modes into one single platform is necessary to attract people from a convenience and sustainability perspective. From this point of view, we construct a conceptual transportation simulation platform which integrates multimodal shared transportation system which contains vehicle, bus, walking, and shared travel modes such as a ridesharing mode and shared autonomous fleet vehicles (SAFVs).

In the real world, some transportation services share a vehicle network, but other modes such as metro, rails and walking share a physically separate network, which is not part of the vehicle network. Due to this physical division, the travel time of users passing through each network needs to be measured differently. With this in mind, we proposed a multi-layered transportation system in our previous research (Nam et al., 2018). We build two distinct travel layers, depending on the property of transportation mobility providers: (a) vehicle network; and (b) transit network. As shown in Figure 4.2, each layer includes several sub-layers. Note that the planar layers in this figure are only representing the spatial network. The underlying model and optimization include a time-expanded form of each layer for time-space ride-matching that is explained subsequently.

The base layer for the network is a vehicle network because the primary travel option of a significant proportion of system participants is private vehicles. It is important to compose the analytical network as a real vehicle network for depicting realistic vehicle movements. The critical challenge in building this base layer, however, is that a high resolution for the network causes computational complexities.

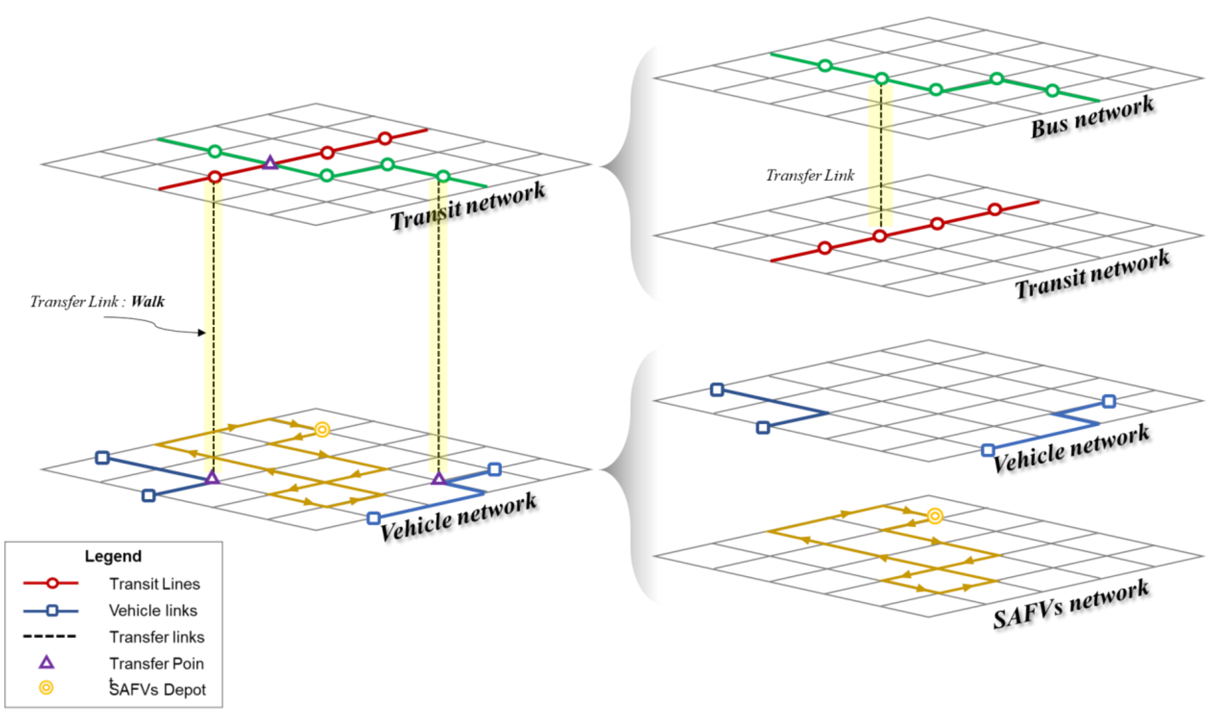


Figure 4.2 Multilayered Transportation Network Overview

Thus, we perform our analysis on an abstraction of the real network and define the new nodes as "go-points." Without any loss of generality, we assume that all trips originate and terminate at the go-points (Masoud and Jayakrishnan, 2017a).

AV and AV fleets may help reduce car-ownership and congestion. However, to accomplish this task, a tremendous number of autonomous vehicles would be needed. Additionally, from a policy perspective, it is currently infeasible to shift all private vehicle demand to shared autonomous fleet vehicle demand because, in reality, a lot of people may still depend on their current primary travel mode (which is a private vehicle) and may not want to relinquish ownership.

The shared autonomous fleet vehicle network is designed for a system with the key locations being vehicle depots. In this sub-layer, we assume that SAFVs have the same features as in the vehicle network, which allows us to consider every go-point in the vehicle network as an intermediate node and so that nearby intermediate nodes from depots in the SAFVs network can be connected. It is worth mentioning that this dissertation considers SAFVs as one of shared mobility options in order to portray a near-future transportation system more realistically, instead of changing all individuals' personal vehicles to autonomous vehicles instantly.

To avoid confusion between go-points in the vehicle layer and the nodes in other layers, here we refer to the nodes in transit and autonomous fleet vehicle networks as "station". In the transit network, buses share network links with vehicles, unlike metro rails which are grade separated from the vehicle network. The difference between buses and private vehicles is that buses follow their own schedule and run only on designated routes. We make a reasonable assumption that the time the bus arrives at the stop is always the same, so that its travel time is not affected by traffic congestion. Thus, we load buses and metro rail onto the transit network layer, which consists of stations and timetables.

The primary assumption in the design of our proposed multi-layer network is that each travel mode cannot utilize other travel mode networks. Thus, we generate transfer links to connect each layer and designate walking as the travel mode for this link.

By introducing the multi-layer networks and go-points and stations, we build a time-expanded network for each layer. The network includes nodes which has both time and location aspects. In addition, we discretize the study time span into a set of indexed time intervals of a small duration, $\Delta t$, expected to be 5 minutes or less (we use 1 minutes) so that time-dependent travel time matrices can be used for analysis. In this network, each node $n_i$ is considered as a tuple $(t_i, s_i)$, where $t_i$ is the time interval during which a user may be located at station $s_i$. In turn, a link can be represented as a tuple $(n_i, n_j) = (t_i, s_i, t_j, s_j)$ (Masoud and Jayakrishnan (2017a)). One of the advantages of this network is that it can intuitively model a waiting movement. Let us suppose that there is a rider who is waiting for another driver who can pick and drop her off to her destination or there is a shared-ride driver who is waiting for another rider who has not yet arrived at a pick-up point. In such cases, their waiting movements can be illustrated as a time-space link that is $(t_i, s_i, t_j, s_j)$ = (1,1,2,1). This means that during one time interval she stays at the station (or go-point) 1. More details of the ride-matching optimization for individual driver on the time-expanded multi-layer networks is given in chapter 5.

In such an integrated shared mobility system and the network structure, the proposed P2P ridesharing service helps a user (i.e., riders) experience a chain of travel modes according to their convenience.

### 4.2.3 Mobility Portfolio Agent

In the proposed shared and automated transportation system, a mobility portfolio agent is a subscription-based service provider that connects the system users and the agents in the system via smartphone applications. The mobility portfolio agent can show available TOC modes that the users can use depending on their system participation status and provide them with a payment system. This allows subscribers to easily use the suggested TOC mode from the mobility portfolio agent. To achieve these tasks, we define three classes of mobility portfolio sub-agents: a mobility portfolio bundle design agent, a solution suggestion agent, and a payment agent.

#### (1) Mobility Portfolio Bundle Design Agent

The travel options in the shared and automated transportation system vary considerably (Table 4.1). Due to a variety of travel options, a large number of TOC modes can be generated, and the system participants enter the system with their own TOC modes in mobility portfolios. However, when people actually participate in the system with a mode determined by them, it is intractable to execute the p2p ridematching process taking all these characteristics into account. Furthermore, people may not use pre-determined TOC modes if no feasible matched partners exist. Note that TOC modes are highly dependent on system participation status (i.e., such as a mobility service provider and/or a receiver). More specifically, once users enter the system with their own participation status, TOC modes are defined as the outputs from the p2p ridematching process. Thus, we introduce a bundle design agent for the mobility portfolio. In this agent, we firstly define the system participants' available travel status. Travel status can be classified in various ways. For example, we can set different travel status depending on the mobility service type such as p2p carsharing providers, public transit users, shared-bike users, p2p shared-ride drivers, p2p shared-ride riders, and so on. It is also possible to group the travel status according to the properties or status of the shared-mobility providers and shared-mobility receivers. Furthermore, even we can include a not-engage-in-shared-mobility status which is a reasonable option for many users in various circumstances. Henceforth, in this dissertation, we define that there are three bundle options in mobility portfolios: a shared-ride provider (i.e., shared-ride driver), a shared-ride user (i.e., shared-ride rider), and a solo-driver.

### (2) Mobility Portfolio Solution Suggestion Agent

Once people enter the system with a travel status from the mobility portfolio bundle, their TOC modes are assigned according to the results from the p2p ridematching process. At this time, people may have various options. For instance, let assume that a person joins the system as a shared-mobility rider. In this platform, he/she requests shared-mobility rides for the trip, and after completing the p2p ridematching process there are 10 feasible TOC modes with different shared-mobility provider sets. In this scenario, this rider needs to compare the cost and benefits between the proposed TOC modes. In addition, it is possible that riders have more than 10 feasible TOC modes if there are plenty of shared-mobility providers who can serve these travel itineraries, and riders have to compare all possible TOC modes manually. Too many choices may cause unnecessary user fatigue and makes the system unattractive. To reduce such fatigue, the mobility portfolio aims to provide the best TOC solution to the users. This dissertation assumes that once the users receive their travel option from the portfolio, they use it without hesitation.

(3) Payment Agent

In the mobility portfolio, each travel option in the system has designated cost. In the consideration of the vehicle cost, TOC mode's price is set in proportion to travel distance. This price can be used as a metric that the suggestion agent considers when making decisions between available TOC modes. Through the smartphone payment system, the mobility portfolio subscriber can easily book the recommended TOC modes.

### 4.2.4 Peer-to-Peer Ridematching Agent

The peer-to-peer ridesharting system is an essential concept through this dissertation, because it is the most comprehensive and relaxed type of ridesharing systems. In this system, people can join the system as either mobility providers or receivers and shift their travel status at any times. This implies that people utilize mobility services not only as service users, but also provide themselves with their vehicles as shared-ride drivers or carsharing providers. By allowing people to easily shift their travel status, we can provide more opportunities people to get matched. In other works, if we divide people into a rider and a driver groups and match, there are people who keep being matched, while there are people who don't have the change to get matched at all.

Moreover, another benefit of the peer-to-peer ridesharing mechanism is that it is flexible to collaborate with a multimodal transportation system that include various mobility services such as shared-ride providers, bike, scooter, walk, public transit and even shared autonomous fleet vehicle;

and it can easily link mobility services providers and service users. Thus, this problem can be solved by formulating a peer-to-peer (p2p) ridematching problem of matching paths in the time-expanded multimodal network.

The goal of the p2p ridesharing agent is to match system participants as much as possible in real-time so that people can instantly begin their trip with their matched partners. In this context, Masoud and Jayakrishnan (2021a) mathematically formulated a real-time p2p ridematching problem of matching paths and solve it with a dynamic programming approach. One of the assumptions they made is that origin and destination are fixed. Variables $OS_r$, $OS_d$, $DS_r$, and $DS_d$ represent origin and destination go-points for both riders and drivers, respectively. Another assumption in the formulation is that each participant's early departure time from origin and late arrival time to destination are randomly generated. Equation (4.5) shows the original ridematching problem formulation. In their study, four binary decision variables have been set in equation (4.1)-(4.4), and using these variables the ridematching problem as shown in equation (4.5).

$$x_l^d = \begin{cases} 1 & Driver\ d\ travels\ on\ link\ l \\ 0 & Otherwise \end{cases} \tag{4.1}$$

$$y_l^{rd} = \begin{cases} 1 & Rider\ r\ travels\ on\ link\ l\ with\ driver\ d \\ 0 & Otherwise \end{cases} \tag{4.2}$$

$$z_r = \begin{cases} 1 & Rider\ r\ is\ matched \\ 0 & Otherwise \end{cases} \tag{4.3}$$

$$u_r^d = \begin{cases} 1 & Driver\ d\ contributes\ to\ the\ itinerary\ for\ rider\ r \\ 0 & Otherwise \end{cases} \tag{4.4}$$

Constraints set (4.5b)-(4.5d) represent drivers' route and (4.5e) ensures the flow conservation of drivers. Constraints set (4.5f)-(4.5h) represent the riders' route that is associated with drivers who serve a rider from his origin to destination.

$$\text{Max} \sum_{r\in R} z_r - \sum_{r\in R} W_r \sum_{d\in D} u_r^d \tag{4.5a}$$

$$\sum_{\substack{l\in L:\\ s_i=OS_d(t_i,t_j)\in T_D}} x_l^d - \sum_{\substack{l\in L:\\ s_j=OS_d(t_i,t_j)\in T_D}} x_l^d = 1 \qquad \forall\, d\ \in D \tag{4.5b}$$

$$\sum_{\substack{l\in L:\\ s_j=DS_d(t_i,t_j)\in T_D}} x_l^d - \sum_{\substack{l\in L:\\ s_i=DS_d(t_i,t_j)\in T_D}} x_l^d = 1 \qquad \forall\, d\ \in D \tag{4.5c}$$

$$\sum_{\substack{t_i,s_i\\ l=(t_i,s_i,t,s)\in L}} x_l^d = \sum_{\substack{t_i,s_i\\ l=(t,s,t_j,s_j)\in L}} x_l^d \qquad \begin{array}{l}\forall\, d\ \in D\\ \forall\, t \in T_d\\ \forall\, s \in S\backslash\{OS_d \cup DS\_d\}\end{array} \tag{4.5d}$$

$$\sum_{l\in L}(t_j - t_i)x_l^d \le \frac{T_d^{TB}}{\Delta t} \qquad \forall\, d\ \in D \tag{4.5e}$$

$$\sum_{d\in D'} \sum_{\substack{l\in L:\\ s_i=OS_r(t_i,t_j)\in T_r}} y_l^{rd} - \sum_{d\in D'} \sum_{\substack{l\in L:\\ s_j=OS_r(t_i,t_j)\in T_r}} y_l^{rd} = z_r \qquad \forall\, r\ \in \mathrm{R} \tag{4.5f}$$

$$\sum_{d\in D'} \sum_{\substack{l\in L:\\ s_j=DS_r(t_i,t_j)\in T_r}} y_l^{rd} - \sum_{d\in D'} \sum_{\substack{l\in L:\\ s_j=DS_r(t_i,t_j)\in T_r}} y_l^{rd} = z_r \qquad \forall\, r\ \in \mathrm{R} \tag{4.5g}$$

$$\sum_{d\in D'} \sum_{\substack{t_i,s_i\\ l=(t_i,s_i,t,s)\in L}} y_l^{rd} = \sum_{d\in D'} \sum_{\substack{t_i,s_i\\ l=(t,s,t_j,s_j)\in L}} y_l^{rd} \qquad \begin{array}{l}\forall\, r\ \in R\\ \forall\, t \in \mathrm{T_r}\\ \forall\, s \in S\backslash\{OS_r \cup DS\_r\}\end{array} \tag{4.5h}$$

$$\sum_{d\in D'} \sum_{l\in L}(t_j - t_i)y_l^{rd} \le \frac{T_r^{TB}}{\Delta t} \qquad \forall\, r\ \in R \tag{4.5i}$$

$$\sum_{r\in R} y_l^{rd} \le C_d x_l^d \qquad \begin{array}{l}\forall\, d\ \in D\\ \forall\, l\ \in L\end{array} \tag{4.5j}$$

$$u_r^d \ge y_l^{rd} \qquad \begin{array}{l}\forall\, r\ \in R\\ \forall\, d \in D\\ \forall\, l \in L\end{array} \tag{4.5k}$$

$$u_r^d \leq \sum_{l \in L} y_l^{rd} \qquad \forall\, r \in R \quad \forall\, d \in D \tag{4.5l}$$

$$\sum_{d \in D} u_r^d - 1 \leq V_r \qquad \forall\, r \in R \tag{4.5m}$$

Constraint set (4.5f) ensure the flow conservation of riders who are successfully matched with drivers. Constraint set (4.5e) and (4.5i) limit the total travel time for both drivers and riders, respectively. Constraint set (4.5j) ensures that the total number of riders that drivers can serve cannot exceed drivers' vehicle capacity. Constraint sets (4.5k) and (4.5l) register drivers who contribute to each rider's itinerary. Constraint set (4.5m) restricts the number of transfers by each rider. The output of the p2p ridematching results is the maximum number of served riders by providing a minimum travel time itinerary using a dynamic programming approach.

In our formulation, we modified the original ridematching problem to account for the extended mobility service providers. Instead of using the driver decision variable, $x_l^d$, we re-define it as shown in equation (4.6). Variable, $d_v$, denotes a vehicle type $v$ that assigned to driver $d$. By doing so, we can now consider heterogenous vehicle types for not only vehicle, public transit, walk but also various vehicle models such SUVs, electric vehicle, 2-seat door vehicle, autonomous vehicle, and so on. It makes possible to set different prices according to vehicle types. We also set a cost variable, $e^{d_v}$, as a designated price for each vehicle type, which allows us to calculate the minimum cost travel time path for riders with their associated shared mobility providers. Note that in the p2p ridesharing agent, we aim to solve the ridematching problem that aims to find the optimal solutions for riders. This is because in the practical standpoint, once people register themselves as a shared-ride drivers in the mobility portfolio system, they cannot find a rider who can optimize their path because firstly they do not know which other riders will have them in eligible set to even optimize. Driver-side optimization is not practical. However, for all riders, once they ask for a ride, they have a can to select a group of drivers who can optimize their path. Thus, in the problem of finding a path for all system participants, the optimization is done for all riders.

$$x_l^{d_v} = \begin{cases} 1 & Vehicle\ v\ that\ is\ assigned\ to\ Driver\ d\ travels\ on\ link\ l \\ 0 & Otherwise \end{cases} \tag{4.6}$$

In the p2p ridematching agent, even though we are focusing on riders' side optimality, the outputs from this agent will a travel itinerary for all system participants with associated cost. This will be explained in the next chapter. In practice, however, the optimization will be done in real-time, for individual riders, to select the best possible drivers for them.

There are certain implications in how the above optimization is used individually in real-time. First of all, it will naturally have to be based on the individual's objectives and not any system objectives such as overall costs or matching ratio. Emphasizing the individual's objective is important, as user-level trust on the system and the app, and their compliance will require the optimization to be done from their standpoint. Just as in the case of "system optimum" and "user equilibrium" in traditional transportation planning, the system objectives may cause some users to be provided solutions that are not best for themselves, and this can lead to lack of trust in the system. Thus user-side objective such as minimum travel time cost and payment are needed. However the collective system performance with individual (distributed) optimizations does become socially beneficial with increased sharing of resources and reduced system costs, in general, as our results will show.

It is perhaps even more important to describe that the above optimization is performed only for riders (who pay for the rides through utilization of their paid portfolio "minutes"). This implies that the drivers' apps are not assumed to optimize from their standpoint. This assumption is based on practicality. The mobility agency (or the portfolio seller) cannot ask any rider, who pays, to select an option that involves higher payment than their best option in terms of the drivers available. However, the drivers who are receiving payment (and thus positive utility from offering the ride) can be asked to offer the service to a rider who is not the best from their standpoint and gives less payment than another rider. That is, they cannot be allowed to select a rider who is best from that driver's standpoint – which may result in the rider getting a suboptimal solution, which cannot be imposed on a "payer". For this reason, the implementation of the above optimization formulation and solution scheme explained in the next chapter are only for riders. The drivers are assumed to offer the service if they get a payment. It is possible and not too challenging to introduce a minimum payment required for any driver to offer the service, but this has not been attempted in this dissertation research.

## 4.3 Discussion

In this chapter, we discussed the limitations of traditional trip modeling when applied to integrated and shareable transportation systems. This led to our concept of travel mode pool to describe the seamless chaining of various travel modes with different characteristics that are more appropriate for these systems. We then describe a conceptual platform based on agent-based modeling techniques to operate different entities that compose the shared and automated transportation system. In the platform, there are three main elements which are the multi-layered network design:

the p2p ridesharing system, and mobility portfolio with the sub-agents that allow users to hop between various travel modes. A mathematical formulation of the transformed ride-matching problem, which serves as an input to the mobility portfolio agents, is provided.

# Chapter 5

# Mobility Portfolio Framework

## 5.1 Overview

The primary role of the mobility portfolio is to serve mobility plans to system users. Mobility plans that are cost-effective can motivate travelers to yield their current travel mode and increase their participation in this shared transportation system. This phenomenon can create network effects in that additional users make the system more efficient in terms of vehicle usage, leading to reduced private vehicle ownership, and consequently, lower overall levels of traffic congestion and emissions. Therefore, the design of mobility portfolios is of utmost importance.

This chapter presents an overview of the framework employed in this book to model an individual level mobility portfolio problem, followed by its various mathematical formulations. The modeling framework in this chapter takes into account every participant's travel itinerary, travel cost, updated travel time perception, and travel status choice dynamics for every decision phase during the mobility portfolio period to eventually provide a mobility portfolio solution. Figure 5.1 shows the different modules and processes that undergird the proposed framework. We describe them in more detail in the following section.

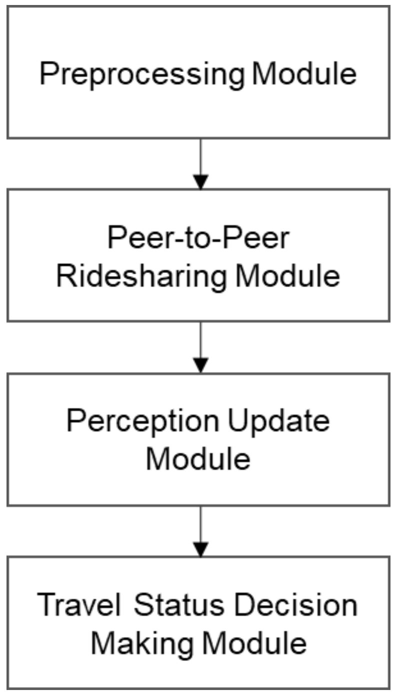


Figure 5.1 Mobility Portfolio Framework

## 5.2 Model Components

The purpose of the mobility portfolio usage plan is to provide a solution, i.e., a set of TOC modes to use at various phases during the mobility portfolio period. As TOC modes are related to travel status, the mobility portfolio subscribers have to decide which travel status to choose at every decision phase within that time frame. In order to explain travel status choice dynamics over time, it is necessary to explicitly model the system participants' perception of travel time and how this perception changes dynamically. Thus, the modeling framework contains the following components: (a) preprocessing module, (b) p2p ridesharing module, (c) perception update module, and (d) travel status decision making module. This section provides a description of these modules in the broad context of mobility portfolio problems.

### 5.2.1 Preprocessing module

The role of this module is to limit the size of the accessible network for the system participants. This is necessary to reduce the p2p ridematching computational time. Masoud and Jayakrishnan (2017a) proposed an Ellipsoid Spatio-Temporal Accessibility Method (ESTAM) that reduces the size of the original time-expanded network for each system user, considering reachable spatiotemporal links within their respective travel time windows. In the preliminary phase of framework, we applied the ESTAM method on a abstract network. The algorithmic details can be found at Masoud and Jayakrishnan (2017a). Mobility services such as metro and buses follow their assigned schedule and routes. Thus, drivers for public mobility services travel on a route-based time-expanded network. Notes that transfer and wait movements do not require any specific vehicles, since we assume that users walk to transfer between stations and wait there, if required. To model this behavior, we set a dummy driver, $d'$, as a vehicle for both walking and waiting movements. One important aspect of dummy drivers is that they can exit anytime. Thus, dummy drivers have access to the entire time spanned spatial network and are not limited by the constraints of spatial reachability.

### 5.2.2 P2P Ridesharing module

In this module, the p2p ridematching problem described in the previous chapter is modeled and solved using a multi-layered time-expanded network. The output of the p2p ridematching problem in the previously described method is the total number of matched riders. However, the outputs of the model in this dissertation are travel itineraries with costs for all system participants (including not only matched riders and drivers, but also unmatched riders and solo drivers) and their TOC modes with vehicle types. Except for riders who are matched with other drivers, all participants are considered to be matched with themselves, so that vehicle types for their trips are the same as the ones they would normally use.

We denote $S_i$ as the set of travel itineraries for participant $i$, and $\ell_n$ to be the $n^{th}$ sequence of links that composes the travel itinerary, $\{\ell_1, \ell_2, \dots, \ell_n\} \in S_i$. Note that link $\ell = (t_j, s_j, t_k, s_k)$ is now spatiotemporal in nature and contains information about the link start-node arrival time and link end-node departure time. The term $\ell_n^{d_v}$ denotes a matched driver with vehicle type for link $\ell_n$. The cost variable $e^{d_v}$, defined in chapter 4.2.4, is used to calculate travel cost. The notations of p2p ridesharing module are similar to the model described earlier, which we extend in order to incorporate potentially new mobility service,

### 5.2.3 Perception Update Module

There are two sub-modules within this module: a travel time perception update module and a travel cost perception module.

Within the mobility portfolio framework, people need to choose to shared-ride drivers, riders, or solo driver for their next decision phase. Their decision is closely related to their travel time, since vehicle costs for its type have already been fixed at this stage. Our developed agent-based simulation platform gathers all system participants travel information, such as travel time, departure time and other trip information. The platform is also able to provide information about system performance, which, combined with their experience during their current decision phase, can be used by participants to update their travel time for the next decision phase. Updated perception of travel time and the change in perception during the mobility portfolio period will be major inputs for the next module.

It is worth mentioning that the network performance is heavily dependent on the number of the matched riders, which, in turn, is closely related to the number of potential shared-ride drivers. This is because more matched riders lead to less loaded vehicles on transportation networks. The network performance can be measured only after the matching process, which means that the system users who start their journey with an expected travel time in their perception, may experience different travel times when they actually travel on the network. To obtain the experienced travel times, we use NeXTA/DTALite (Zhou and Taylor, 2014), a mesoscopic simulation for dynamic traffic analysis. The mesoscopic model allows us to obtain a vehicle's trajectory, without incurring the computation costs of microsimulation models.

There are various studies that focus on updating the perceived travel time by users (Jha et al., 1998; Zhang et al., 2014; Lin and Yang, 2019). The broad class of simulation-based day-to-day learning methods is considered a well-known approach for modeling perception updates. Bayesian inference is also considered a useful statistical method that uses Bayes' theorem to update hypothesis probabilities as more information becomes available. The method usually involves two aspects: expected information and experienced information. These data of travel time between same origin-destination (OD) pairs can be easily updated using traffic network information and historical perception of travel time between same origin-destination (OD) pairs. In Zhang et al.

(2014) and Jha et al. (1998) collect traffic network information with the help of transportation simulation models, then combine the information and drivers' historical perceptions to update perception on routes. However, these studies focus on one particular traveler group for travel choice model. For instance, Zhang et al. (2014) uses the updated travel time to estimate travel routes and using the updated data when drivers choose their route and departure time. Unlike in previous studies, the travel status decision-making module in this dissertation is executed across the entire system. In addition, our framework makes a more realistic assumption that system participants have different matching experiences, which means that even though people may enter the system as a shared-ride riders, some of them may not find a match. We assume that unmatched riders would need to drive themselves on their privately-owned vehicles.

Thus, in this dissertation, we firstly separate people who travel on same OD pairs and then calculate the expected travel time using a Bayesian inference model with accumulated experienced travel time data and real travel time data from NeXTA/DTALite simulation model with their current decision phase travel status. With this updated travel time, we can estimate expected travel costs for each travel status for people who have the same origin and destination. The first step of the cost estimation is to develop a payoff table method which can illustrate potential profits for each item, based upon the characteristics of the ridesharing environment. Using this method, expected payoffs, or expected travel cost values in other words, of travel status can be calculated by multiplying travel costs in a perfect information scenario by the probability of the matching success.

Thus, in this dissertation, we firstly separate people who travel on same OD pairs and then calculate expected travel time using Bayesian inference model with accumulated experienced travel time data and real travel time data from NeXTA/DTALite simulation model with their current decision phase travel status. With this updated travel time, we can estimate expected travel costs for each travel status for people who have the same origin and destination by multiplying the current experienced average travel cost. In this context, we apply a payoff table method which can illustrate potential profits for each item, based upon the characteristics of the ridesharing environment. Using this method, expected payoffs, or expected travel cost values in other words, of travel status can be calculated by multiplying travel costs in a perfect information scenario by the probability of the matching success.

### 5.2.4 Travel Status Decision Making Module for Portfolio Usage Plan

The expected travel costs for each travel status from the previous module can be directly used to make travel status choices for the next decision phase within the mobility portfolio period. A key aspect of the mobility portfolio framework is that system participants' sequential decision making within the period can be updated during successive iterations. This is intended to simulate a person's decision-making processes in that an individual user's travel status decision choice is influenced by not only their previous decision phase experience but also the experiences of the same decision phase during previous iterations. The Ant Colony optimization (ACO) algorithm, a popular metaheuristic algorithm, has the capability to mathematically incorporate these two learning phases. Thus, we adopt a ACO algorithm with some modifications, and apply it to the mobility portfolio problem. The details of the algorithm are described in section 6.3.

## 5.3 Mobility Portfolio Problem

### 5.3.1 Mathematical Formulation

We formulate the mobility portfolio problem mathematically with the objective of maximizing savings for each individual. To that effect, we define a decision variable as follows:

$$h_\ell^{id} = \begin{cases} 1 & if\ driver\ d\ travels\ on\ link\ \ell\ contributes\ to\ on\ traveler\ i\ itinerary \\ 0 & otherwise \end{cases} \tag{5.1}$$

$$g_\ell^{ir} = \begin{cases} 1 & if\ traveler\ i\ travels\ on\ link\ \ell\ with\ rider\ person\ r \\ 0 & otherwise \end{cases} \tag{5.2}$$

The objective function, representing individual's savings is described in equation (5.3)

$$max\ s_i \tag{5.3}$$

We set variable $s_i$ to represent user $i$'s travel cost savings. The travel cost savings can be calculated using the following equation:

$$s_i = \sum_n^N (Z_i - c_{i,n}) \tag{5.4}$$

We set variable $Z_i$ to represent user $i$'s total travel expenditures with primary travel mode (which is a private vehicle), and it can be calculated in equation (5.5). Variable $e^{d_v}$ represents the unit cost of vehicle type $d_v$, and variable $\bar{t}_i$ shows the average value of the minimum and maximum travel times that can be traveled from origin to destination within the time window.

$$Z_i = e^{d_v} \cdot \bar{t}_i \tag{5.5}$$

Variable $c_{i,n}$ to represent the travel cost for individual $i$ at the $n^{th}$ decision phase within the portfolio period. Note that $|N|$ represents the length of mobility portfolio period, and $I$ represents the set of all system participants regardless of their travel status, so that $I = \{D \cup R \cup SO\}$ where $D, R,$ and $SO$ represent the group of people who enter the system as drivers, riders, and solo drivers, respectively.

The travel cost for each individual can be calculated after the ridematching results. Equation (5.6) represents the travel cost calculation considering a set of links that contribute to a user's itinerary.

$$c_{i,n} = \begin{array}{l} \displaystyle\sum_{\ell=(t_j,s_j,t_k,s_k)\in L} \sum_{d\in A} t_{i,\ell}^{d} \cdot e^{d_v} \cdot h_{\ell}^{id} \cdot \delta \cdot \theta \\ \displaystyle + \sum_{\ell=(t_j,s_j,t_k,s_k)\in L} t_{i,\ell}^{d} \cdot e^{i_v} \cdot g_{\ell}^{ir} \cdot \delta \cdot (1-\theta) \end{array} \qquad \begin{array}{l} \forall\, d \in A \\ \forall\, r \in R \end{array} \tag{5.6}$$

where,

$$\theta = \begin{cases} 1 & if\ traveler\ i\ is\ rider \\ 0 & otherwise \end{cases}$$

$$\delta = \begin{cases} 1 & if\ person\ i\ travels\ alone \\ \alpha & incentive\ ratio\ if\ person\ i\ is\ a\ rider\ and\ pay\ to\ driver\ d \\ (1-\alpha) & incentive\ ratio\ if\ person\ i\ is\ a\ driver, and\ receive\ from\ rider\ r \end{cases}$$

The first term in equation (5.6) indicates riders' travel cost and the second term shows drivers' travel cost after the ridematching process, respectively. The travel time variable, $t_{i,\ell}^{d}$, represents user $i$'s link $\ell$ travel time with driver $d$. Note that except for matched riders, individual $i$ and driver $d$ are the same. This means that, from a modeling standpoint, a driver and a rider are considered the same agent. To account for all mobility service providers such as public transit services, $T$, and dummy drivers, $D'$, we define the set of mobility providers as $A = \{D \cup T \cup D'\}$. Variable $\delta$ represents ride-match benefits. For instance, if a person $i$ does not matched whether she is a rider or a driver, she has to drive herself without incentives, and thus $\delta$ become 1; and $\alpha$ is an incentive ratio that riders have to pay their matched drivers which is negotiated.

$$\sum_{n=1}^{N} t_i^{d_v} \leq CR_{d_v}^{max} \tag{5.7}$$

Equation (5.7) is related to the mobility portfolio scheme. This equation ensures that the amount of used travel time on a driver's vehicle type $d_v$ must not exceed the maximum travel time credit allowable for it. Putting restrictions on vehicle time usage can be seen as similar to placing restrictions on travel options provided by the mobility portfolio framework. For instance, if a shared-ride driver's travel itinerary is composed of a set of links, $(\ell_1, \ell_2, \ell_3)$, and he shares link $\ell_2$ with a rider, then, his travel mode can be a set of TOC modes as follows: ('drive-alone & drive yourself', 'drive yourself & share empty seat', 'drive-alone & drive yourself'). His travel mode is composed of three travel options: drive-alone, drive yourself, and share empty seat, with his vehicle type for each option being his private vehicle. Thus, the travel time incurred by vehicle types is equivalent to the travel time for travel options. The same logic applies to shared-ride riders as well. Equation (5.7) represents a constraint that prevents participants from abusing a certain type of travel option and induces them to use other travel options. When some amount of maximum travel time credit on travel options is given, this mathematical formulation leads to the optimal solution.

### 5.3.2 Problem Variants – Multimodal Transportation System Expansion

#### (1) Shared Autonomous Fleet Vehicle

While hewing to the structure of mobility portfolio problem, various problem environments can be created by expanding the ridematching formulation described in model (5.5) to include various system characteristics. In this section, we review how incremental changes to the formulation allow us to model different current and future ridesharing scenarios.

The travel option pool in model (5.5) contains shard-ride drivers and public transit. The travel option pool that is utilized in this dissertation is expanded by incorporating autonomous vehicles in shared fleet systems. Even though autonomous vehicles by definition do not actually have a driver, for modeling purposes, we assume that there is a virtual driver $sd$. The set of mobility providers, $A$, is also expanded to become $A = \{D \cup T \cup SD \cup D'\}$. Shared autonomous fleet vehicles (SAFVs) travel routes depend on the passengers origin and destination stations, with depots, $o_{sd}$, representing their initial trip origin stations. The route for an SAFVs is a sequence of partial destinations which indicates pick-up and drop-off points of passengers. Thus, we modify constraint set (5.5b)-(5.5c) to consider the routes of the fleet vehicles as shown in Equation (5.8a)-(5.8b).

$$\sum_{\substack{l \in L: \\ s_i = OS_d (t_i, t_j) \in T_D}} x_l^{d_v} - \sum_{\substack{l \in L: \\ s_j = OS_d (t_i, t_j) \in T_D}} x_l^{d_v} = 1 \qquad \forall\, d \in A \tag{5.8a}$$

where
$$\begin{cases} s_k = \{o_{sd} \cup OS_d\} & if\ driver\ is\ virtual\ driver\ sd \\ s_k = OS_d & Otherwise \end{cases}$$

$$\sum_{\substack{l \in L: \\ s_j = DS_d (t_i, t_j) \in T_D}} x_l^{d_v} - \sum_{\substack{l \in L: \\ s_i = DS_d (t_i, t_j) \in T_D}} x_l^{d_v} = 1 \qquad \forall\, d \in A \tag{5.8b}$$

where
$$\begin{cases} s_k = \{o_{sd} \cup DS_d\} & if\ driver\ is\ virtual\ driver\ sd \\ s_k = DS_d & Otherwise \end{cases}$$

### (2) Shared Autonomous Fleet Vehicle and Peer-to-Peer Carsharing Systems

The modified ridematching problem can be further extended to implement a peer-to-peer carsharing service. Unlike commercial carsharing services such as Zipcar, the p2p carsharing mobility providers are private vehicle owners. By registering themselves as p2p carsharing providers, a user can allow other participants in the system to use their car while it is not operating. In this scenario, shared-ride riders can also be p2p carsharing drivers. Thus, we define a variable $d_v^{pq}$ to denote a vehicle $v$ that is assigned to participant $p$ and operated by $q$. This service is different from regular fleets in that the carsharing vehicle owners' trip destinations are origins for the carsharing services, and carsharing users' destinations become carsharing vehicles' destinations. Furthermore, the decision variables $x_l^d$ in equation (4.1), that were previously defined from a drivers' standpoint, is redefined from the perspective of the vehicle and its owner. Equation (5.9) represent new the decision variable.

$$x_l^{d_v^{pq}} = \begin{cases} 1 & \textit{Vehicle v that owned by participant p and operated by q travels on link l} \\ 0 & \textit{Otherwise} \end{cases} \tag{5.9}$$

In accordance with the modified decision variable, the constraint sets in equation (5.5b)-(5.5c) are redefined in equation (5.10a)-(5.10b).

$$\sum_{\substack{l \in L: \\ s_i = OS_{d^{pq}}(t_i, t_j) \in T_D}} x_l^{d_v^{pq}} - \sum_{\substack{l \in L: \\ s_j = OS_{d^{pq}}(t_i, t_j) \in T_D}} x_l^{d_v^{pq}} = 1 \qquad \forall\, d \in A \tag{5.10a}$$

where $\begin{cases} s_k = \{DS_p \cup OS_{d^{pq}}\} & \textit{if } p \neq q \\ s_k = OS_{d^{pq}} & \textit{Otherwise} \end{cases}$

$$\sum_{\substack{l \in L: \\ s_j = DS_{d^{pq}}(t_i, t_j) \in T_D}} x_l^{d_v^{pq}} - \sum_{\substack{l \in L: \\ s_i = DS_{d^{pq}}(t_i, t_j) \in T_D}} x_l^{d_v^{pq}} = 1 \qquad \forall\, d \in A \tag{5.10b}$$

where $\begin{cases} s_k = \{DS_p \cup DS_{d^{pq}}\} & \textit{if } p \neq q \\ s_k = DS_{d^{pq}} & \textit{Otherwise} \end{cases}$

Defining the p2p carsharing system in this manner makes it possible to maximize the total cost savings by adding the extra carsharing cost benefit variable $c'_{i,n}$. The extra cost benefit variable is added to the objective function as follows:

$$S_i = \sum_{n}^{N} (Z_i - c_{i,n} + c'_{i,n} \cdot \mu) \tag{5.11}$$

By replacing the cost variable $c_{i,n}$ defined in equation (5.6) with $x_l^{d_v^{pq}}$, the first term and the second term representing the extra cost benefits can be calculated using equations (5.12a)-(5.12b).

$$c_{i,n} = \sum_{\ell=(t_j,s_j,t_k,s_k)\in L} \sum_{d\in A} t_{i,\ell}^{d_v^{pq}} \cdot e_1^{d_v} \cdot h_\ell^{i,d_v^{pq}} \cdot \delta \cdot \theta + \sum_{\ell=(t_j,s_j,t_k,s_k)\in L} t_{i,\ell}^{d_v^{pq}} \cdot e_1^{i_v} \cdot g_\ell^{ir} \cdot \delta \cdot (1-\theta) \quad (5.12a)$$

$$c'_{i,n} = \sum_{\ell=(t_j,s_j,t_k,s_k)\in L} t_{i,\ell}^{d_v^{pq}} \cdot e_2^{d_v} \cdot h_\ell^{i,d_v^{pq}} \quad (5.12b)$$

The vehicle cost variables $e_1^{d_v}$and $e_2^{d_v}$ are determined based on which travel option was used while driving the vehicle. The vehicle owner $p$ and driver $q$ are same for the first term, but different in the second term.

In the modified objective function, $\theta$ is the additional decision variable as defined in equation (5.13).

$$\mu = \begin{cases} 1 & if\ participant\ i\ register\ as\ a\ p2p\ carsharing\ service\ provider \\ 0 & Otherwise \end{cases} \quad (5.13)$$

In the limiting case, all shared-ride riders become p2p carsharing providers by yielding their cars parked at the origin to others. In this case, the mobility provider set $A = \{D \cup T \cup SD \cup D' \cup R\}$ and constraint sets (4.8a) and (4.8b) are modified as in the equations (5.14a)-(5.14b):

$$\sum_{\substack{l\in L: \\ s_i = OS_{d^{pq}}(t_i,t_j)\in T_D}} x_l^{d_v^{pq}} - \sum_{\substack{l\in L: \\ s_j = OS_{d^{pq}}(t_i,t_j)\in T_D}} x_l^{d_v^{pq}} = 1 \qquad \forall\ d\ \in A \qquad (5.14a)$$

where $\begin{cases} s_k = \{OS_q \cup\ OS_{d^{pq}}\} & if\ p\ \neq q \\ s_k = OS_{d^{pq}} & Otherwise \end{cases}$

$$\sum_{\substack{l\in L: \\ s_j = DS_{d^{pq}}(t_i,t_j)\in T_D}} x_l^{d_v^{pq}} - \sum_{\substack{l\in L: \\ s_i = DS_{d^{pq}}(t_i,t_j)\in T_D}} x_l^{d_v^{pq}} = 1 \qquad \forall\ d\ \in A \qquad (5.14b)$$

where $\begin{cases} s_k = \{DS_q \cup DS_{d^{pq}}\} & if\ p \neq q \\ s_k = DS_{d^{pq}} & Otherwise \end{cases}$

### 5.3.3 Mobility Portfolio Problem Applications

#### (1) Subscription Service Demand Model

The goal of mobility portfolio service providers is to prescribe a mobility solution set to the subscribers. As business, it is in the interest of the service providers to maximize the total number of subscribers. On the other hand, existing and potential users could be driven away from this platform if they experience unsatisfactory situations such as low matching success rates or low cost savings. Therefore, it is necessary to build a service demand model that combines the proposed mobility portfolio model with a real-time survey-based decision process that provides information about the current sentiments of users to the platform owners.

#### (2) Mobility Portfolio Profit Maximization Problem

The mobility portfolio problem can be configured to provide the maximum profits for the mobility portfolio service providers by adding constraints sets or by introducing additional terms to the objective function. For instance, to model a system that contains SAFVs as one of the mobility providers, we can formulate a multi-objective function that optimizes both SAFVs' profits and mobility portfolio users' cost savings by introducing an additional term $\sum_i \sum_f w_{i,f} \cdot \pi_{i,f}$. Here $\pi_i$ is a binary decision variable which is 1 if a SAFVs $f$ serves a rider $i$; otherwise, it is 0. A new variable, $w_{i,f}$, indicates the profit generated by individual $i$ when using a SAFV, $f$.

## 5.4 Discussion

We presented the core mathematical formulation of the mobility portfolio problem in this chapter and discussed its variations. The modeling framework presented in this chapter is employed throughout the thesis to model and optimize mobility portfolio problems as well as to simulate and analyze the impacts of integrated mobility services including p2p ridesharing, p2p carsharing and autonomous fleet vehicle sharing. The four components described in this chapter effectively capture the travel status choice dynamics and arrive at optimal mobility portfolio solutions. In the next chapter, we propose a methodological framework for mobility portfolios with bundling mechanisms, one of the most promising avenues for research in shared mobility transportation systems.

# Chapter 6

# Mobility Portfolio Problem

## 6.1 Overview

The simplest form of a mobility portfolio with bundles has three discretized travel statuses: shared-ride drivers, shared-ride riders, and solo-driver options. In this chapter we propose an iterative method rooted in a learning-based travel cost perception update model to solve the mobility portfolio problem by providing the minimum mobility portfolio cost for the system participants. Performing case studies on a real network, we confirm that the proposed mobility portfolio framework converges to a stable state for system participants and improves system performance by generating incentives for people to use shared mobility options.

## 6.2 Mobility Portfolio with Bundle Structure

### 6.2.1 Illustrative Example

Bundles contain a set of options that are tied to limited travel credits. Existing MaaS options are simply a set of transportation modes. For the purposes of the dissertation, to distinguish our framework from existing MaaS options, we call our proposed version as the "Mobility Portfolio (MP) bundle." Our MP bundle is composed of travel statuses – which can be shared-ride driver, shared-ride rider, or solo driver – as mobility options. The reason for including a solo driver as an option is to consider realistic situations such as people failing to be matched with others or to account for situations when they do not want to share their car. Within the bundle platform, mobility users are allowed to use any TOC mode available in the shared transportation system. Personal mobility providers (i.e., ridesharing drivers) also use those modes by changing their status.

Figure 6.1 shows a graphical representation of an n-period MP bundle. In this graph, each node represents one day, and each edge represents a possible travel status that subscribers can choose. Note that each day in the figure represents a period of one or more days when a subscriber uses a certain mode of travel and has a certain amount of usage credits available to them (e.g., "20 hours on a 4-seater car in ridesharing mode"). Travel time credits are set for each travel status option.

We assume that the MP bundle is provided as a smartphone application and the mobility supplier agency or company can collect travel information regarding the subscribers' travel experience such as matching result, travel mode, and travel cost. Also, we adopt a 'Pay-for-Only-What-You-Use' pricing approach, meaning that subscribers will only pay the costs associated with their travel mode and time.

It is important to mention that bundles are always specified for a period. During the bundle period, people can change their status based on their previous experiences. In the context of this dissertation, the bundle period is 5 weekdays, and the decision phase is 1 day. The updating process for the next day is influenced both by the user's experience of the previous day and the same day of the previous week. We can also conceptualize each day in our framework as a set of days as well. It is critical to incorporate in our design that travelers enter the system at various stages of their personal portfolios. Therefore, we model the day-to-day change of status of each user by simply modeling in an aggregate fashion representative people in the population making decisions, with the entire user pool split into 5 sets. The concept of a day in our framework is used only to describe a unit of a mobility period, but in reality, that unit can be any number (i.e., a "day" here can refer to any number of days, or a week, though we expect it to be 1 day in practice). The only concern is that if the unit is a large number of days, say, 30, the computation to find a steady final state of usage of different mode options will be more formidable.

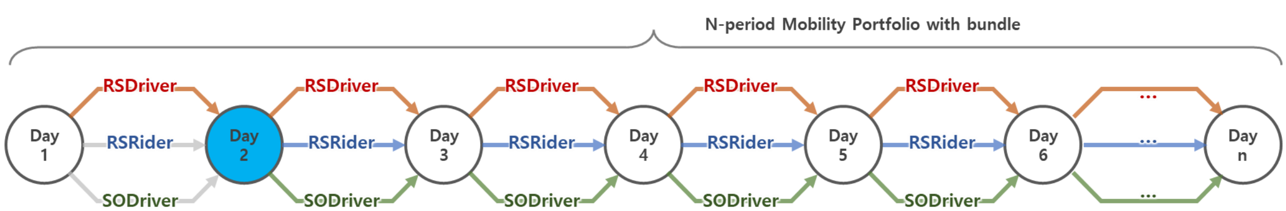

Figure 6.1 A graph visualization of an n-period mobility portfolio (MP) bundle

## 6.3 Solution Methodology

### 6.3.1 Iterative Approach

The objective function in the mobility portfolio problem is a nondifferentiable function. Therefore, we apply a heuristic algorithm, which in this case is an iterative method in order to execute the interlinked modules described previously. Our proposed iterative approach is bi-level with an outer and an internal iterative process. As shown in Figure 6.2, the internal iteration represents a daily travel status update process during a N-period mobility portfolio. This internal process is necessary to update the system participants' travel status for the next day based on their current day's experience of traveling on the current travel option. The role of the outer iteration is to find a convergence point, i.e., a set of travel options, that incentivizes the system participants to not change their travel status for each day within the period. Once the outer iteration has converged, we assume that system users have found a personalized mobility portfolio solution that is stable. During the internal iteration, all modules except the preprocessing module are performed sequentially. A detailed description of algorithms applied in each module is provided in the next section.

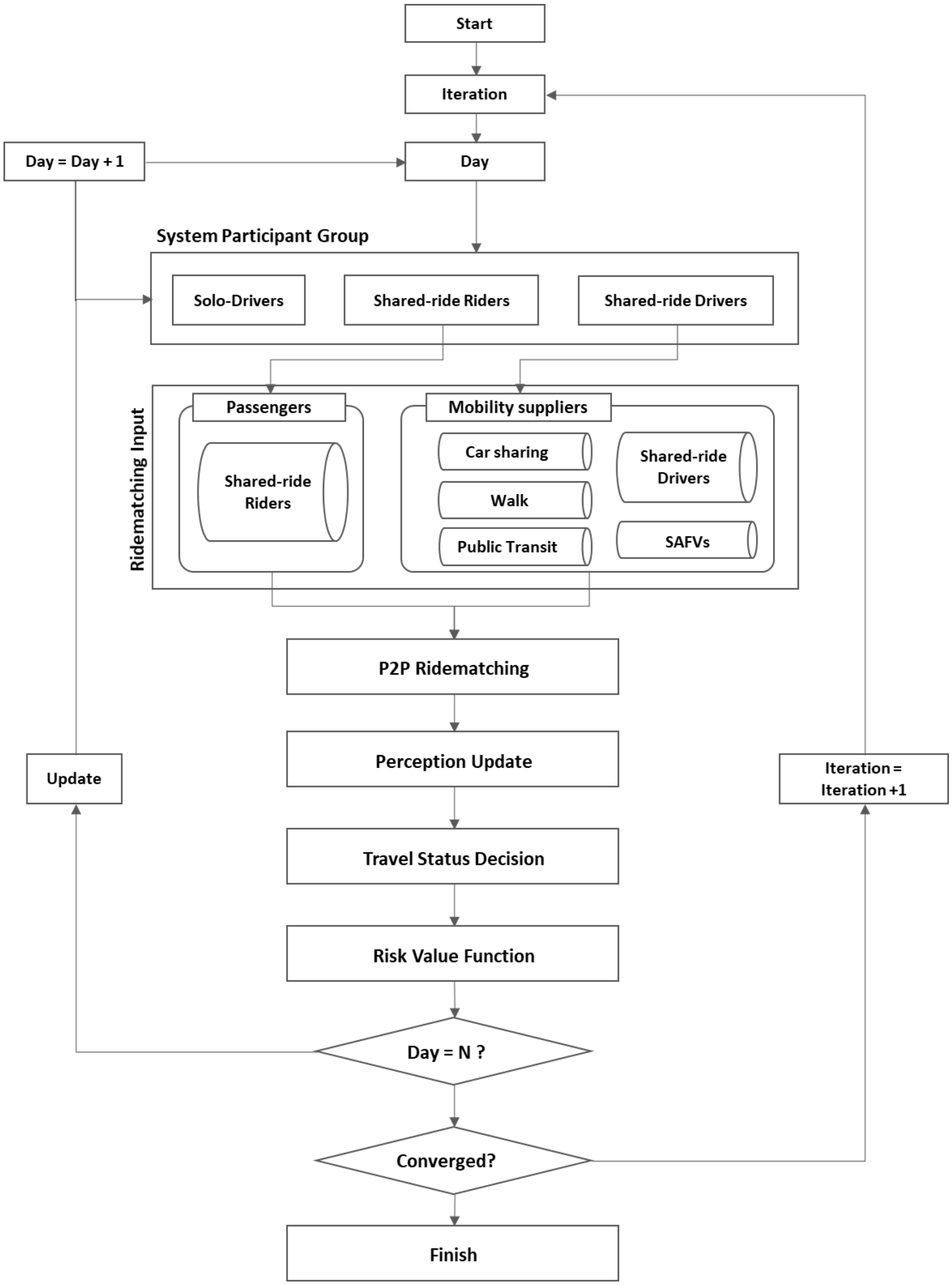


Figure 6.2 Overview of the iterative process

### 6.3.2 Real-time Ridematching Algorithm

In this dissertation, we assume that people expect to use their shared-mobility service options as soon as they become available. Keeping this in mind, we adopt a real-time ridematching algorithm described in chapter 5 that can match system participants with their partners immediately. We solve a many-to-one ridematching problem considering shared-ride drivers and riders and create a reduced time-expanded feasible network for both drivers and riders using the Ellipsoid Spatiotemporal Accessibility Method (ESTAM). We conduct a depth first search (DFS) to determine whether there are drivers who can serve a rider's entire itinerary. If the drivers found by DFS cannot serve the entire itinerary of a given rider, then we assume there is no match. For the matched drivers and riders, we run a dynamic programming (DP) method to find the minimum travel time path. Link travel time between nodes is a key element to find riders' itineraries.

In this dissertation, by considering various shared mobility service providers such as shared-ride drivers, public transit, walking and shared autonomous fleet vehicles (SAFVs), we modify the previously developed DP algorithm to include the mobility provider's vehicle cost. By doing so, the riders can be given a more realistic minimum cost itinerary and the system manager is able to know TOC modes for both shared-ride riders and drivers. It is worth mentioning that operational problems such as fleet dispatching problems are beyond the scope of our study. The system matches participants to SAFVs if their trip information does not violate both SAFVs' on-boarding passengers' trip and travel time constraints (i.e., waiting times to be picked up or SAFVs' in-vehicle travel time).

Figure 6.3 shows a time-expanded feasible network for a shared-ride rider 1 that is generated from the preprocessing module. Let $(i, t)$ represent a node that includes a go-point id $i$ and time index $t$. As shown in Figure 6.3, links that connect two nodes can be served by drivers $d$. Furthermore, let $c_{d_v}$ be the vehicle cost depending on driver $d$'s vehicle type $v$. For illustrative purposes, we assume that vehicle costs (per minute) for drivers 1, 2, and 3 are \$ 0.8, \$ 0.5, and \$ 0.7, respectively. Also, vehicle costs for waiting and walking are set to be \$ 0.1. In this example, the origin node is (10,5), i.e., 5 is the earliest departure time from the origin, and the destination node is (20,12), meaning 12 is the latest arrival time to the destination. Without considering the vehicle cost and the number of transfers, this rider's trip itinerary can be served in two ways, both of which are equivalent to each other: by driver 1, and by driver 2 who then transfers the rider to a driver 3. When vehicle cost is considered, the route served by driver 2 who carries the rider to the destination at 11 is the best matching result.

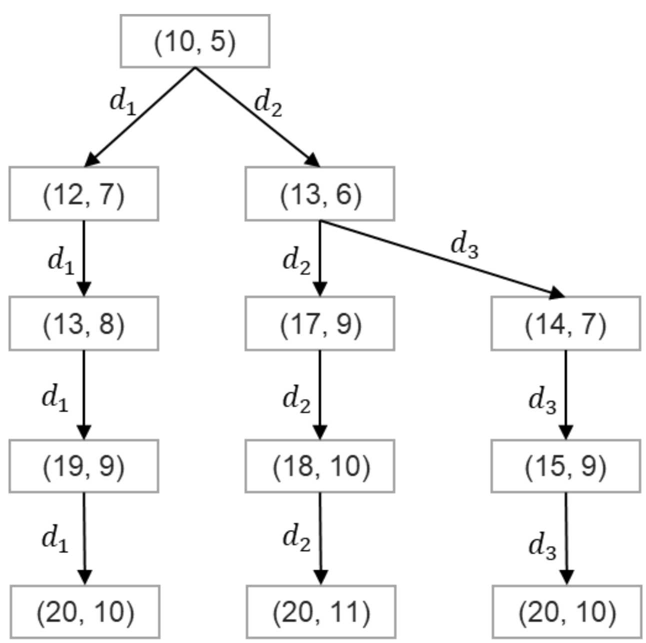


Figure 6.3 Time-expended feasible network for rider i

### 6.3.3 Perception Update

Simulation-based day-to-day learning methods are widely accepted approaches in research literature to model the process of perception updating. The method usually involves two aspects: expected information and experienced information. In Zhang et a. (2014), with the help of the artificial urban transportation system (AUTS), traffic information and drivers' historical perceptions are combined to update users' perception on routes to be selected for the current day's trip. Jha et al., (1998) develop a Bayesian updating model for updating travelers' travel time perceptions with information provided by Advanced Traveler Information Systems (ATIS). However, it is not practical to directly apply the existing learning models to our framework. This is because the learning process for the MP bundles relies on travel experiences that have occurred at two different points in time. Our perception update method is a period-to-period process, not a day-to-day process, modeled with representative units of times, that can be single days or a set of days. Since mobility portfolio systems do not exist currently, the learning process in our model is essentially a mechanism that captures changes in the system and iteratively leads to convergence to a final state which reflects the postulated real behavior of the travelers.

As mentioned earlier, we propose a two-stage learning process: (a) micro level update process, which involves applying a Bayesian model to update the expected travel time and cost for the next day based on the current day's experience and (b) macro-level update process, in which we apply a modified ant colony algorithm to combine the expected travel cost and the accumulated experiences onto the next day.

(1) Bayesian Inference Model

In this dissertation, we introduce a Bayesian inference model to update agents' perception based on the expected travel time before starting the trip (which corresponds to the prior in Bayesian terms) and the experienced travel time after finishing the trip on the same day (which corresponds to the posterior) with a dynamic traffic simulation model, DTALite/NeXTA. The benefit of the Bayesian model is that it allows us to use our prior belief with an uncertainty as the true value of the parameters (i.e., known as the prior distribution) to help us calculate the posterior distribution of the parameters by using the observed data. A detailed explanation can be found in (Tebaldi and West, 1998). In this dissertation, we consider travel time as a parameter to be updated. It is worth mentioning that the proposed travel status selection model is a disaggregated choice model because each agent's behavior depends on their trip information (e.g., departure time and origin/destination information) and their travel status. However, in this case, the OD travel time data that agents can refer to becomes too limited, which can lead to biased choice behavior. To prevent this situation from occurring, we aggregate the one-minute time step into a 10-minute time interval. Subsequently, we assign the same travel status to agents who have the same OD pair during this 10-minute time interval. We assume that the travel time is a normally distributed random variable, with mean travel time ($\mu$) and known variance ($\sigma^2$).

After performing the previous ridematching processes, the system participants with their own travel status are now divided into two sub-groups: matched and unmatched. Furthermore, people who choose the solo-driver option are also considered in this step. So, we have a total of five different groups: matched shared-ride driver group, an unmatched shared-ride driver group, a matched shared-ride rider group, an unmatched shared-rider group, and a solo-driver group.

Before starting the simulation, we create a prior distribution of OD travel time for the five different groups for each 10-minute period, using the expected travel times. At the end of the simulation, we collect the actual travel time values. Considering these values as true data, we create a likelihood distribution, which is then used to calculate a posterior distribution. The posterior distribution is considered as a new prior distribution for the next day. Note that we assume that the posterior and the likelihood distribution follow a normal distribution.

- The notation employed in this procedure is given below:

  $BT_{k,s}^{1,i,w}$ : Mean expected travel time parameter by individual *i* on day *w* for OD pair *k (o,d)* at time interval *s* before starting the simulation.

  $\tau_{k,s}^{1,i,w}$ : Belief of the travel time on day w by individual I for OD pair *k (o,d)* at time interval *s* before starting the simulation.

  $AT_{k,s}^{i,w}$ : Mean experienced travel time parameter by individual *i* on day *w* for OD pair *k (o,d)* at time interval *s* after finishing the simulation.

  $\sigma_{k,s}^{i,w}$ : Belief of the travel time on day w by individual *i* for OD pair *k (o,d)*at time interval *s* after finishing the simulation.

  $BT_{k,s}^{2,i,w}$: Updated travel time parameter of $BT_{k,s}^{1,i,w}$

  $\tau_{k,s}^{2,i,w}$ : Updated belief of updated travel time parameter, $BT_{k,s}^{2,i,w}$

  $x_{k,s}^{i,w}$ : Experienced travel time on day w by individual *i* for OD pair *k (o,d)* at time interval *s*.

  $n_{k,s}^{w}$ : Number of individuals who travel OD pair *k (o,d)* at time interval *s*.

The Bayesian update model is given by equation (6.1)-(6.4). The prior distribution on $BT_{k,s}^{i,w}$ is denoted by $N(BT_{k,s}^{1,i,w}, \tau_{k,s}^{1,i,w})$ and the likelihood distribution on $AT_{k,s}^{i,w}$ is denoted by $N(AT_{k,s}^{i,w}, \sigma_{k,s}^{i,w})$. By Bayes theorem:

$$Pr(\mu|y,\sigma^2) \propto Pr(y|\mu) \cdot Pr(\mu) \tag{6.1}$$

$$N\left(BT_{k,s}^{2,i,w}, \tau_{k,s}^{2,i,w}\right) = N(AT_{k,s}^{i,w}, \sigma_{k,s}^{i,w}) \cdot N(BT_{k,s}^{1,i,w}, \tau_{k,s}^{1,i,w}) \tag{6.2}$$

- where the posterior mean and variance:

$$BT_{k,s}^{2,i,w} = \left(\frac{1}{\tau_{k,s}^{1,i,w}} + \frac{n}{\sigma_{k,s}^{i,w}}\right)^{-1} \cdot \left[\frac{BT_{k,s}^{1,i,w}}{\tau_{k,s}^{1,i,w}} + \frac{n}{\sigma_{k,s}^{i,w}}\left(\frac{1}{n_{k,s}^{w}}\sum_{i=1}^{n} x_{k,s}^{i,w}\right)\right] \tag{6.3}$$

$$\tau_{k,s}^{2,i,w} = \left(\frac{1}{\tau_{k,s}^{1,i,w}} + \frac{n}{\sigma_{k,s}^{i,w}}\right)^{-1} \tag{6.4}$$

It is worth noting the value that we want to estimate is a ‘travel time’ value which is non-negative. However, it is possible to see the distributions that have negative values in travel time. Particularly, we can easily observe this situation when the average travel time is short, and the variance is large. To prevent this and provide better estimated solutions, we can apply a truncated normal distribution. The benefit from a truncated normal distribution form is to eliminate the unnecessary variables and thus to provide better estimates with a designated range. For example, if we precisely model a prior travel time distribution that truncated at zero, it could be shown as follows:

$$N\left(BT_{k,s}^{1,i,w}, \tau_{k,s}^{1,i,w}\right) \in (0, \infty)$$

(2) Payoff Approach

The output of the Bayesian model gives us the 5 time-dependent prior distributions of travel times for every OD pair for the next day. The expected travel time values from the prior distributions are now utilized to compute the next day's expected travel cost (note: we consider the mean travel time value). As mentioned above, the travel costs are automatically captured after the ridematching process. To provide the expected travel cost expenditure ($V$) for the next day, we apply the payoff method as shown in Figure 6.4.

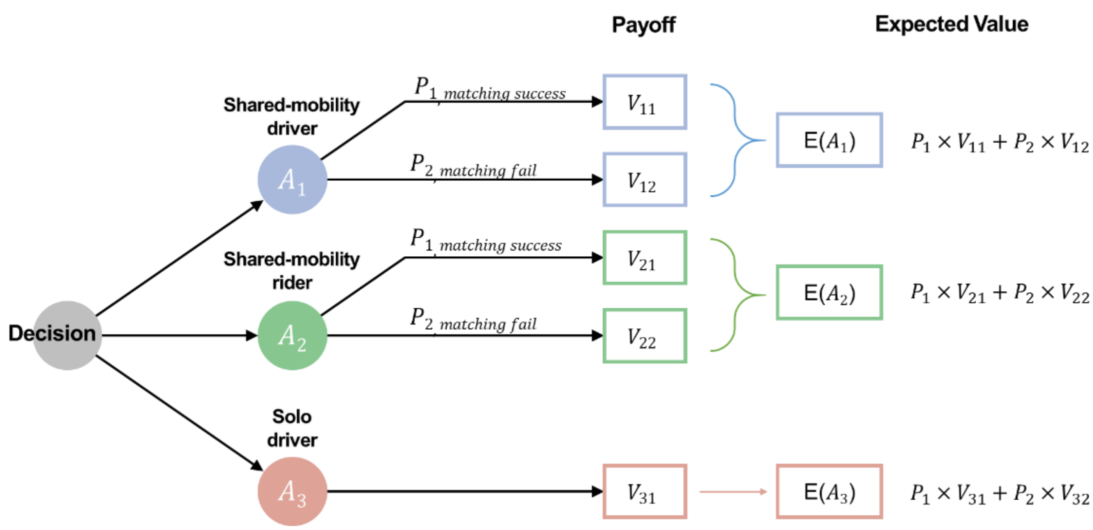


Figure 6.4 Payoff method

The next day's expected travel cost for each individual $i$ is calculated by the following equation:

$$V_{m,n}^{i,w+1} = BT_{k,s}^{2,i,w} \cdot C_{k,s}^{1,i,w} \tag{6.5}$$

The variable, $V_{m,n}^{i,w+1}$, represents an expected travel cost for individual $i$ for the next day *(w+1)* depending on travel status $m$ and matching outcomes $n$. The variable, $C_{k,s}^{1,i,w}$ represents the experienced travel cost on day $w$ by individual $i$ for OD pair $k(o,d)$ at time interval $s$.

The expected value for each travel status option *m* is estimated by equation (6.6):

$$E(A_m) = \sum_{n=1}^{N} V_{m,n}^{i,w+1} \cdot P_n{}^w = \sum_{n=1}^{N} BT_{k,s}^{2,i,w} \cdot \ C_{k,s}^{1,i,w} \cdot P_n{}^w \tag{6.6}$$

The variable, $P_n{}^w$, represents a matching ratio on day $w$ based on matching results.

The ridematching ratio is often used as a metric to measure the performance of a ridesharing transportation network system, and it is generally associated with the number of riders who are served by other drivers (Jha et alk 1998; Masoud et al., 2017; An et al., 2019). The number of drivers who serve those riders is not considered in this calculation. That is because, in most cases, those who act as mobility providers come from the group of trip-purposeless drivers, thus, whether or not a match is made does not affect their decision to continue as drivers. However, in our study, the drivers' experience of getting matches are just as important as the riders' experiences. To calculate the matching success ratio ($P_1$), we divide the total number of the matched drivers and riders by the total number of people who make shared trips as drivers or riders. The matching failure ratio ($P_2$) is simply (1- $P_1$). The number of solo drivers is not considered because their travel experiences do not depend on the matching process. The expected travel value for a solo-driver travel status is the same as the expected travel cost.

*Proof*. The expected value for solo drive travel status is calculated as follows.

$$E(A_3) = P_1 \cdot V_{31} + P_2 \cdot V_{32} = P_1 \cdot V_{31} + (1 - P_1) \cdot V_{32}$$

Also, $V_{31} = \cdot V_{32}$.

Thus, $E(A_3) = P_1 \cdot V_{31} + (1 - P_1) \cdot V_{31} = V_{31}$ ■

Referring to the MP bundles shown in Figure 6.1, each travel status edge will have the calculated expected value from equation (6.6).

### 6.3.4 Modified Ant Colony algorithm

In the macro level update module, we apply the concepts of the Ant colony optimization (ACO) algorithm. The ACO algorithm aims to find an optimal path in a graph by running artificial ants (i.e., simulation agents) with pheromones (Yang et al., 2008). In the ACO algorithm, each ant constructs a solution path within the graph, considering the intensity level of the cumulated pheromones on the edge. Edge selection can be modeled as follows:

$$p_{ij}^k = \frac{\tau_{ij}^{\alpha} \cdot \eta_{ij}^{\beta}}{\sum_{k \in available_i} \tau_{ik}^{\alpha} \cdot \eta_{ik}^{\beta}} \tag{6.7}$$

- where,

$p_{ij}^k$ : probability of moving from position *i* to *j*

$\tau_{ij}$ : amount of pheromone deposited on the edge from position *i* to *j*.

$\eta_{ij}$ : attractiveness of the edge from position *i* to *j*.

$\alpha, \beta$ : parameters to control the influence of $\tau_{ij}$ and $\eta_{ij}$, respectively. ($0 \leq \alpha;\ \beta \geq 1$)

The attractiveness of the edge is calculated by $\frac{1}{d_{ij}}$, where *d* is the distance. When the ants find the feasible path solutions, they leave their pheromones along each segment of the path. The pheromone updating rule can be written as follows:

$$\tau_{ij} \leftarrow (1-v) \cdot \tau_{ij} + \sum_{x}^{m} \Delta\tau_{ij}^{k} \tag{6.8}$$

- where,

  $v$ : pheromone evaporation coefficients.

  $m$ : total number of ants who traverse the edge from position *i* to *j*.

  $\Delta\tau_{ij}^{k}$ : amount of pheromone deposited by the $k^{th}$ ant on the edge from position *i* to *j*.

In this dissertation, each traveler has their own MP bundle graph, and the graph is completely independent of other users' graphs. Each traveler bases their travel decision on their own experiences which are accumulated from their own iteration process. Thus, we modify equation (6.7)-(6.8) as follows:

$$p_{is}^{k} = \frac{\tau_{ij}^{s,\alpha} \cdot \eta_{ij}^{s,\beta}}{\sum_{k \in available_{ij}} \tau_{ij}^{k,\alpha} \cdot \eta_{ij}^{k,\beta}} \tag{6.9}$$

$$\tau_{ij}^{s} \leftarrow (1-v) \cdot \tau_{ij}^{s} + v \cdot \sum_{e} \Delta\tau_{ij}^{s,e} \tag{6.10}$$

- where,

  $\tau_{ij}^{s,e}$ : memory of ridematching experiences on travel status edge *s* from day *i* to *j*.

  $\eta_{ij}^{s}$ : expected value on the next travel status edge *s* from day *i* to *j*.

  $\sum_{e=0}^{e-1} \Delta\tau_{ij}^{s,e}$: accumulated memory of ridematching experiences on travel status edge *s* from day *i* to *j* deposited by $e^{th}$ traveler.

We consider a pheromone to represent the memory of the travel experiences. We assume that even though an agent enters the system as a ridesharing driver or a rider, if he fails to be matched with other agents, the memory on the edge will be counted as 1, otherwise 2. If the driver selects an edge and is also matched then the memory is 2, to induce him/her to use the edge more in the future. Other memory numbers can be used as well, but no parametric study was attempted in our research.

For the solo drivers, their travel status edges will be counted as 1 as well. Unselected edges will have a value of 0. The term $\eta_{ij}^{s}$ is automatically replaced by the value obtained from equation (6.6). We assign the same weight to $\tau_{ij}^{s,\alpha}$ and $\eta_{ij}^{s,\beta}$, thus, we do not consider the control parameters $\alpha$ and $\beta$. Unlike the original AOC algorithm, in the mobility portfolio problem when travelers select a travel status edge, other travelers' travel experiences on certain edges do not affect their choice. This fact allows us to convert the term $\sum_e \Delta\tau_{ij}^{s,e}$ as $\Delta\tau_{ij}^{s}$ because $e = 1$. Figure 6.5 shows an example of the $j^{th}$ iteration and day 2 travel status updating process.

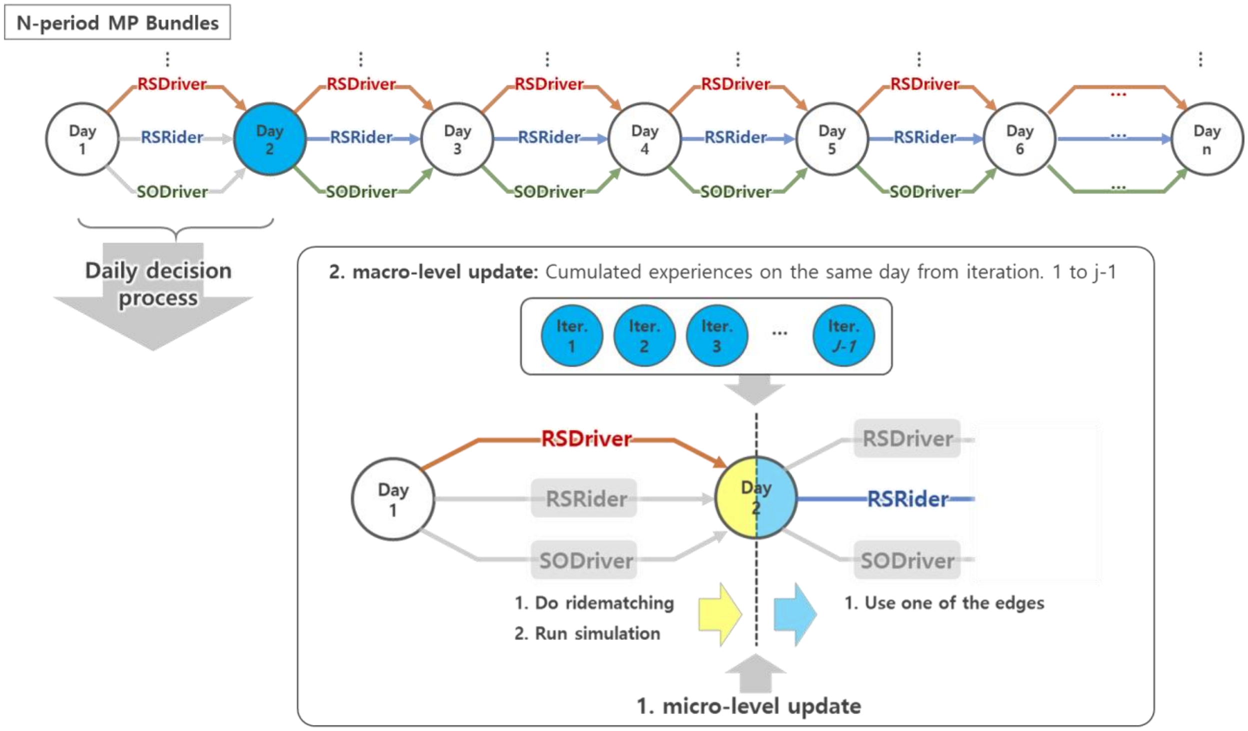


Figure 6.5 Mobility portfolio framework: $j^{th}$ iteration and travel status update (day 2 example)

## 6.3.5 Risk Value Function

With the results from the previous module, users can now select the most desirable edge. If there are no credit limits on the edge, they can keep using that edge as their travel status option. However, in the proposed MP bundles model, each option has a limit on usage time. If a person exceeds a certain travel option, he can no longer use the option. Moreover, due to the lack of experience, some people may have fewer opportunities to use other travel status that can provide a better mobility portfolio solution. To prevent the situation of time credits on any mobility portfolio option being exhausted before the expiration of the bundled plan period and to provide a chance to select less-desirable options, we propose a risk function that calculates the level of risk *(r)* for an individual. This risk function is as follows:

$$r = \frac{ToT^{s*} - (T^{s*,e} + \sum_{e=0}^{e-1} \sum_{s} T^{s,e} \cdot \varphi)}{ToT^{s*}} \tag{6.11}$$

where $T^{s*,e}$ is the expected travel time with the selected travel status $s*$ at iteration $e$. This travel time is calculated from equation (6.3). The term $ToT^{s*}$ is a total time credit for the selected travel status $s*$ and $\delta$ is an indicator to capture the previous travel time experienced on $s*$.

$$\varphi = \begin{cases} 1 & if\ travel\ status\ s*\ \ is\ selected\ at\ iteration\ e \\ 0 & otherwise \end{cases} \tag{6.12}$$

If the value of risk is smaller than a random number ($\theta$) with a value between 0 to 1, the system will randomly select other travel types. The random number could be replaced by a fixed number or could be reduced gradually as the days pass.

### 6.3.6 Convergence

We discuss the convergence of the learning process explained earlier. The output of iterative methods can get arbitrarily close to some specific value; however it is computationally infeasible to converge to a single optimal point. Thus, we propose a convergence rule. First, before proceeding to the next outer iteration, at the end of the mobility portfolio period we check the travel status of the system participants on the same $n^{th}$ day of the current and the previous outer iteration, then calculate the status change ratio on each day. If the average of the sum of the ratios is less than or equal to a tolerance level of 0.025, it is assumed that it converges, and each individual has a stable mobility portfolio solution. Equation (6.13) is used to check for the convergence of the iterative process.

$$\frac{1}{|N|}\sum_{n=0}^{N}\left(\frac{1}{I}\sum_{I=0}^{I}u_n^i\right) \leq 0.025 \tag{6.13}$$

The variable, $u_n^i$, is a binary variable and its value is 1 if an individual $i$'s $n^{th}$ day travel status on the current iteration, and the previous iteration are different, and 0 otherwise. The variable $N$ indicates the total length of the mobility portfolio period and variable $I$ denotes the total number of system participants.

# 6.4 Numerical Experiments

## 6.4.1 General Simulation Setting

### (1) Integrated multimodal transportation network in Irvine area

A portion of the city of Irvine, California was selected as our study area. We constructed a multi-layered network of the region, including the possible travel modes in the area. First, we built a base layer for the vehicle network. As we assumed in section 4.2.2, go-points in the vehicle network are created including the center of TAZ (Traffic Analysis Zone). To build the base layer in the study area, we used the California Statewide Transportation Demand Model (CSTDM). Each go-point is connected to its nearby go-points, and each link travel time is calculated based on the link free-flow speeds. In this layer, the ridesharing drivers travel in their vehicle. Second, we added a public transit network layer on top of the base layer. For the bus layer, we utilized the general transit feed specification (GTFS) data for the area. There are six bus lines in our search scope in GTFS. We also obtained the location of each bus station and timetables for buses. A network for the shared autonomous fleet vehicle (SAFVs) is added to the base layer network. We assume that there are three SAFV depots which are evenly distributed within the city. The total number of SAFVs operating in the system is 10 and each depot has 3, 3, and 4 vehicles, respectively. Walk nodes are depicted by pink nodes, as shown in Figure 6.6. Travelers, especially ridesharing riders, can use the walk links to transfer between the different travel modes in the different layers. To improve computational speed, we discretize the time horizon with 1-minute time intervals.


(a) CSTDM network (b) Go-points network

Figure 6.6 Irvine area network with the I-5/I-405/SR-55 triangle and SR-73 freeway

## (2) Mobility Portfolio Setting

In this dissertation, we set a 5-day MP bundle period, considering weekdays. Considering the size of the research area, we give the following usage credits for each option: 180 minutes as a driver, 200 minutes as a rider, and 150 minutes as a solo-driver for the five-day period.

### (3) MP Bundle Subscriber Demand Generation

Referring to the CSTDM model, 262,487 trips are generated during the morning-peak-period. We randomly select 45,000 trips as potential subscribers for the mobility portfolio system. Among them, we also randomly choose 12,000 people and set their initial travel status as a shared mobility rider. In the same fashion, 25,000 people start their first trip in the system as a ridesharing driver, and the remaining people make their initial trip as solo-drivers. Travel time windows and departure times for each individual are randomly assigned. We randomly assign a travel time flexibility between 1 and 15 minutes to each user.

### (4) Vehicle Cost and Discount Value Setting

To reflect diversity in vehicle price, we assume that there are five different classes of private vehicles: electric vehicle, conventional vehicle, luxury conventional vehicle-new, SUV, luxury SUV and set prices as \$0.2, \$0.3, \$0.4, \$0.5, and \$0.6 per minute per vehicle. We assign a random class number to each individual vehicle. Furthermore, for public transit we set a price of \$0.1 per minute and for the SAFVs we set an average vehicle cost of \$0.4 per minute. In addition, we assume that if anyone shares a trip with others, then people who are involved in the shared trip will have a 50% discounted travel cost based upon the length of the shared trip. Note that different discount values could be set for each travel mode, however, as an initial study, we consider a single value and apply it to all travel modes, including SAFVs, and buses. To consider walk time and waiting time penalties, the discount value is not applied for those travel modes.

### (5) Simulation Setting

We set the simulation time to be the same as the morning peak period and the trip purpose of travelers is set as a work trip. We also evaluate the performance of the network by using the proposed framework for the test study in DTALite/NeXTA. In the simulation model, we assign all of the travel demand (i.e., 262,487 trips) to study the effects of network traffic congestion on the mobility portfolio users' experience.

There are several assumptions made in this simulated mobility portfolio framework:

1) It is a subscription-based transportation system so that the system already knows the participants' origins, destinations and their corresponding time windows.
2) A user's travel time window cannot be violated.
3) Each trip starts or ends only in the predefined Travel Analysis Zones (TAZs), called go-points.
4) Every user's primary travel mode is a combination of drive-yourself option and drive-alone option (i.e., same as solo-driver in the traditional mode choice model).
5) Participants (subscribers) comply with the trips suggested by the mobility portfolio.
6) The simulation time horizon is a set of 1-min discretized time intervals spanning a total of 3 hours.

### 6.4.2 Uniform Distribution of Mobility Portfolio Starting Date

It is reasonable to assume that travelers can initiate (or purchase) the bundle on any day of the week. Therefore, we uniformly divide people in each travel status group and assign them to different weekdays to start their MP bundle plan. Thus, on each mobility portfolio day at iteration

1, there are 25,000 drivers, 5,000 riders and 2,400 solo drivers. Note that at iteration 1 the demand of each travel status group doubles as each day passes compared to the previous day. One thing to mention is that after performing the day 1 simulation at iteration 1, people who traveled on day 1 with mobility portfolios learned from their experience, which affects their next day (i.e., day 2) travel status decision. Therefore, the total number of the system participants for each travel status group in practice may not be exactly double. Note that for the problem instances, we generate 10 different mobility portfolio participants groups. The results we report in this section are averaged over 10 simulation runs for each problem.

### (1) Convergence Test

Combining the proposed mobility portfolio scheme and the agent-based traffic simulation model, we gain insight on the performance of the proposed learning methodology. The interest here is in observing the convergence of the model for each of the days of the bundling period. To test the convergence, we run 10 different simulations. Figure 6.7 shows that the travel status shift ratios for each travel status converge to 0.025, which is less than the tolerance level, so the model is assumed to converge. Except in the first iteration, the travel status shift ratio in each iteration (which represents the 5-day simulation period) varies initially but stabilizes after the fourth iteration. This is because the mobility portfolio subscribers are more confident about their choices as the days and the iterations progress. Once people are satisfied with a particular travel allocation, they tend to make a similar choice as in the previous iteration.

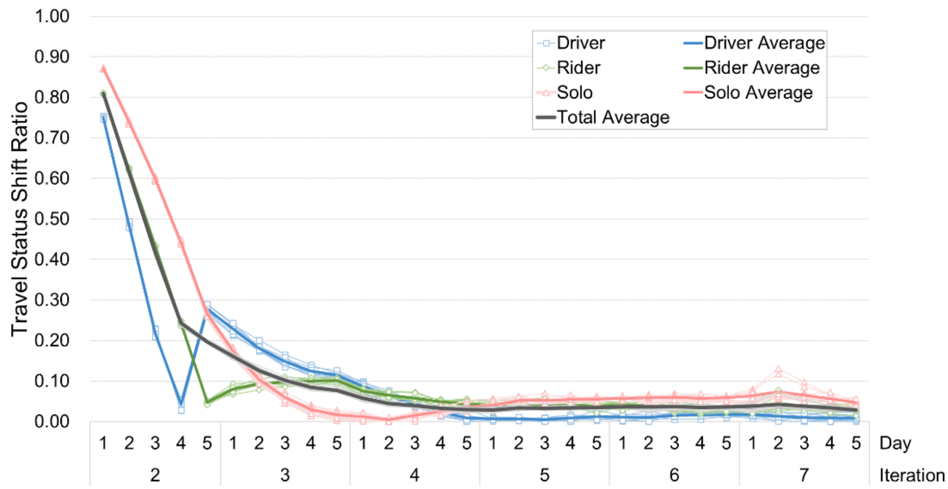


Figure 6.7 Iterative convergence of Travel status change ratio, averaged over 10 runs

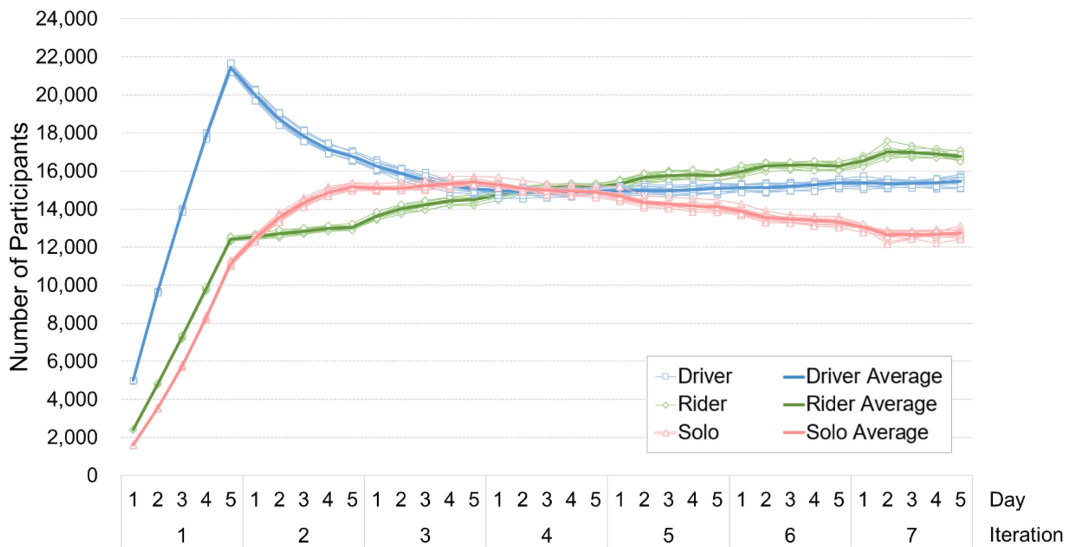


Figure 6.8 Changes in the number of shared-ride drivers, shared-ride riders, and solo-ride drivers, over 10 runs

Figure 6.8 shows the variation in the number of people who join the system with a particular travel status. Similar to the convergence test results, after the fourth iteration the number of shared-ride drivers is stabilized. It is interesting to note that the number of shared-ride riders increases while the number of solo-ride drivers tends to decrease. This result indicates that the proposed mobility portfolio framework induces people to join and participate in the shared-mobility transportation system.

Note that we consider the first iteration as a network warming period to load people with different portfolio starting days, thus it is reasonable to see that the total number of system participants is smaller in this iteration than in later iterations.

### (2) Mobility Portfolio Cost Savings

Figure 6.9 shows the total mobility portfolio cost savings, defined here as the cost savings compared to the default option of not using a mobility portfolio. The savings increase as the iterations progress. The total cost savings initially are small because not enough people use the suggested solution recommended by mobility portfolio framework, and user have not yet acquired the travel experience to make a better choice. At the final iteration, the total cost savings over 5 days is almost $300K.

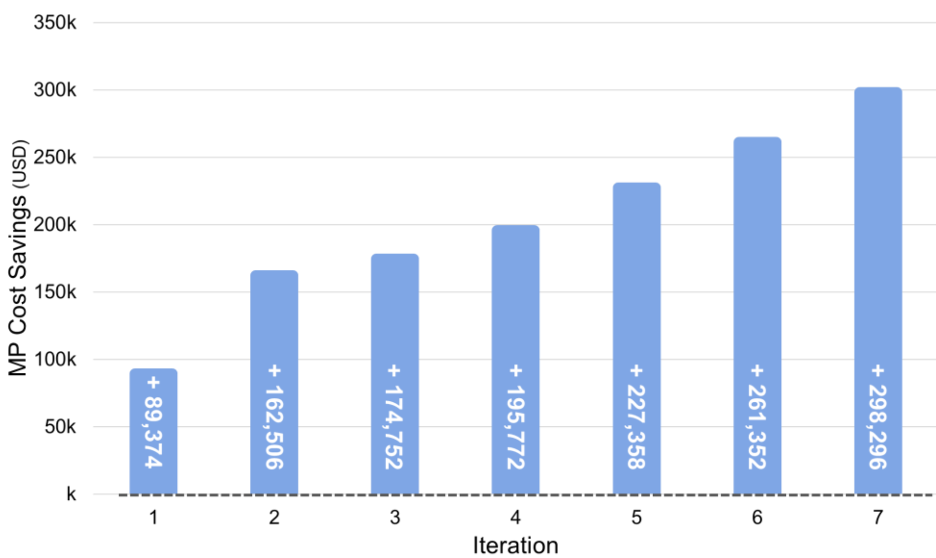


Figure 6.9 Total mobility portfolio cost savings, averaged over 10 runs

Figure 6.10 shows the total weekly travel costs that spend by people in each travel status group. The group with the largest cost savings is the shared-ride riders, who saved $3.77 on average. People who enter the system as shared-ride drivers are expected to have their costs reduced by $2.35. People in the solo-ride drivers group experience the least cost savings, which is to be expected, since their travel option does not change significantly from their existing option. However, the number of solo-ride drivers is reduced after the iterative process, resulting in overall system savings.

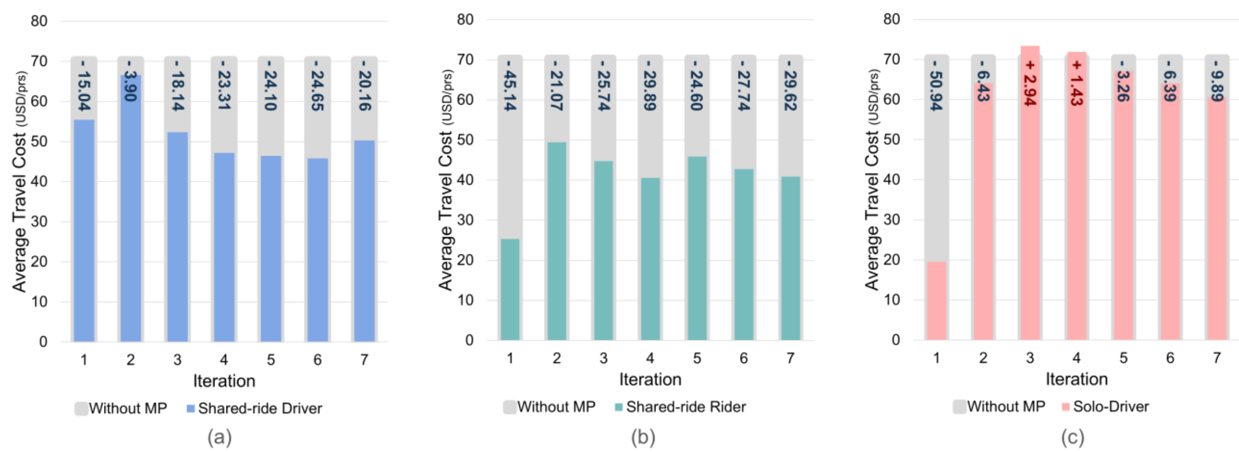


Figure 6.10 Average travel cost by travel status: (a) Shared-ride driver, (b) Shared-ride rider, and (c) Solo-Driver

## (3) Matching Results

In the mobility portfolio framework, we allow the travel status shifts which leads to changes in the matching ratio as the iteration progresses. Figure 6.11 shows the number of matched riders and the matching ratio. The number of matched riders continues to increase as the iterations progress. The ratio increases until the fifth iteration, drops slightly, and then increases again. This appears to be due to the difference between the total number of the potential shared-ride riders and the served riders.

We also analyze the number of the potential shared-ride drivers and the drivers who actually serve riders. Intuitively, more shared-ride drivers lead to more matched riders (An et al., 2019). The results presented in Figure 6.12, however, are contrary to this common belief. The horizontal distance between the bars represents the number of drivers who are willing to share their car with others but drive alone because they are not matched. The largest gap occurs in the first two iterations. Especially, in the case of day 5 at iteration 1, approximately one third of drivers are matched with riders, and the rest of drivers remain unmatched. By learning from these unsatisfying experiences, people shift their travel status and eventually the total number of the potential shared-ride drivers is stabilized, and the number of matched drivers increases. This figure illustrates the effectiveness of our proposed mobility portfolio framework in maintaining an acceptable matching level (Figure 6.11) with fewer cars.

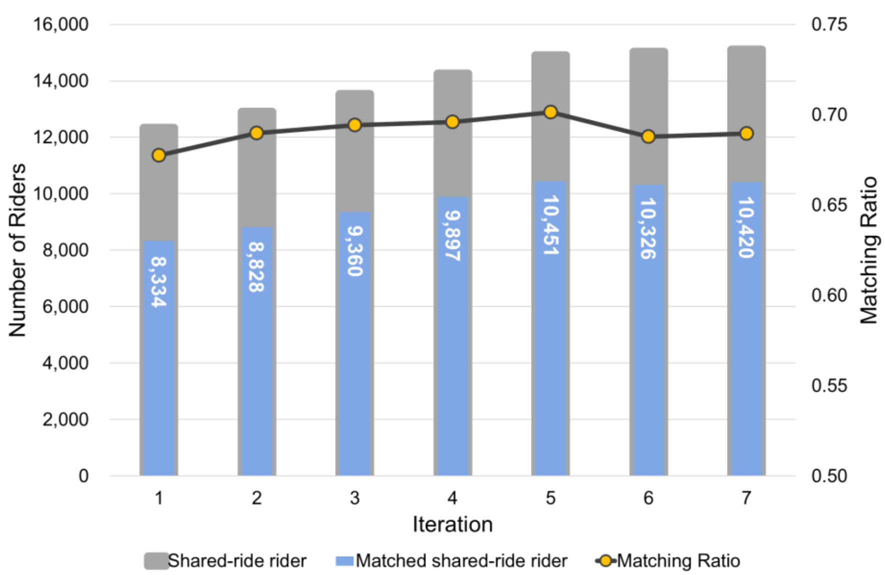


Figure 6.11 Changes in matching ratio results, averaged over 10 runs

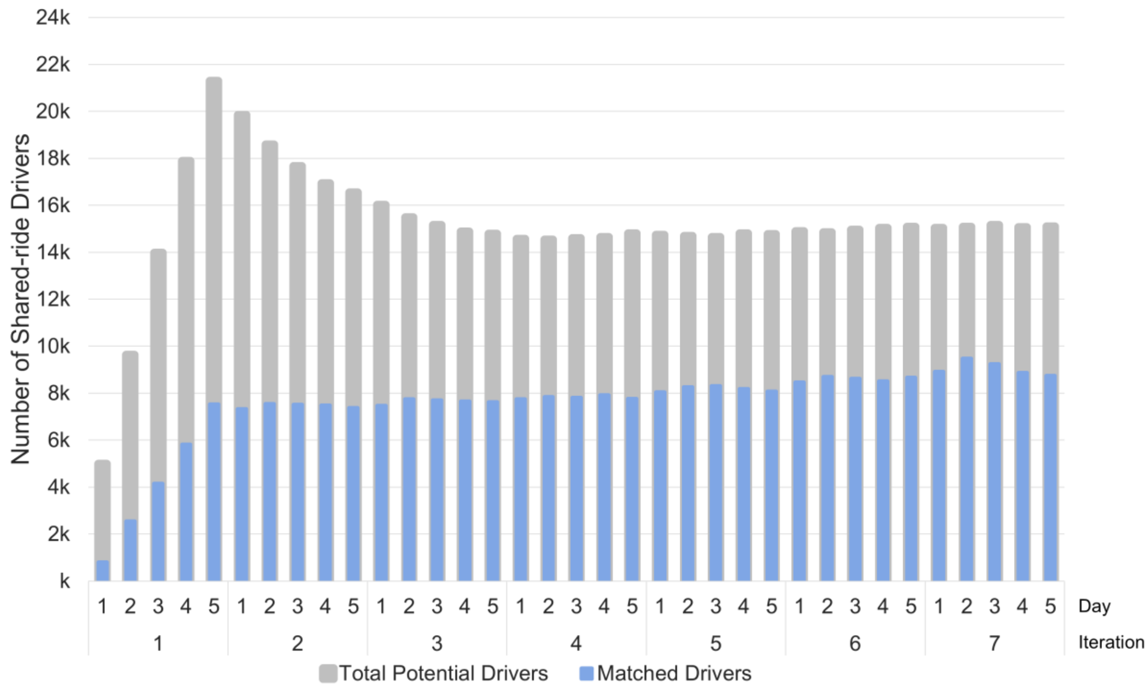


Figure 6.12 Comparisons of the total number of the potential shared-ride drivers and the matched drivers, over 10 runs

## (4) System Performance

We also analyze vehicle-mile-traveled (VMT) to evaluate the performance of the integrated shared transportation system with the portfolio scheme. Figure 6.13 depicts the results of the reduced VMT after every iteration, showing that convergence is achieved. When comparing the VMTs of the first and last iterations, we find a reduction of VMT to be over 1.5M units which indicates that the mobility portfolio scheme has induced the system into a more beneficial state.

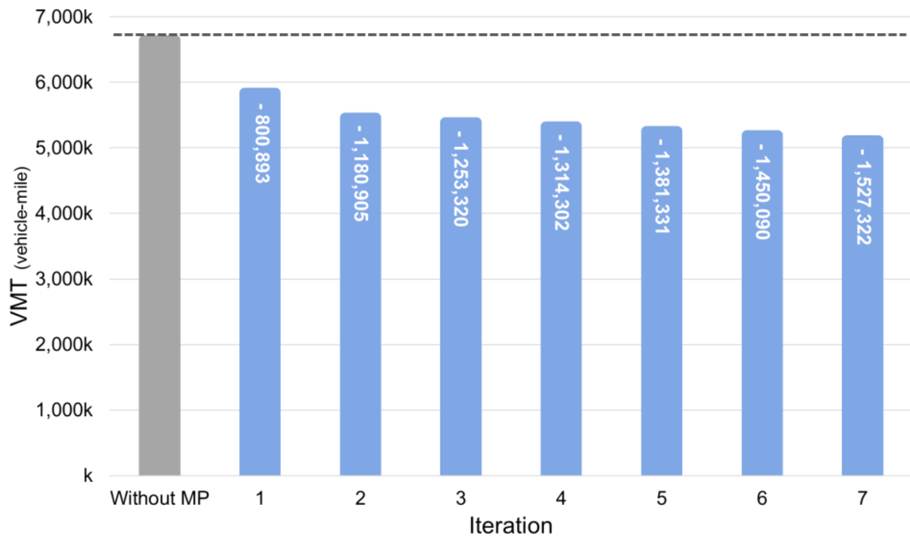


Figure 6.13 Total VMT reduction

## (5) TOC Mode Share Ratio

Within the mobility portfolio framework, we divide the system participants into three groups using bundles. By using the TOC mode concept presented in chapter 3 it is possible to describe each system participant's actual trip movement.

Table 6.1 shows 6 TOC modes considered in our framework. They are basic TOC mode (i.e., *TOC mode-B*), a basic element which can be combined together to generate the other 5 TOC modes called TOC mode combination (i.e., *TOC mode-C*).

As shown in Table 6.1, TOC mode-B 1 through 6 mean solo-ride driver, shared-ride driver, autonomous vehicle users, shared-ride rider, public transit passenger, and walk, respectively. Note that a vehicle type depends on the ridematching results, so it is denoted as $x$, except walk. Using these fundamental TOC modes, we can generate several other TOC mode-Cs. Table 6.2 shows the TOC mode combination list. TOC mode-C 7 refers to solo-ride driver + shared-ride driver.

Table 6.1 Basic TOC modes

| TOC Mode-B | Travel Options (level) | | | | | | |
|---|---|---|---|---|---|---|---|
| | **Driving Mode** | **Parking Space** | **Shared Empty Seat** | **Public Transit** | **Walk** | **Owner -ship** | **Vehicle Type** |
| 1 | 0 | 0 | 0 | 0 | 0 | 0 | $x$ |
| 2 | 0 | 0 | 1 | 0 | 0 | 0 | $x$ |
| 3 | 1 | 1 | 1 | 0 | 0 | - | $x$ |
| 4 | 2 | 1 | 1 | 0 | 0 | - | $x$ |
| 5 | 2 | 1 | 1 | 1 | 0 | - | $x$ |
| 6 | 2 | 1 | 0 | 0 | 1 | - | Walk |

The difference between TOC mode-C 7 and 8 is that people who experience TOC mode-C 8 serve two shared-ride riders and continue to travel alone after dropping off riders. TOC mode-C 9 through 16 are applicable for shared-ride riders. TOC mode-C 9 and 11 represent the modes shared-ride rider + shared-ride rider (i.e., 1 transfer), and shared-ride rider + walk + shared-ride rider (i.e., 1 transfer). The 'Number of Connection' column in Table 6.2 conveys the number of transfers, thus, TOC mode-C 7 and 8 have a value of 0. Note that we do not count walking as a transferrable mode, so that even though TOC mode 12 and 16 contain two TOC mode-B 6s, the number of connections for these modes are 2 and 0. The TOC mode columns in TOC mode combination list can be extended depending on the number travel path segments which are obtained from the ridematching process.

Table 6.3 shows the TOC mode share for each travel status. The basic TOC Mode 1 is present in shared-ride driver, solo-ride driver, and shared-ride rider travel status group. This is obvious because unmatched drivers and riders, and solo-ride drivers have to drive themselves.

Table 6.2 TOC mode combinations

| TOC Mode-C | TOC mode combination | | | | |
|---|---|---|---|---|---|
| | **TOC mode** | **TOC mode** | **TOC mode** | **TOC mode** | **Number of Connection** |
| 7 | 1 | 2 | - | - | 0 |
| 8 | 1 | 2 | 2 | - | 0 |
| 9 | 4 | 4 | - | - | 1 |
| 10 | 4 | 6 | - | - | 1 |
| 11 | 4 | 6 | 4 | - | 1 |
| 12 | 4 | 6 | 4 | 6 | 2 |
| 13 | 4 | 6 | 5 | 4 | 3 |
| 14 | 4 | 6 | 5 | 6 | 2 |
| 15 | 6 | 4 | 6 | - | 1 |
| 16 | 6 | 6 | - | - | 0 |

Table 6.3 shows the TOC mode share for each travel status. The basic TOC Mode 1 is present in shared-ride driver, solo-ride driver, and shared-ride rider travel status group. This is obvious because unmatched drivers and riders, and solo-ride drivers have to drive themselves. Except the basic TOC Mode 1, most of shared-ride drivers serve 1 or 2 riders. Furthermore, 136 shared-ride drivers pick up and drop off a rider from their own origins and destinations, thus, they have another basic TOC Mode 2. For shared-ride riders, most of the matched riders are served directly without transferring (TOC Mode-B 4). The next most popular TOC mode is 9 which connects two different shared-ride drivers without walk links. This is possible because we use a go-point based network structure. These results confirm that by using the TOC option tables (Table 4.1) we can model diverse travel movements in any shared transportation system.

Table 6.3 TOC mode share by travel status

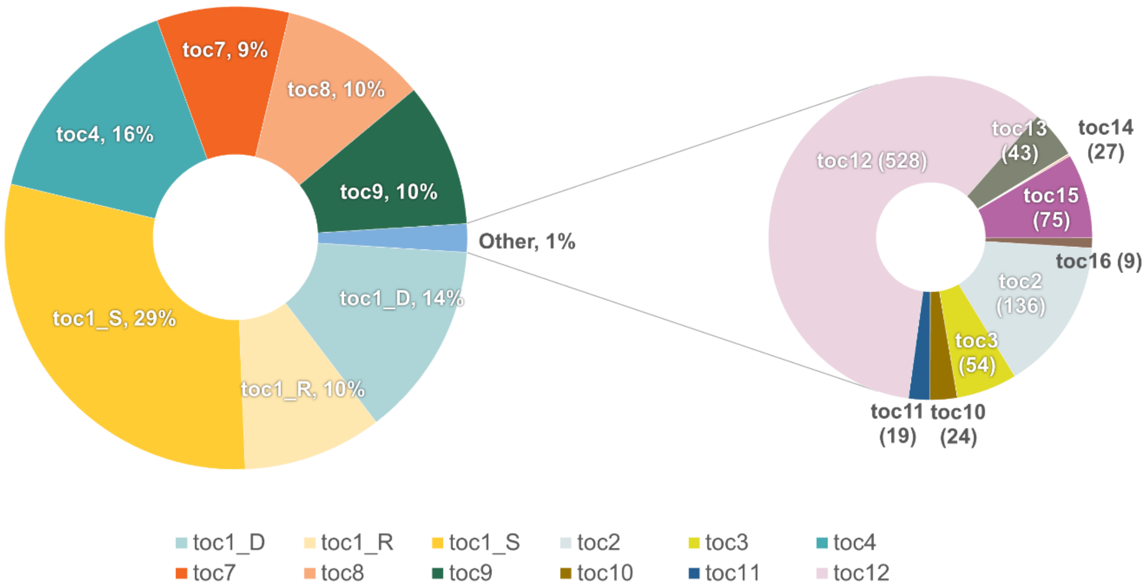


| **Travel Status** | **TOC Mode** | **Number of Participants** | **Travel Status** | **TOC Mode** | **Number of Participants** |
|---|---|---|---|---|---|
| Shared-ride Driver | 1 | 6,141 | Shared-ride Rider (continue) | 9 | 4,523 |
| | 2 | 136 | | 10 | 24 |
| | 7 | 4,170 | | 11 | 19 |
| | 8 | 4,604 | | 12 | 528 |
| Solo-ride Driver | 1 | 13,229 | | 13 | 43 |
| Shared-ride Rider | 1 | 4,375 | | 14 | 2 |
| | 3 | 54 | | 15 | 75 |
| | 4 | 7,068 | | 16 | 9 |

## (6) Public Transit Ridership

The ridership of SAFVs and buses resulting from the mobility portfolio is shown in Figure 6.14. The number of SAFVs operating during the morning peak hours is set to be 10. The results show that the average number of passengers on the each SAFV is approximately 6.5. During the same time period, the total number of bus passengers is 31, on average. Although at first glance it might seem like the usage of public transit systems is not significant, it should be noted that it still represents an improvement over current ridership statistic. More importantly, the results exemplify the potential of strategies such as incentives or benefits for public transit to promote public transit ridership using this framework.

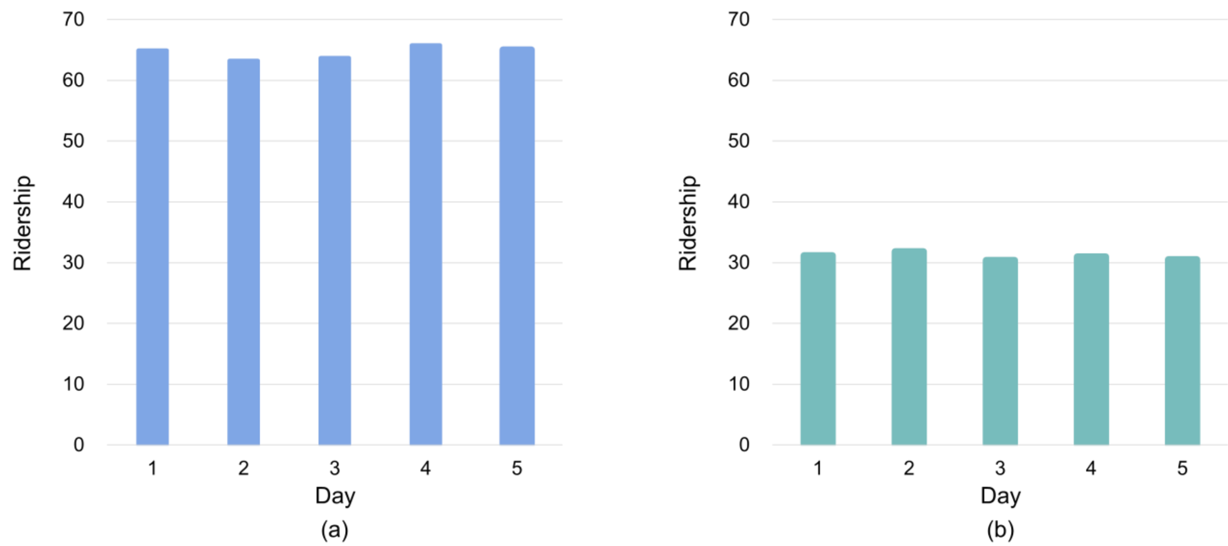


Figure 6.14 Ridership in (a) SAFVs and (b) Bus at Iteration 7

## 6.4.3 Changes in the Number of Shared Autonomous Fleet Vehicles

In the previous section, we assumed that the people can initiate their mobility portfolio at any day of the mobility bundling period. Keeping that assumption, in this section we perform a sensitivity analysis on the number of SAFVs in the system. This analysis can show the relationship between system performance and the number of matched participants. From this section, we reduce the sample size in half, and so that the total number of the potential shared-ride rider and driver are 6,000 and 12,500, respectively.

### (1) System Performance

First, we analyze the impacts of changes in the number of SAFVs without the learning process. Table 6.4 and Figure 6.15 show the percentage of matched riders, as the total number of SAFVs increases from 10 to 100. We find that the matching rate shows a modest increase as the number of vehicles increases. We observe a significant decrease in Vehicle-Miles-Traveled (VMT) as the number of SAFVs increases. The VMT reduction gap between the SAFV 10 and SAFV 100 cases is 4,000 units.

Table 6.4 Changes in matched riders and SAFV passengers

| Number of SAFVs | Matched Riders | Matching Ratio | SAFV Passengers |
|---|---|---|---|
| 10 | 4,595 | 0.766 | 53 |
| 20 | 4,606 | 0.768 | 104 |
| 30 | 4,613 | 0.769 | 148 |
| 40 | 4,623 | 0.77 | 198 |
| 50 | 4,639 | 0.773 | 247 |
| 60 | 4,651 | 0.775 | 301 |
| 70 | 4,662 | 0.777 | 354 |
| 80 | 4,673 | 0.779 | 404 |
| 90 | 4,683 | 0.78 | 446 |
| 100 | 4,691 | 0.782 | 484 |

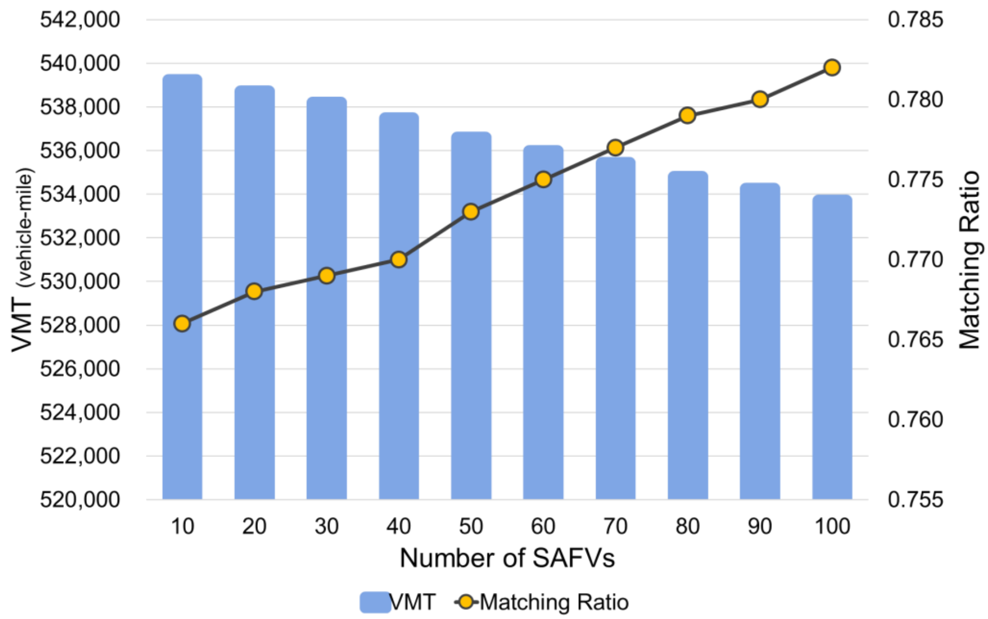


Figure 6.15 Variation in VMT with respect to the number of SAFVs

### (2) Mobility Portfolio Cost Savings

We perform the mobility portfolio learning process for four different SAFV numbers (10, 20, 50, and 100) and Figure 6.16 shows the average travel cost of shared-ride drivers and riders for each case after 7 iterations. Without the mobility portfolio scheme, the average travel cost for each participant is $14.82. It is interesting to note that in all cases both drivers and riders incur cost savings of $9.73 and $8.1 respectively.

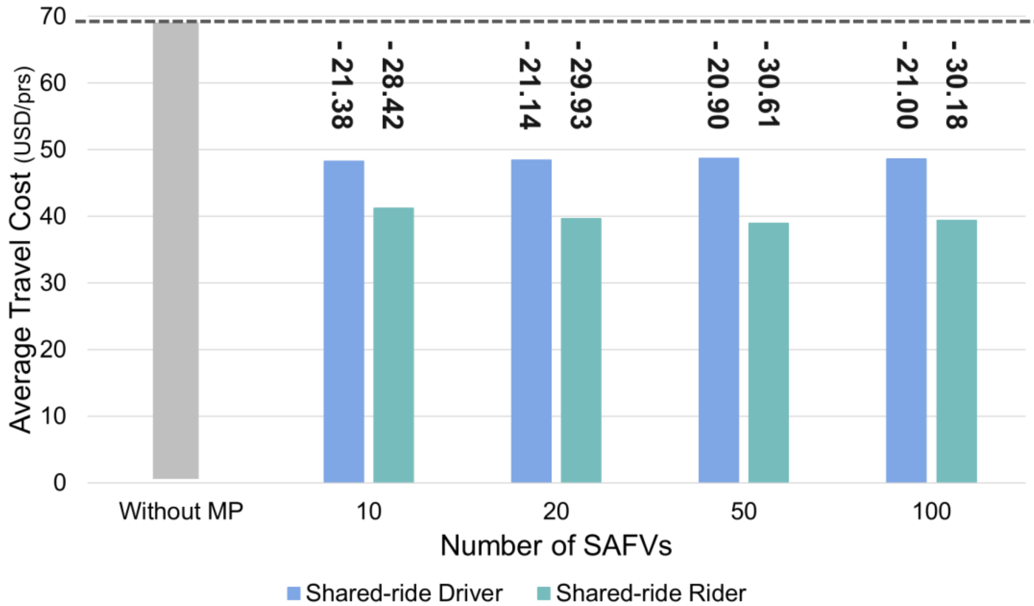


Figure 6.16 Individual's average travel cost at convergence state

### 6.4.4 Extended TOC mode pool

In this section, we introduce a carsharing service to the system. Unlike commercial carsharing services (i.e., carsharing vehicles are owned by companies and it has designated depos), we propose a peer-to-peer (P2P) carsharing system composed of private vehicle owners who are willing to lend their car when it is being used by them.

In this shared transportation system, both shared-ride riders and drivers can be carsharing owners. The difference in the owner types comes from where the carsharing vehicles are parked. For shared-ride riders, their car is located at their origins (i.e., home) while for shared-ride drivers, their vehicles are parked near their destinations (i.e., work). Furthermore, the amount of time that can be rented is shorter if a car belongs to a shared-ride driver because they have to use it to go back to their home. On the other hand, it is longer if a car belongs to a shared-ride rider because they are less reliant on one vehicle. The amount of time will be an important factor especially when we extend the mobility portfolio scheme to cover the entire day rather than the morning peak hours. This is because, in that case, we would need to consider system participants' daily activities, their activity type, and durations, that will impact their decision to be a shared-ride driver or riders. This will also influence the availability of P2P carsharing services can be changed every day or even every time.

To simplify the problem, we consider that only shared-ride drivers provide their car for P2P carsharing services. To make an effective comparison, we also adhere to the same simulation settings and the sample size described in section 6.4.1. To perform the multimodal ridematching problem, we utilized the function that we defined in section 5.3.2 (2). Furthermore, we assume that riders do not need to return carsharing vehicles to owners. This means that we consider only one bound trip (i.e., work trip) only, guaranteeing that one P2P carsharing vehicle can be matched to one shared-ride rider.

### (1) Sensitivity Analysis

In this section, we perform a sensitivity analysis on the number of carsharing participants in the system with the 12,500 drivers and 6,000 riders. Figure 6.17 shows the impact of the carsharing services. The base scenario for comparison is 0%, which represents no P2P carsharing vehicles in the system. As more people become P2P carsharing providers, the number of people using it increases until the carsharing percentage reaches 60%. After that point, the carsharing usage gradually plateaus.

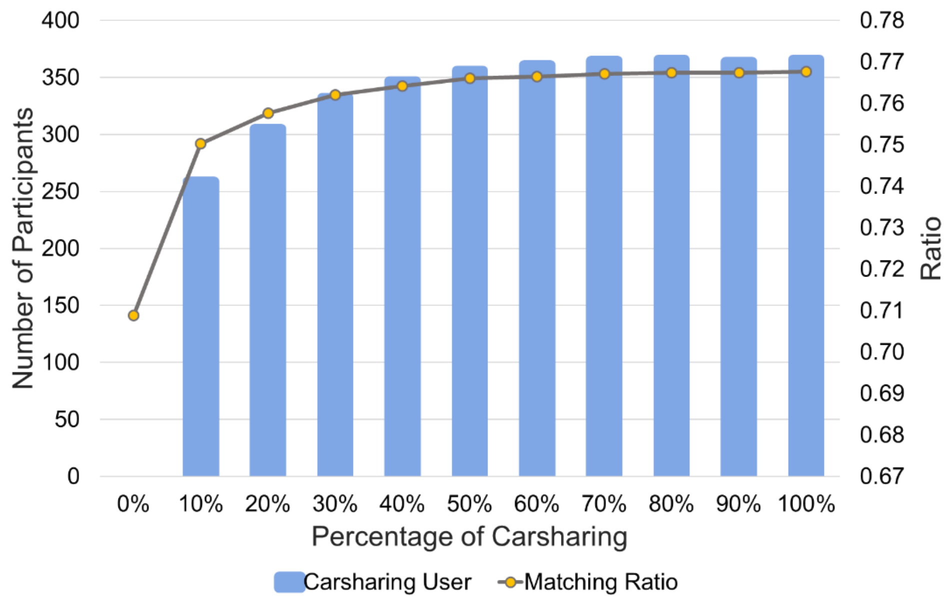


Figure 6.17 Sensitivity analysis over the number of carsharing participants in the system

Figure 6.18 illustrates the P2P carsharing usage as the total number of shared-ride drivers increases from 10,000 to 15,000. For a given number of participants, we generate multiple random problem instances by changing the ratio of P2P carsharing providers. While keeping the number of shared-ride riders fixed, Figure 6.18 suggests that when the total number of drivers become increases, the carsharing usage decreases. It is intuitive to expect this result because shared-ride rides have a greater chance to be matched with drivers when there are sufficient number of drivers, and vice versa. For example, in the 'Driver 10,000' case, shared-ride drivers are only about 1.6 times the number of riders, therefore a smaller number of riders can be served by drivers. It leads to riders to drive themselves by using carsharing services. Similar to the results depicted in Figure 6.17, after the number of carsharing providers reached 60%, the number of users does not increase significantly.

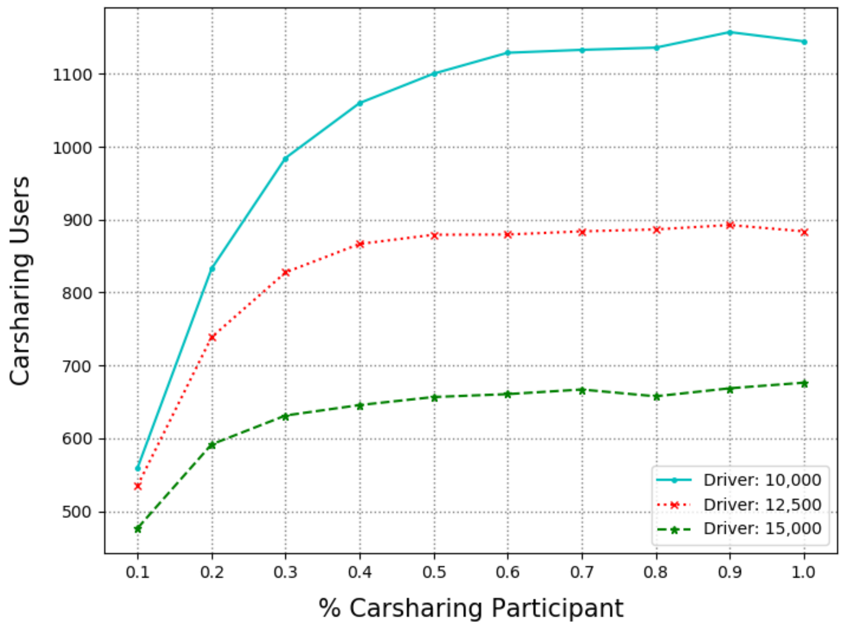

Figure 6.18 Sensitivity analysis over the carsharing users in the system

We also varied the number of shared-ride riders to study its impact on system performance. Figure 6.19 depicts the distribution of number of matched participants under different number of shared-ride drivers and riders, while changing the proportion of P2P carsharing providers. The results suggest that higher number of drivers results in higher matched riders. Table 6.5 depicts the matching ratio and the travel cost. The highest matching ratio is observed in the case of Driver 15,000 – Rider 6,000. Furthermore, the average travel cost becomes smaller when the number of drivers increases. As shown in Figure 6.19, P2P car sharing has significant impacts on the Driver 10,000 case. This result is consistent with the previous results shown in Figure 6.18.

Table 6.5 Individual's average travel cost and matching ratio over changes in the number of riders and drivers

| **Driver** | **Rider** | | | | | |
|---|---|---|---|---|---|---|
| | **6,000** | | **9,000** | | **12,000** | |
| | **Average travel cost** | **Matching ratio** | **Average travel cost** | **Matching ratio** | **Average travel cost** | **Matching ratio** |
| **10,000** | 9.63 | 0.710 | 9.57 | 0.615 | 9.94 | 0.513 |
| **12,500** | 9.71 | 0.751 | 9.17 | 0.689 | 9.34 | 0.596 |
| **15,000** | 9.99 | 0.766 | 9.13 | 0.733 | 8.97 | 0.671 |

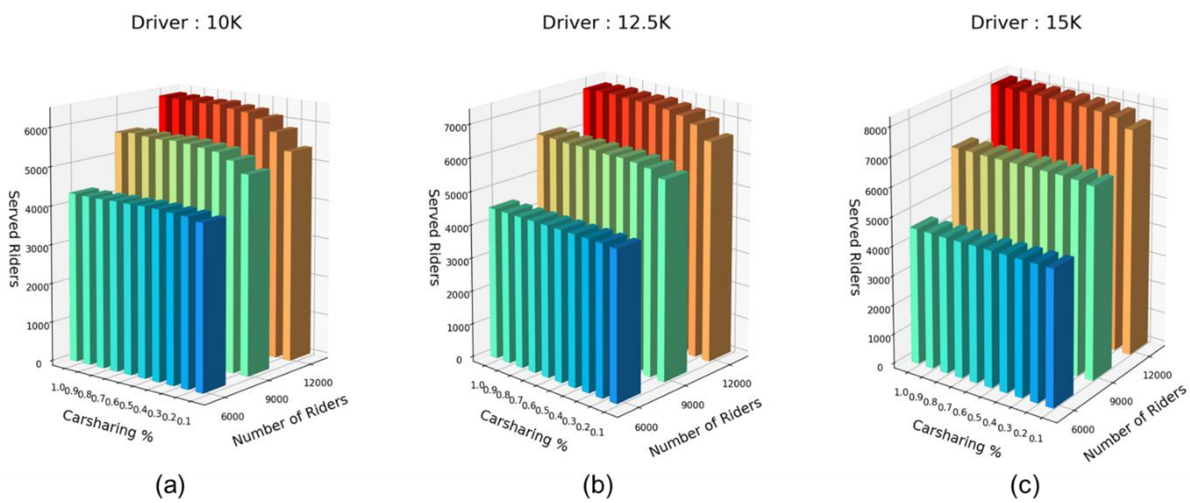


Figure 6.19 Distribution of number of matched riders: (a) Driver – 10,000, (b) Driver – 12,500, and (c) Driver – 15,000

## (2) TOC Mode Share Ratio

The introduction of P2P carsharing expands the TOC mode pool. Combining with the original TOC modes, it is possible to create additional TOC mode combinations. There are two basic TOC modes related to P2P carsharing mode (Table 6.6). The TOC mode-B 17 in Table 6.6 represents

P2P carsharing providers that have ‘not drive + Own (Share)’ travel option properties. TOC mode-B 18 presents P2P carsharing users with a chain of travel options such as Drive yourself, Need parking space, and ‘Not Own (Share).

Using these basic TOC modes, we generate 4 different types of TOC mode combinations. Table 6.7 shows the extended TOC mode combination lists. TOC Mode-C 19 shows a unique travel movement by including drive-alone and P2P carsharing options. This mode illustrates that shared-ride drivers, who do not share their empty seats while traveling, have riders after finishing their trip. In addition, TOC Mode-C 20 illustrates shared-ride drivers who serve other users and then allow their car to be used for P2P carsharing purposes. As mentioned previously, we do not consider the case where shared-ride riders can become P2P carsharing providers. If such shared-ride riders enter the system, we can easily depict their travel movement by integrating basic TOC Mode 4 and 18. TOC Mode-C 21 through 23 are used for shared-ride riders. TOC Mode-C 21 illustrates the SAFVs and P2P carsharing movement. TOC Mode-C 22 and 23 show the collaboration between public transit and walking with carsharing. The length of the extended TOC mode combination list can be increased arbitrarily depending on the combinations and their order.

Table 6.6 Extended TOC modes with P2P carsharing

| **TOC Mode** | **Travel Options (level)** | | | | | | |
|---|---|---|---|---|---|---|---|
| | **Driving Mode** | **Parking Space** | **Shared Empty Seat** | **Public Transit** | **Walk** | **Owner-ship** | **Vehicle Type** |
| … | … | … | … | … | … | … | … |
| 17 | 2 | 0 | 0 | 0 | 0 | 1 | X |
| 18 | 0 | 1 | 0 | 0 | 0 | 2 | X |

Table 6.7 Extended TOC mode combinations with P2P carsharing

| TOC Mode-C | TOC mode combination | | | |
|---|---|---|---|---|
| | TOC mode | TOC mode | TOC mode | Number of Connection |
| 19 | 1 | 17 | - | 0 |
| 20 | 2 | 17 | - | 1 |
| 21 | 4 | 18 | - | 2 |
| 22 | 4 | 5 | 18 | 2 |
| 23 | 4 | 6 | 18 | 1 |
| … | … | … | … | … |

Table 6.8 shows the TOC mode share results by each travel status when P2P carsharing is introduced (in the case of Driver 15,000 – Rider 6,000). Approximately half of the drivers are needed to serve around 75% of riders in the system indicating an acceptable level of ridematcing.

Table 6.8 Extended TOC mode share by travel status

| Travel Status | TOC Mode | Number of Participants | Travel Status | TOC Mode | Number of Participants |
|---|---|---|---|---|---|
| Shared-ride Driver | 1 | 6,325 | Shared-ride Rider (continue) | 9 | 1,513 |
| | 2 | 103 | | 10 | 16 |
| | 7 | 5,908 | | 11 | 11 |
| | 8 | 164 | | 12 | 143 |
| | 19 | 115 | | 13 | 5 |
| | 20 | 140 | | 14 | 0 |
| Solo-Driver | 1 | 6,744 | | 15 | 24 |
| Shared-ride Rider | 1 | 1,508 | | 16 | 4 |
| | 3 | 63 | | 21 | 255 |
| | 4 | 2,459 | | 22 | 0 |

## 6.5 Discussion

In this chapter, we developed a mobility portfolio modeling framework via an agent-based simulation platform and used it to implement various shared mobility services. To provide the best transportation itinerary plan, we proposed a mobility portfolio with a bundled plan and developed a mathematical formulation to find the mobility solution with the minimum travel cost. A two-stage learning mechanism is adopted to reflect the decision-making process of system participants who continually shift to find a better solution on another day or time period by shifting their travel statuses. Results obtained from a test study conducted with an agent-based simulator, DTALite/NeXTA, lends support to our hypothesis that the proposed mobility portfolio scheme provides the best solution for each individual and improves the system performance. Furthermore, since the mobility portfolio framework arrives at a least cost solution, it provides incentives to potential users to switch to shared mobility options in the future. From the numerical experiments, we also find the impacts of not only the mobility portfolio scheme itself, but also the changes in mobility providers in the shared transportation systems. From an individual point of view, the mobility portfolio scheme results in cost savings, and from an overall system perspective, it results in VMT reduction. In addition, by using the TOC mode concept proposed in this dissertation, it is possible to model complex shared travel movements comprising continuously shifting modes and ownership. Results show that the proposed scheme can promote the ridership of buses as a feeder to the next leg of their trips. Overall, results indicate that implementing the mobility portfolio schemes in shared transportation systems effectively improves the performance at the individual and system level.

We evaluate the performance of the proposed model using a simplified network and assume a single depot location which can limit accessibility to people who live far away from the depot. We assign a fixed travel cost discount value for every travel mode which may influence an individual's travel status choice behavior. Applying this framework on a more detailed and realistic network is expected to yield more insights into the behavioral effects of mobility portfolios and is part of our future research.

# Chapter 7

# Multi-Hop Ridematching Optimization Problem

## 7.1 Motivation

Since the purpose of the ridematching module in the mobility portfolio framework is to provide real-time matching results to the individual riders and the ridematching optimization is done by the individuals' apps for their benefits, a system-optimal matching is naturally improbable to happen. The ridematching module's suggestions are expected not to be optimal in terms of a system-wide matching ratio, total VMT, cost savings, etc. From the perspective of a service provider such as governments and regional planners, however, system-wide benefits cannot be overlooked. One advantage of a centralized mobility portfolio platform is that the system has access to every participant's trip information including origin/destination, departure/arrival time and their travel status during their mobility portfolio service subscription periods. Thus, it is reasonable to say that the portfolio provider can find the individually-optimal ridematching solution for each system participant before they start trips and provide it before they ask. The system informs users details such as when to start their trip, where to go to pick up riders or to wait until shared-ride providers arrive to pick them. In this chapter, we propose a novel approach to solve the multi-hop ridematching optimization problem, which is the backbone of many-to-one and many-to-many ridematching problems, by using a linear program.

## 7.2 Problem Description

We are interested in finding matched pairs that maximize system-wide benefits. The benefits could be defined in terms of VMT savings or cost savings generated by the matched pairs. Let $(i, j)$ denote a temporally matched pair of rider $i$ and driver $j$. If we disallow transfers between drivers then any rider can only be matched by a single driver. Thus, the set of matched drivers for rider $i$, $k_i$, can be represented as $k_i = \{j_1\}$ where $j_1$ indicates the first driver who serves rider $i$.

If we allow transfers, the set can be formed as $k_i = \{j_1, j_2, \dots, j_{V+1}\}$. Note that this is an ordered list whose number of elements cannot be greater than the allowable number of transfers, $V$ + 1. A path, $P_i$, that rider $i$ takes can be described as follows: $P_i = \{p_0, p_1, p_2, \dots, p_v, \dots, p_{V+1}\}$ where $p_0$ and $p_{v+1}$ represent origin and destination points of rider $i$ and $p_v$ represents a transfer point. Thus, driver $j_v$'s pickup and drop-off points for a matched rider $i$ are $(p_{v-1}, p_v)$ for all transfer points in $P_i$. Furthermore, if a rider makes several transfers during a trip, the rider is associated with a set of ordered multiple matched pairs, $M$, as follows: $M = \{(i, j_1), (i, j_2), \dots, (i, j_{V+1})\}$. Riders may also be associated with several sets representing different combination of drivers. So, a rider $i$ can have a group of sets of drivers described as follows $K_i = \{k_i^1, k_i^2, \dots, k_i^m\}$. Note that the total number of sets in a group is not limited.

To evaluate the benefits of a particular match, we calculate the VMT, or cost savings compared with traveling alone, which represents the base case scenario, in which riders use their car to drive to their destination alone if no ride-share can be identified. We define variables $v(i)$ and $u(i)$ to denote participant $i$'s origin and destination points, and a variable $h_{p,q}$ to denote the travel distance between node $p$ and $q$. The variable $h^*_{p,q}$ is actual travel distance that the $n^{th}$driver $j$ in rider $i$'s $m^{th}$driver set $k_i^a$ travels until he finishes his trip. The variable can be formulated as shown in equation (7.1):

$$h^*_{v(j_n),u(j_n)} = h_{v(j_n),p_{n-1}} + h_{p_{n-1},p_n} + h_{p_n,u(j_n)} \qquad \begin{array}{l} \forall n = (1,2,3,\dots,V+1) \\ \forall p_n \in P_i \\ \forall j_n \in k_i^m \end{array} \tag{7.1}$$

The first term in equation (7.1) represents the distance to pick rider $i$ up from driver $j$'s origin, and the second term is the distance between transfer point $p_{n-1}$ and $p_n$. The third term represents the distance between $p_n$ and driver $j$'s destination point. The VMT savings that are generated from a matched pair related to rider $i$ and his associated drivers is equivalent to the summation of each VMT saving, $w^m_{i,j}$, associated with matched rider $i$ and driver $j$ through the $m^{th}$ intermediate node in his matched driver set, $k_i^m$. The VMT savings for the matched pair can be calculated as follows:

$$w^m_{i,j} = h_{v(i),u(i)} + \sum_{\substack{n=1 \\ j_n \in l_i}}^{V+1} h_{v(j_n),u(j_n)} - \sum_{\substack{n=1 \\ j_n \in l_i}}^{V+1} h^*_{v(j_n),u(j_n)} \qquad \begin{array}{l} \forall n = (1,2,3,\dots,V+1) \\ \forall p_n \in P_i \\ \forall j_n \in k_i^m \\ \forall k_i^m \in K_i \\ k_i^m \in K_i \;\; \forall m = \{1,2,\dots,m\} \end{array} \tag{7.2}$$

We can use equation (7.2) to calculate the cost savings for the matched pair by multiplying it by the vehicle cost associated with participant $p$, $c_p$. Thus, equation (7.2) can be modified as follows:

$$w_{i,j}^{m} = h_{v(i),u(i)} \cdot c_i + \sum_{\substack{n=1 \\ j_n \in l_i}}^{V+1} h_{v(j_n),u(j_n)} \cdot c_{j_n} - \sum_{\substack{n=1 \\ j_n \in l_i}}^{V+1} h_{v(j_n),u(j_n)}^{*} \cdot c_{j_n} \tag{7.3}$$

Without considering transfers, several studies have formulated a one-to-one ridematching problem using a maximum-weight bipartite matching model (Figure 7.1a) and have solved it using a linear programming approach (Agatz et al., 2011; Wang et al.,2017). Wang et al., (2017) extend a one-to-one matching problem to a one-to-many matching problem by formulating that a driver can serve multiple riders, with the assumption that the driver can cover the entirety of riders' routes.

The bipartite graph approach is an efficient tool that arrives at a one-by-one matching solution without conflicts. However, there are some limitations of this approach when it is applied to the one-to-many matching problem. To illustrate this, let us assume that rider $r_1$ has two matched driver sets, $\{d_1, d_2\}$ and $\{d_3, d_4\}$. As shown in Figure 7.1b, the rider has four edges, $e_{i,j}$, that connect rider *i* and each matched driver $d_j$. Also, let us set the costs of each edge as follows: $c\left(e_{r_1,d_1}\right), c\left(e_{r_1,d_2}\right), c\left(e_{r_1,d_3}\right)$, and $c(e_{r_1,d_4})$ are 10, 2, 7, and 4 unites respectively. S, the costs of drivers set $\{d_1, d_2\}$ and $\{d_3, d_4\}$ are 12 and 11, respectively.

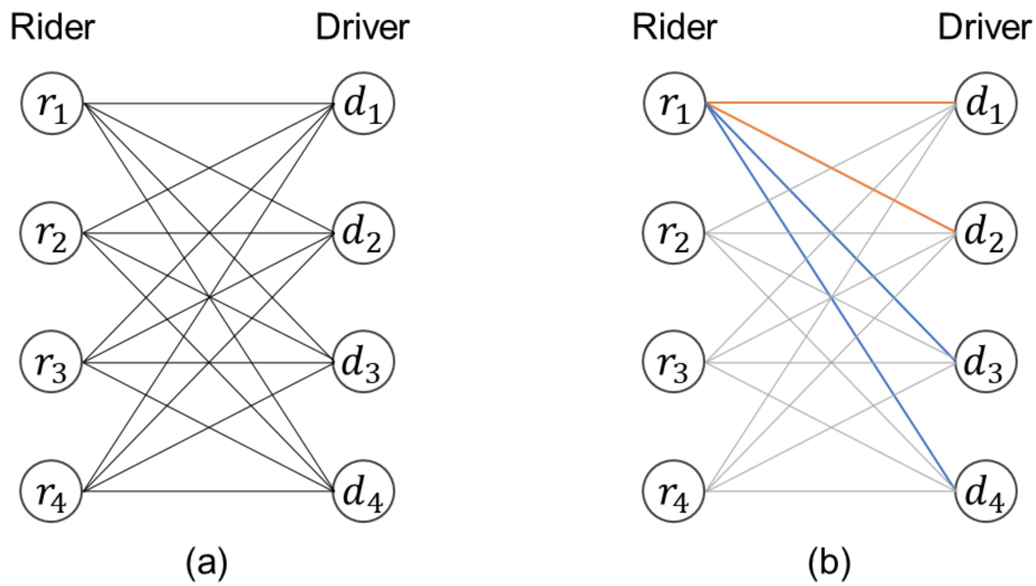


Figure 7.1 Bipartite graph examples for ridematching problems

Thus, the best matched set for rider $i$ is $\{d_1, d_2\}$. Using a learning-based programming method, however, rider $i$ is matched to $\{d_1\}$ or $\{d_1, d_3\}$ if and only if we set the decision variable as 2 or 0. Both solutions are incorrect because drivers in the solutions cannot finish the rider's trip. To mitigate this problem, we propose a novel graphical approach by adding intermediate nodes, $k_i^m$, between rider and driver groups. The purpose of the intermediate nodes is to discretize the feasible matched driver sets and to distinguish the riders' set associated with driver $j$ . From the definition of the intermediate nodes, it follows that each intermediate node is only connected to a single rider. Figure 7.2 illustrates the proposed graphical transformation.

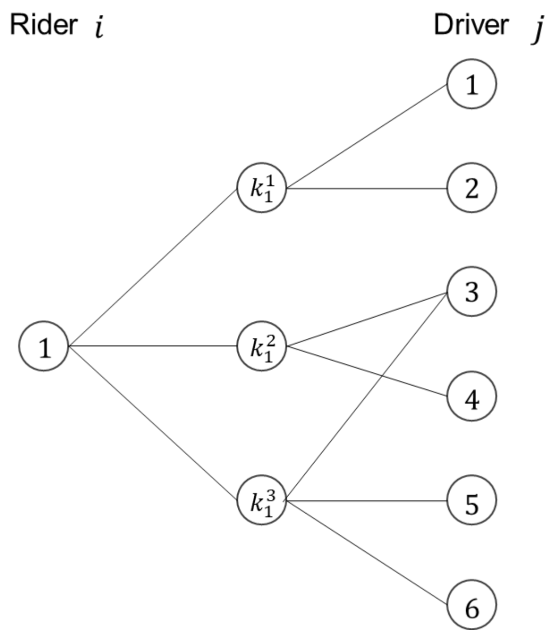

Figure 7.2 Graphical approach for one-to-many matching problem

As shown in Figure 7.2, it follows that rider 1 has three available driver sets and driver 3 can be associated with two different sets. Also, the maximum number of transfers is 2, because there are three drivers in set 3. It is worth mentioning that the costs for edges which connect riders and intermediate points are 0, because these edges are virtual and are only used to separate the feasible driver sets. The costs for rider 1 and its feasible driver sets can be automatically calculated by adding costs generated from edges associated with each set. For instance, from the edge $(k_1^1, 1)$, we know that rider 1 is matched with driver 1 who belongs to the first matching set. We can also calculate also cost savings between rider 1 and driver 1 using equation (7.3).

In the case of many-to-many ridematching problem, drivers can serve multiple riders and riders can use multiple drivers. The proposed graphical approach can be easily implemented in this scenario by adding another type of intermediate node named $g$-intermediate node that includes a driver who serves more than 2 riders, henceforth known as $g$-driver to the graph. The $g$-

intermediate nodes contain a list of multiple riders, $lr = \{p, q, \dots, r\}$. Thus, we set a $g$-intermediate node as follows: $g^{z}_{lr} = \{k^{n}_{p}, k^{m}_{q}, \dots, k^{w}_{r}\}$. The graph may have a set of g-intermediate nodes, $G$. Note that the length of the $g$-intermediate nodes cannot be greater than vehicle capacity, $VC$. Figure 7.3 exemplifies a graph that is applicable for the many-to-many matching problem.

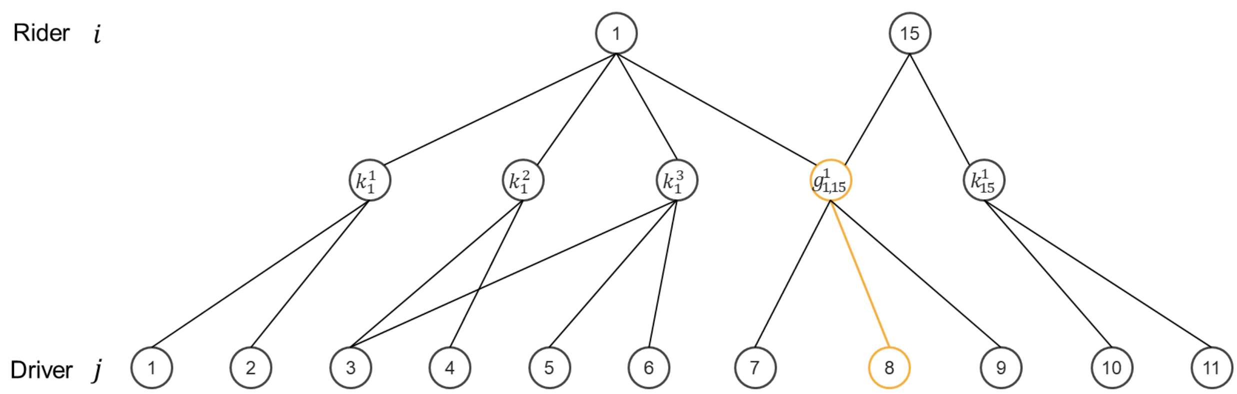


Figure 7.3 Graphical approach for the many-to-many matching problem

VMT savings for driver 8 can be calculated by modifying equation (7.1) as follows:

$$h^{*}_{v(j_n),u(j_n)} = h_{v(j_n),p_{n-1}} \cdot \varphi + h_{p_{n-1},p_n} \cdot \omega + h_{p_n,u(j_n)} \cdot \tau \qquad \begin{array}{l} \forall n = (1,2,3,\dots,V+1) \\ \forall p_n \in P_i \\ \forall j_n \in k^{m}_{i} \\ k^{m}_{i} \in K_i \ \ \forall m = \{1,2,\dots,m\} \end{array} \tag{7.4}$$

Variables $\varphi, \omega$ and $\tau$ are binary variables whose values are defined as follows:

- if $j_n$ is a $g$-driver and rider $i$ is the first passenger of $j_n$, then $\varphi = 1, \omega = 1, \tau = 0$;
- if $j_n$ is a $g$-driver and rider $i$ is the last passenger of $j_n$, then $\varphi = 0, \omega = 1, \tau = 1$;
- if $j_n$ is a $g$-driver and rider $i$ is not the first or the last passenger of $j_n$, then $\varphi = 0, \omega = 1, \tau = 0$;
- if $j_n$ is not a $g$-driver, $\varphi = 1, \omega = 1, \tau = 1$ which is the same as equation (7.1).

Furthermore, to find the total pickup distance among passengers who use the same vehicle, we use equation (7.5), where the term $lr_n$ indicates the $n^{th}$ passenger in list $lr$.

$$h' = \sum_{n=1}^{VC-1} h_{u(lr(n)),v(lr(n+1)} \qquad \begin{array}{l} \forall n = (1,2,3,\dots,VC-1) \\ \forall lr(n) \in lr \end{array} \tag{7.5}$$

Equation (7.6) shows the total VMT savings in the many-to-many ridematching problem formulation.

$$\begin{aligned} w_{i,j}^m = h_{v(i),u(i)} &+ \sum_{\substack{n=1 \\ j_n \in l_i}}^{V+1} h_{v(j_n),u(j_n)} \\ &- \left( \sum_{\substack{n=1 \\ j_n \in l_i}}^{V+1} h^*_{v(j_n),u(j_n)} + h' \cdot \sigma \right) \end{aligned} \qquad \begin{array}{l} \forall n = (1,2,3,\dots,V+1) \\ \forall p_n \in P_i \\ \forall j_n \in k_i^m \\ k_i^m \in K_i \;\; \forall m = \{1,2,\dots,m\} \end{array} \tag{7.6a}$$

$$\sigma = \begin{cases} 1 & if\ list\ 'lr'\ contains\ rider\ i\ in\ g_{lr} \\ 0 & otherwise \end{cases} \tag{7.6b}$$

To calculate the cost savings for the matched pair, we first transform equation (7.5) into equation (7.7) by multiplying it with the vehicle cost related to participant $p$, $c_p$. Using equation (7.7), we finally arrive at the total cost savings as shown in equation (7.8).

$$h' = \sum_{n=1}^{VC-1} h_{u(lr(n)),v(lr(n+1)} \cdot c_{j_n} \qquad \begin{array}{l} \forall n = (1,2,3,\dots,VC-1) \\ \forall lr(n) \in lr \end{array} \tag{7.7}$$

$$\begin{aligned} w_{i,j}^m = h_{v(i),u(i)} \cdot c_i &+ \sum_{\substack{n=1 \\ j_n \in l_i}}^{V+1} h_{v(j_n),u(j_n)} \cdot c_{j_n} \\ &- \left( \sum_{\substack{n=1 \\ j_n \in l_i}}^{V+1} h^*_{v(j_n),u(j_n)} \cdot c_{j_n} + h' \cdot \sigma \right) \end{aligned} \qquad \begin{array}{l} \forall n = (1,2,3,\dots,V+1) \\ \forall p_n \in P_i \\ \forall j_n \in k_i^m \\ k_i^m \in K_i \;\; \forall m = \{1,2,\dots,m\} \end{array} \tag{7.8a}$$

$$\sigma = \begin{cases} 1 & if\ list\ 'lr'\ contains\ rider\ i\ in\ g_{lr} \\ 0 & otherwise \end{cases} \tag{7.8b}$$

## 7.3 Methodology

In the following sections, we formulate a multi-hop ridematching optimization problem that allows transferring between shared-ride mobility providers, and then provide a mathematical programming approach to maximize the total cost savings for all system participants.

### 7.3.1 Ride-share Match Graph Generation

As described in Figure 7.2, paths in the graph represent ride-share matches between riders and drivers. The key elements of the ride-share graph are rider nodes, mobility provider nodes, intermediate nodes, and links between these nodes. In the graph, all riders in the rider group, $R$, are considered as a rider node $i$. Similarly, drivers in share-ride driver group, $D$, are considered as a mobility provider node $j$. Other travel modes such as public transit, walk, and shared-bike, are considered mobility provider nodes. Links connect a node $i \in R$ on one side of the graph with a node $j \in D$ on the other side if and only it is feasible to establish a ride-share match with rider $i$ and driver $j$. If rider $i$ has multiple drivers, we create an intermediate node $k$.

We begin by preprocessing data for both shared-ride riders and drivers to reduce the size of the network by considering only the accessible spatiotemporal network within their travel time window. Instead of using the DP algorithm described in section 6.3.2 that provides an instant minimum travel cost matched partner to riders, we only perform a depth first search (DFS) on the reduced network for riders to find all possible combinations of mobility providers that complete a rider's entire trip itinerary. If there are mobility providers sets that cannot serve a rider's complete itinerary, we consider those mobility provider sets are infeasible.

Let assume that a rider has multiple feasible sets, each representing a different combination of mobility providers, and that the ride-share providers allow at most one transfer. The graph associated with this scenario becomes as shown in Figure 7.4a. Rider 1 in the figure has two direct matched pairs with driver 2 and driver 6 and two matched pairs with intermediate nodes. The maximum number of segmented pathways a rider can take is 2. Therefore, the total amount of flow that rider 1 can send to the segmented pathways is 0, 1, or 2. Note that the flow value are integers because they represent actual users. Considering the flow as a decision variable, we can formulate a maximum ridematching problem using a binary decision variable to represent a dummy driver for riders. As shown in Figure 7.4b, we add a dummy driver node, $d'$, and create four intermediate nodes, each connected to two links. By assigning a weight of 0 to the link connected to the dummy nodes, we ensure that these links do not impact total system cost savings, which is our objective function. In this example, the decision variable is a binary variable whose value is either 2 or 0, depending on the maximum number of transfers.

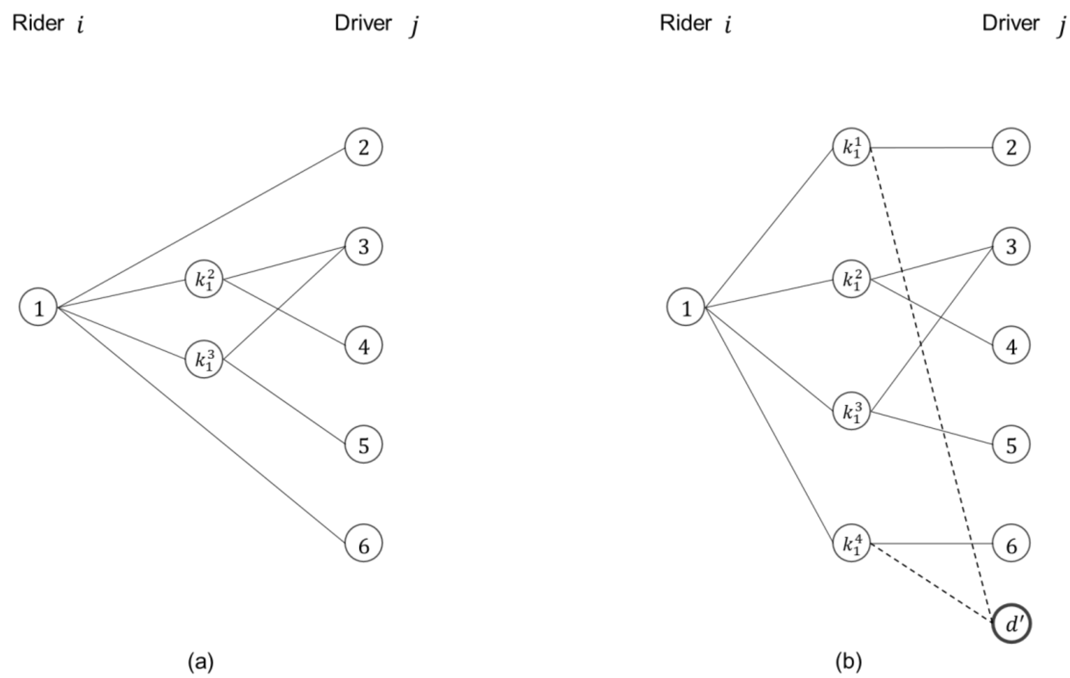


Figure 7.4 Example of feasible ride-share match graph

### 7.3.2 Mathematical Formulation

The multi-hop ridematching problem is structurally similar to the transshipment network problem which is a special case of the transportation problem in which the shipment of goods passes an intermediate destination before reaching their final destination. There are three different nodes defined in the transshipment problem: transshipment nodes, and supply and demand nodes. Transshipment nodes can have both incoming and outgoing links, whereas supply and demand nodes are points where goods enter or leave the network.

Using the properties of nodes in transshipment problem, we model shared-ride riders as supply nodes $R$, shared-ride drivers as demand nodes $D$, and intermediate nodes as transshipment nodes

$K$. Thus, the ride-share match graph has a set of all nodes $N = R \cup D \cup K$, and a set of links $A$. Depending on the objective function, the weight of each link in the ride-share matching graph is calculated using equations (7.6) and (7.8). A key difference between the transshipment problem and the multi-hop ridematching problem is that in the ridematching problem the weights of the links entering the intermediate nodes are assigned to be 0. Note that demand nodes can be extended if we consider other types of travel modes.

For the multi-hop ridematching problem, we use two decision variables as defined in equations (7.9)-(7.10). Equation (7.9) indicates that if rider $i$ uses the $m^{th}$ intermediate node $k$ then rider node $i$ will send its flows to the link that connects rider node $i$ and the $m^{th}$ intermediate node $k$. The amount of the flows is equivalent to the number of segmented pathways, and is calculated as the maximum number of transfers, $V + 1$.

$$x_i^m = \begin{cases} V+1 & if\ rider\ i\ use\ m^{th}\ intermediate\ node\ k \\ 0 & otherwise \end{cases} \tag{7.9}$$

$$x_{i,j}^m = \begin{cases} 1 & if\ a\ path\ is\ generated\ that\ connects\ rider\ i, driver\ j\ and\ m^{th}\ intermediate\ node\ k \\ 0 & otherwise \end{cases} \tag{7.10}$$

Now we proceed to outlining a problem that is not optimized based on the objectives of only the riders in the system but one that includes both riders and drivers. Referring to the earlier discussion in section 4.2.4, this problem would be one that leads to a system-level optimum, unlike the ridematching problem which is a rider-centric problem implemented for individual riders in temporal sequence. In addition, if we include information on all future riders and drivers into the problem, unlike in the ridematching problem that is implemented in real time with only information on the drivers and riders who have entered the system thus far, then this new problem can be considered a benchmark problem that yields the best-possible solution for the system. We formulate this best-solution as a linear program (LP) and solve it, so that the ridematching solutions can be compared against that benchmark.

Equation (7.11a) represents the objective function of the system-wide LP problem. Constraint sets (7.11b) and (7.11c) limit the total number of travel segments for rider $i$ and driver $j$'s vehicle capacity, $VC_j$. Equation (7.11d) is needed to ensure flow conservation. We add a new constraint set (7.11e) that indicates all edges which originate from the same intermediate node to have the same value (i.e., either 1 or 0). Therefore, this equation guarantees that riders are matched to drivers who are located in the same ride-share match list.

$$max \sum_{(i,j)\in A} w_{i,j}^m \cdot x_{i,j}^m \qquad (7.11a)$$

subject to

$$\sum_m x_i^m \leq V + 1 \qquad \forall m = \{1,2,\dots,m\} \qquad (7.11b)$$

$$\sum_i \sum_m x_{i,j}^m \leq VC_j \qquad \forall j_n \in k_i^m \; k_i^m \in K_i \;\; \forall m = \{1,2,\dots,m\} \qquad (7.11c)$$

$$\sum_m x_i^m = \sum_{j\in k_i^m} x_{i,j}^m \qquad \forall j_n \in k_i^m \; k_i^m \in K_i \;\; \forall m = \{1,2,\dots,m\} \qquad (7.11d)$$

$$x_{i,j_1}^m = x_{i,j_2}^m = \cdots = x_{i,j_{V+1}}^m \qquad \forall j_n \in k_i^m \; k_i^m \in K_i \;\; \forall m = \{1,2,\dots,m\} \qquad (7.11e)$$

$$x_i^m, x_{i,j}^m \geq 0 \qquad (7.11f)$$

It is worthwhile to mention that if we assume the capacity of driver $VC_j = 1$, then the multi-hop ridematching problem becomes a many-to-one problem; and if $VC_j \geq 2$, it results in a many-to-many problem. For the many-to-many ridematching problem cases, some driver may connect to several k-type and g-type intermediate nodes. In order to ensure that the drivers' path is not obstructed by infeasible riders and only matched to rider(s) coming from a single $m^{th}$ k-type intermediate node or a single $n^{th}$ g-type intermediate node, we add more constraints as follows:

$$\frac{\sum_i \sum_m x_{i,j}^m}{VC_j^m} + \frac{\sum_i \sum_n x_{i,g}^n}{VC_j^n} = 1 \tag{7.11g}$$

$$\sum_i x_{i,j}^n = \sum_j x_{i,j}^n \tag{7.11h}$$

In equation 7.11g, the variable $VC_j^m$ is always equal to 1; and $VC_j^n$ depends on the number of riders that a driver can serve. Note that if a driver $j$ associated with a $n^{th}$ g-node can serve multiple riders then his $VC_j^n$ is equal to the number of served riders; however, a driver $k$ in the same g-node is only serve a single rider, his $VC_k^n$ is equal to 1. Equation 7.11h shows the flow conservation rule for riders who are matched to drivers in the $n^{th}$ g-type node.

In next section, we generate several ridematching problem instances. All problems are solved on a PC with Core i5 3.5GHz and 24GB of RAM, using the PYTHON programming language and PULP solver with standard tuning.

## 7.4 Results

### 7.4.1 System Performance

#### (1) Cost Savings

We first investigate the relationship between the number of drivers in the system and total cost savings. To that effect, we generate two many-to-one ridematching problem instances: single-hop, single-rider (1 transfer, 1 occupancy) and multi-hop, single-rider (2 transfers, 1 occupancy), and vary the number of drivers from 6,000 to 12,000 while keeping the number of riders constant at 6,000. Figure 7.5 shows the results of this analysis. Cost savings for both problem instances increase as the number of drivers increases. Overall, the multi-hop, single-rider problem instance exhibits higher cost savings than its single-hop, single-rider counterpart. The biggest cost savings gap between the two problem instances is attained when the number of drivers is 7,500. In the case of 11,000 drivers, the cost savings for both instances are within 1 % of each other, after which it widens again.

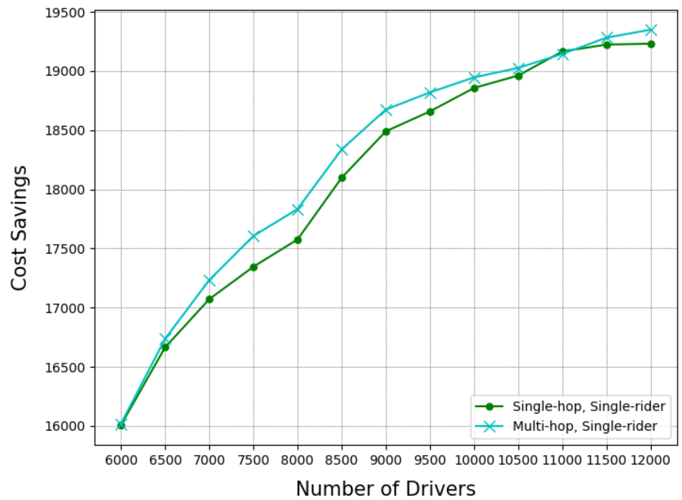


Figure 7.5 Optimal cost savings for many-to-one matching problems

### (2) Percentages of Served Riders

We compare the ridematching performance measure of the two problems using the linear programming (LP) method proposed above (Equations 7-11a through 7-11f) and compare the results with those obtained from a real-time ridematching algorithm utilized in chapter 6 for comparison. The intent here is to investigate how close to the system optimality the ridematching solutions come. It should be noted that the LP solutions are not practically feasible, both due to lack of future information availability and due to the agency's usual inability to force any rider to pay more for mobility so that another rider pays sufficiently less to reduce the system level costs and payments by riders.

Table 7.1 shows comparative results for the single-hop, single-rider scenario. In terms of the number of served riders and the average cost savings per person, the values obtained from the LP method are higher than the ones from the real-time matching algorithm. This indicates, even though it does not guarantee the optimal cost savings or matched pair for each individual, from the system standpoint, the LP method provides more matching opportunities, though practically they may be infeasible to achieve. Alternatively, it can be said that a practical ridematching solution will be suboptimal though still beneficial from the system standpoint.

The most important conclusion is indeed that the ridematching solutions are yielding system level benefits not substantially below the benchmark LP optimum. Another key insight from this analysis is that the number of transfers goes down as more drivers are present in the system. This is to be expected; as more drivers are available, the probability of being matched to riders without transferring increases.

Table 7.1 Performance comparison in a single-hop, single-rider scenario

| | Num. (%) served rider | | Avg. cost savings | | Avg. num. transfer | |
|---|---|---|---|---|---|---|
| Driver | Real-time | LP | Real-time | LP | Real-time | LP |
| 6,000 | 1,719 (29%) | 2,142 (36%) | 5.72 | 7.39 | 0.52 | 0.59 |
| 6,500 | 1,842 (31%) | 2,270 (38%) | 5.58 | 7.29 | 0.49 | 0.58 |
| 7,000 | 1,968 (33%) | 2,377 (40%) | 5.40 | 7.15 | 0.47 | 0.55 |
| 7,500 | 2,124 (35%) | 2,505 (42%) | 5.29 | 6.95 | 0.45 | 0.54 |
| 8,000 | 2,209 (37%) | 2,564 (43%) | 5.17 | 6.89 | 0.43 | 0.53 |
| 8,500 | 2,325 (39%) | 2,686 (45%) | 5.10 | 6.76 | 0.41 | 0.52 |
| 9,000 | 2,415 (40%) | 2,747 (46%) | 4.99 | 6.71 | 0.40 | 0.50 |
| 9,500 | 2,497 (42%) | 2,816 (47%) | 4.93 | 6.56 | 0.38 | 0.48 |
| 10,000 | 2,567 (43%) | 2,870 (48%) | 4.80 | 6.51 | 0.37 | 0.47 |
| 10,500 | 2,616 (44%) | 2,908 (48%) | 4.69 | 6.42 | 0.35 | 0.46 |
| 11,000 | 2,681 (45%) | 2,983 (50%) | 4.62 | 6.32 | 0.34 | 0.45 |
| 11,500 | 2,752 (46%) | 3,034 (51%) | 4.55 | 6.22 | 0.32 | 0.43 |
| 12,000 | 2,819 (47%) | 3,055 (51%) | 4.51 | 6.13 | 0.31 | 0.43 |

Table 7.2 shows the same comparison for a multi-hop, single-rider model. The results suggest that the LP method shows better results in all ridematching performance measures than the real-time matching algorithm. Compared with the single-hop single-rider scenario, we find that the average number of transfers in the multi-hop, single-rider scenario is slightly higher.

Table 7.2 Comparisons of matching performance measures with a multi-hop, single-rider model

| | Num. (%) served rider | | Avg. cost savings | | Avg. num. transfer | |
|---|---|---|---|---|---|---|
| Driver | Real-time | LP | Real-time | LP | Real-time | LP |
| 6,000 | 1,811 (30%) | 2,155 (36%) | 5.79 | 7.44 | 0.64 | 0.61 |
| 6,500 | 1,924 (32%) | 2,277 (38%) | 5.67 | 7.34 | 0.61 | 0.59 |
| 7,000 | 2,071 (35%) | 2,369 (39%) | 5.56 | 7.22 | 0.57 | 0.57 |
| 7,500 | 2,169 (36%) | 2,477 (41%) | 5.38 | 6.99 | 0.53 | 0.54 |
| 8,000 | 2,265 (38%) | 2,535 (42%) | 5.19 | 6.92 | 0.50 | 0.54 |
| 8,500 | 2,368 (39%) | 2,651 (44%) | 5.14 | 6.77 | 0.47 | 0.52 |
| 9,000 | 2,452 (41%) | 2,733 (46%) | 5.06 | 6.74 | 0.45 | 0.51 |
| 9,500 | 2,542 (42%) | 2,814 (47%) | 4.96 | 6.61 | 0.43 | 0.49 |
| 10,000 | 2,585 (43%) | 2,851 (48%) | 4.85 | 6.51 | 0.41 | 0.48 |
| 10,500 | 2,663 (44%) | 2,925 (49%) | 4.72 | 6.45 | 0.39 | 0.47 |
| 11,000 | 2,713 (45%) | 2,983 (50%) | 4.65 | 6.32 | 0.38 | 0.45 |
| 11,500 | 2,770 (46%) | 3,035 (51%) | 4.59 | 6.24 | 0.36 | 0.44 |
| 12,000 | 2,848 (47%) | 3,076 (51%) | 4.56 | 6.21 | 0.34 | 0.44 |

## 7.4.2 Scenario Analysis

In this section, we evaluate the proposed graphical method on several ridematching problems. We set an OD-based matching problem as a base scenario and create several scenarios by varying the number of transfers for riders and the number of served riders for drivers. Table 7.3 shows the summary of the created scenarios. The difference between scenario 1 and 4 is the number of transfers that riders can make. Similarly, the number of riders that drivers can serve is different in scenario 2 and 3. For instance, in scenario 2, we allow users 1 transfer as rider and restrict the total number of riders for a driver to 2. We analyze the performance of each scenario with both the real-time matching algorithm and the LP method with the graphical approach. We set the maximum number of transfers as 2 and set the maximum number of drivers a rider can accept to 3 (Masoud and Jayakrishnan, 2017b).

The number of drivers and riders are fixed at 12,500 and 6,000 respectively, Figure 7.6 shows the cost savings in each scenario. The solutions for all scenarios converge at optimal points which are, by definition, greater than the cost savings obtained without the optimization approach. The results also confirm our intuition that relaxing the problem, i.e., by increasing the allowable number of transfers and riders, leads to higher cost savings.

Table 7.3 Scenario setting

| **Scenario** | **Property** | | **Matching Problem Type** | **Description** |
|---|---|---|---|---|
| | **Transfer** | **Capacity** | | |
| Base | 0 | 1 | One-to-One | OD-based |
| 1 | 1 | 1 | Many-to-One | Single-hop (1), Single-rider (1) |
| 2 | 1 | 2 | Many-to-Many | Single-hop (1), Multi-rider (2) |
| 3 | 1 | 3 | Many-to-Many | Single-hop (1), Multi-rider (3) |
| 4 | 2 | 1 | Many-to-One | Multi-hop (2), Single-rider (1) |
| 5 | 2 | 2 | Many-to-Many | Multi-hop (2), Multi-rider (2) |
| 6 | 2 | 3 | Many-to-Many | Multi-hop (2), Multi-rider (3) |

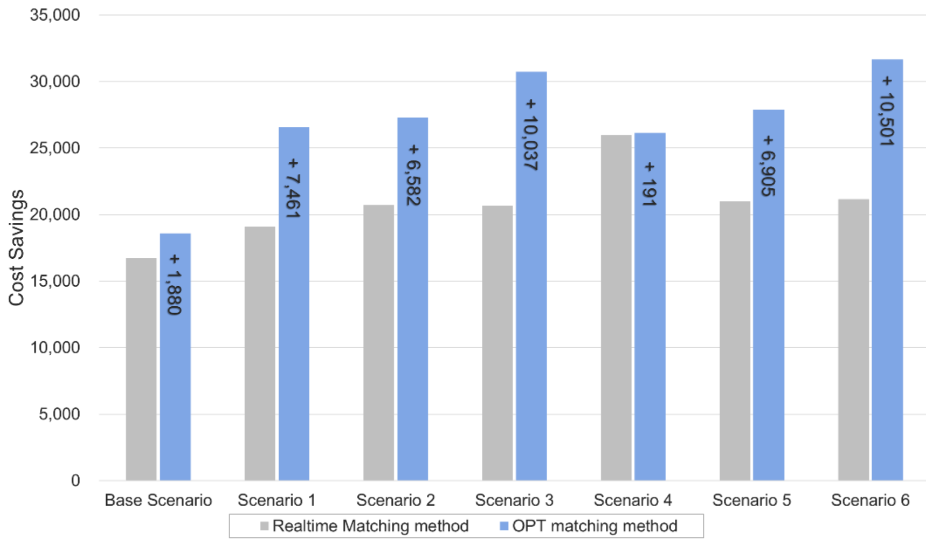

Figure 7.6 Cost savings comparisons by scenarios

Table 7.4 shows the comparative results of all scenarios. In the base scenario, the number of served riders is 2,899 which also represents the lowest matching ratio of 48%. The highest number of served riders is found in scenario 6 which has the most relaxed matching requirements.

The computational time shows a commensurate increase as the number of served riders increases. This is because every served rider generates at least two subsequent edges in the abstract transshipment network. The number of intermediate nodes that a single rider generates depends on the number of elements in their associated driver set, which can include multiple drivers. For instance, if a rider has five potential driver sets and each set has three drivers (i.e., 2-transfer allowing case), then there are five edges are created from a ride node to five intermediate nodes, and each intermediate node has three edges which connect to driver nodes. Therefore, for a single rider, 15 edges are generated, which contributes to the computational time.

Table 7.4 Comparisons of matching performance for different scenarios

| Scenario | Num. of served riders (%) | Num. of transfers | Avg. vehicle occupancy | Wait in transfer (min) | | | Computational time (sec) |
|---|---|---|---|---|---|---|---|
| | | | | Min. | Avg. | Max. | |
| Base | 2,899 (48%) | NA | 1.08 | NA | | | 2.30 |
| 1 | 4,102 (68%) | 0.44 | 1.02 | 1.00 | 2.99 | 10.00 | 4.24 |
| 2 | 4,269 (71%) | 0.40 | 1.52 | 2.00 | 2.83 | 9.00 | 5.19 |
| 3 | 4,334 (72%) | 0.39 | 1.54 | 2.00 | 2.75 | 9.00 | 4.35 |
| 4 | 3,766 (63%) | 0.53 | 1.01 | 1.00 | 2.78 | 10.00 | 4.29 |
| 5 | 4,069 (67%) | 0.38 | 1.53 | 2.00 | 2.71 | 9.00 | 7.77 |
| 6 | 4,656 (78%) | 0.42 | 1.55 | 2.00 | 2.72 | 9.00 | 7.71 |

Figure 7.7 depicts the optimality characteristics of the matching algorithm. Before the optimization is performed, there are potential riders who are temporarily matched with drivers and some drivers who are also temporarily tied with multiple riders. A driver can serve the riders who are associated with him if and only if their travel paths are not in conflict with each other, and if the vehicle capacity constraints are not violated. If these conditions are not met, drivers can only serve a subset of riders associated with them. This accounts for the gap between the potential matched riders and the optimal matched riders. The base scenario, which has the tightest matching constraints, shows the largest gap between the potential and optimally matched riders. The optimality gap is reduced as the matching requirements are relaxed, indicating that the ridematching performance depends on how the ridematching problem conditions are configured.

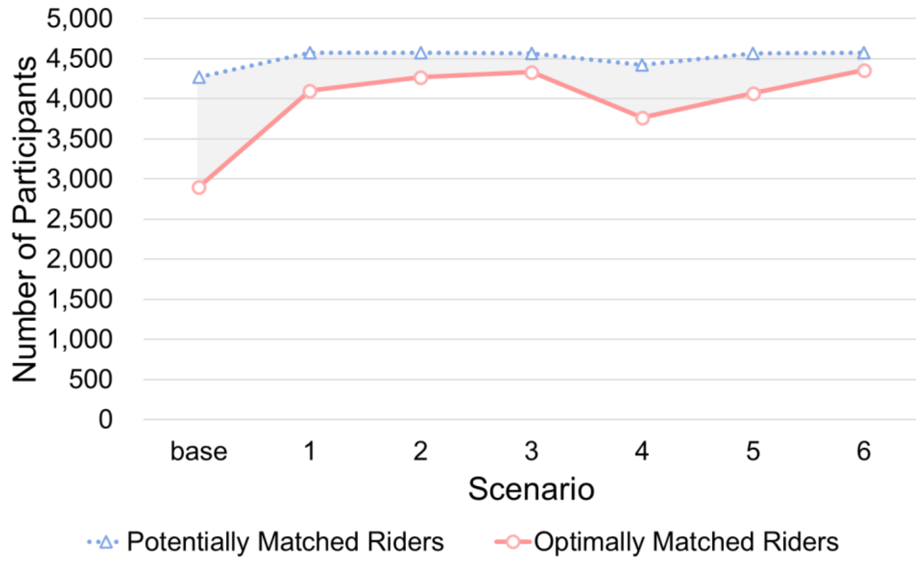


Figure 7.7 Optimal matched riders vs potential matched riders

### 7.4.3 Numerical Experiments

#### (1) Varying Rider Demand

We also evaluate the performance of the graphical approach in terms of the cost savings and computational time, by varying the number of riders and keeping the number of drivers fixed. Several test scenarios representing different types of matching problem instances are generated. In the case of the many-to-many matching problem instance, riders are able to transfer up to 2 times and drivers can serve no more than 2 riders. In the many-to-one matching scenario, we retain the same constraint for riders, but we limit the number of riders that a driver can serve to 1.

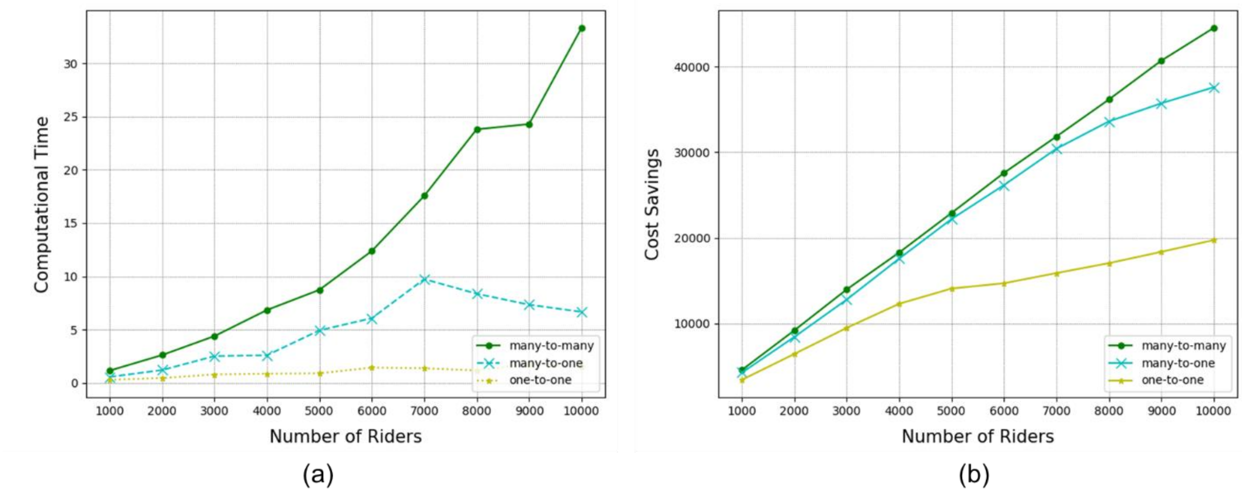


Figure 7.8 Computational time comparison

The computational times are depicted in Figure 7.8a. For the one-to-one matching instance, the computational times do not vary significantly as the number of riders increases. That is because in this case, the addition of new drivers does not generate intermediate nodes, and the maximum number of edges that one rider can create is equal to the number of total drivers, which remain constant. However, once we consider transferring, we need to generate intermediate nodes, which leads to the creation of an additional edge that connects riders and intermediate nodes. For illustrative purposes, if a driver has 3 intermediate nodes and each intermediate nodes has 2 edges that link two drivers, 10 new edges are generated in the graph. Therefore, the many-to-many matching instance incurs longer computational times compared to other scenarios. Figure 7.8b shows the cost savings for each instance. In line with our previous results, increasing the number of riders leads to higher cost savings.

Figure 7.9 shows the number of matched riders for various problem sizes and ridematching instances. In figures 6.9b and 6.9c, the gap between matched drivers and riders represents the proportion of all drivers who are required to serve riders. In the many-to-one matching instance, the number of drivers needed is higher than the number of riders in all cases. The biggest difference occurs when the number of riders is 10,000, needing twice as many drivers to serve riders. In the many-to-many matching instance, the gap between matched drivers and served riders is almost negligible. The number of drivers needed is less than the number of riders when the number of riders rises above 7,000 (shaded red in Figure 7.9c), which has implications for the system operators in terms of economies of scale. The distinguishing features of the many-to-many and the many-to-one matching scenario is the number of required drivers. Based upon the results, we can conclude that more restrictive ridematching constraints reduce the vehicle usage efficiency for drivers.

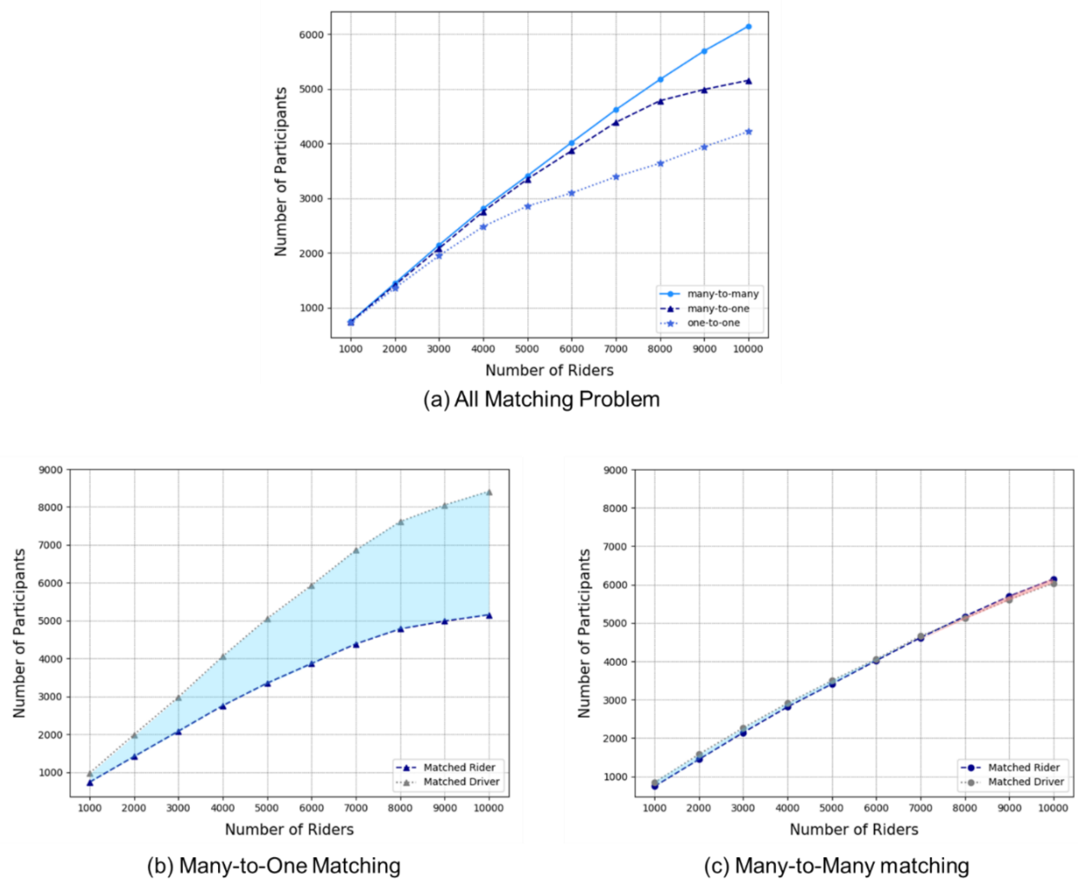


Figure 7.9 Percentage of successful matches

## (2) Varying Demand and Supply

In the previous section, we analyzed the performance of the algorithm in different matching problem scenarios while keeping the number of drivers sized. In this section, we vary both ridesharing drivers (i.e., from 10,000 through 15,000) and riders (i.e., from 1,000 through 10,000), and evaluate the graphical algorithm.

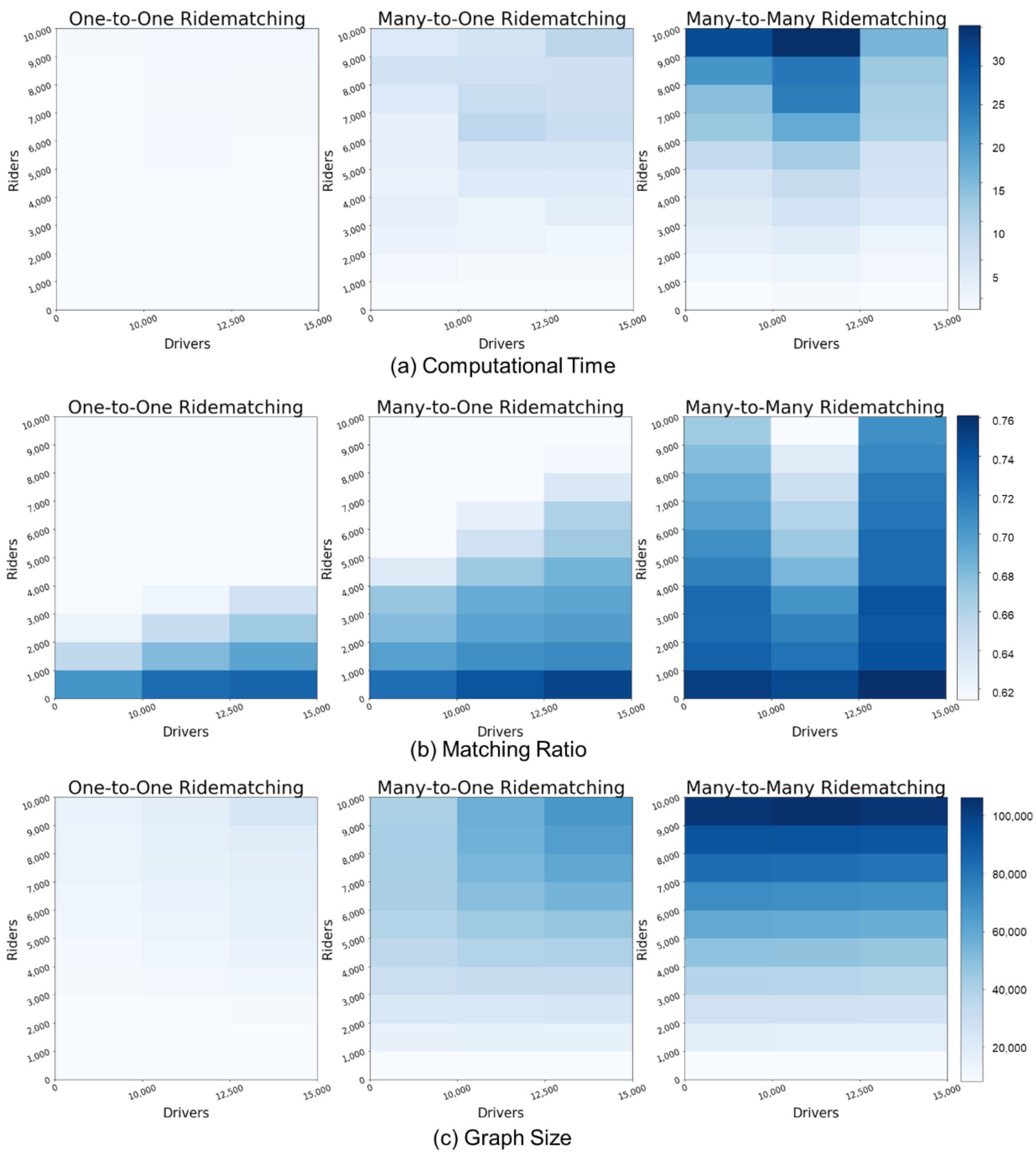


Figure 7.10 Distribution of computational time

Figure 7.10 depicts the performance measurements of the algorithm under the three different matching instances. In all scenarios, the computational time increased as the number of system participants increase, because additional participants generate more edges in the graph (Figure 7.10c). Furthermore, we confirm that the matching ratio increases as the number of drivers increase. This tendency appears more conspicuous as the matching requirements are relaxed. It is worth mentioning that, in the case of the many-to-many ridematching instance and 12,500 drivers, the matching ratio is relatively smaller than in other instances. That can be explained by the gap between the potential riders and the actual matched riders, shown in Figure 7.11. The number of the potential matched riders are similar regardless of drivers as the number of drivers increases from 10,000 to 15,000. However, when in optimal matched riders case with 12,500 drivers, the riders who were actually matched are significantly reduced compared to the potentially matched ones.

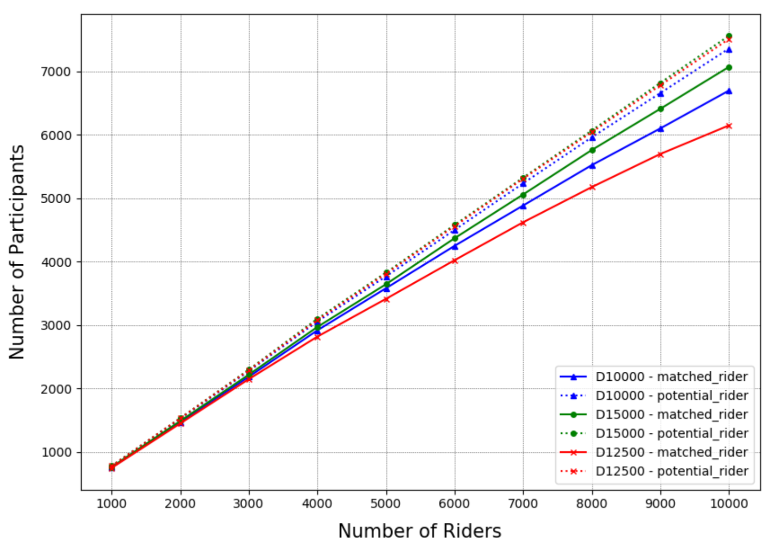


Figure 7.11 Gap between the optimal and potential matched riders

Figure 7.12 demonstrates the cost savings in the three problem instances. The most restricted matching problem shows the least cost savings. In addition, we confirm that in every instance, introducing more participants in the system led to more cost savings benefits.

Figure 7.13 dhows the distribution of transfers for the many-to-one and many-to-many matching instances. We observe that by relaxing the constraint of served riders per driver from 1 to 3, the number of transfers is significantly reduced. The results indicate that vehicle occupancy, which is a key vehicle efficiency metric, is improved. Fewer transfers also represent an important in the quality of the overall rider experience.

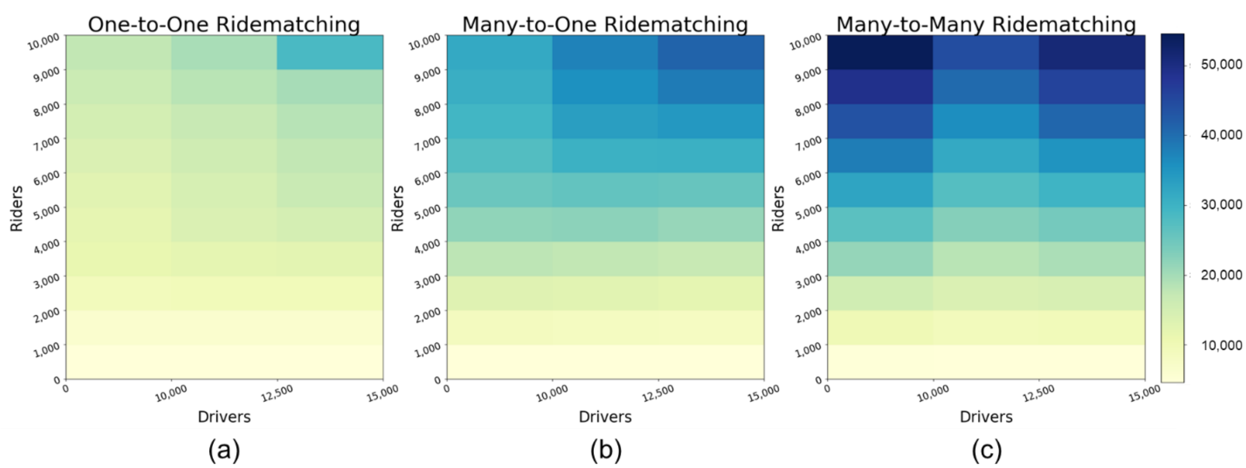


Figure 7.12 Distribution of cost savings

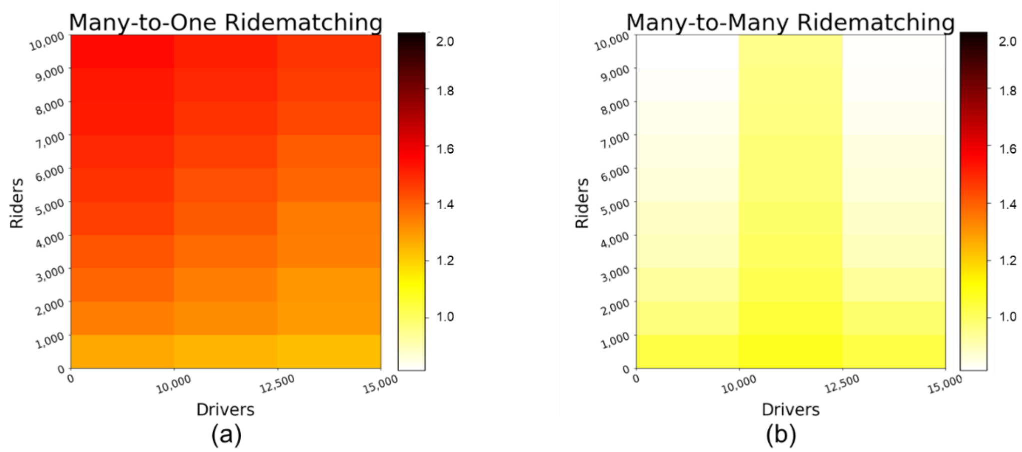


Figure 7.13 Distribution of transfers

## 7.5 Discussion

In this chapter, we developed a graphical method to find the optimal cost savings applicable to diverse ridematching problems. Contrary to the traditional bipartite graph approach which connects matched riders and drivers with direct links, we introduced modeled the problem using a transshipment network structure with intermediate nodes. The role of the intermediate nodes is to guarantee a set of drivers who can serve all itineraries and to prevent the possibility that realistically unconnected drivers will arise and be chosen by riders. We used a linear programming method to find the optimal cost savings, to use as a benchmark.

We applied the proposed method to a relatively large network and analyzed the impacts of changes in demands and supplies in the ridematching system. The proposed graphical approach performs better than the real-time matching algorithm in terms of the cost savings. Furthermore, we generated different ridematching problem instances by varying the number of transfers and vehicle capacity.

We evaluate the system performance under these diverse scenarios. Numerical experiments show that the graphical approach results in the optimal cost saving solutions, compared to the real-time ridematching solution methodology. We also evaluated the system performance when the number of transfers and vehicle occupancy are varied. From system user point of view, the relaxed ridematching constraints, coupled with an appropriate rider-driver ratio, leads to fewer transfers. From an overall system perspective, we confirmed that the proposed algorithm leads the improvements of the successful matched riders.

The proposed graphical algorithm, technically, performed over one optimization time period. However, it can also be applied dynamically by decomposing the time period into smaller time periods, then using a rolling time-horizon approach. A key insight from the results shown in Figure 7.11 is that the gap between the optimal and the potential matched riders suggests that there are 'super' drivers who can serve multiple riders. At the same time, there are riders who have similar trip itineraries, who are likely to experience matching failures since there are not enough available drivers. From the system management point of view, shareable resources are being wasted in these circumstances. If some riders were to decide to be drivers, more people can be matched through improved system efficiency. This underscores the importance of combining the optimal ridematching algorithm with the mobility portfolio framework, which can lead to behavioral changes in system participants, resulting in a more efficient system.

# Chapter 8

# Conclusion

## 8.1 Summary and Contributions

Shared transportation systems continue to gain wide acceptance in societies all over the world. Mobility being increasingly viewed as a shareable good as well as property has led to the rise of diverse services related to shared mobility. These systems allow people to travel efficiently without having to own a vehicle. In addition, autonomous vehicles can greatly expand the travel choices of people and incentivize the development of more innovative transportation systems, by leveraging real-time information about people's movements and behavioral choices. Through an elaborate study of a comprehensive model of ridesharing, mobility portfolios and the associated optimization, the major research objective accomplished in this dissertation are the development of a smart transportation platform that can help optimize the individual travelers' complex movements in a shared and multimodal environment and can provide a smart mobility portfolio plan under the system. In this process, the thesis proposed new conceptual frameworks to describe the modal options from a continuous combination spectrum, provided formulations and algorithms for the associated individual-level optimizations, and developed an agent-based modeling platform to study the collective performance of the system over a multiple-day (or longer) period of time.

First, we develop a new trip modeling concept decomposing previously strict and discrete traditional travel modes (i.e., personal, public transit, and walk) into a flexible combination of several travel options. We define these as travel option chain (TOC) modes. The benefit of the TOC mode concepts is its flexibility. The TOC modes can be utilized universally for any type of shared-mobility services, depending on the characteristics of each travel options, and explicitly incorporates vehicle ownership (or partial ownership) in their formulation through price/payment structures.

Using the TOC mode as an underlying concept, we designed a platform to model a subscription-based mobility portfolio framework for shared and autonomous transportation systems. The platform was built using agent-based modeling techniques to simulate various agents for individual travelers, the system/network/vehicle supply elements, and the optimization elements, so as to analyze their interactions and the resulting individual and collective performance.

We developed a mobility portfolio framework to provide the optimal mobility option for each system subscriber based on their travel preferences and previous travel experience. The core of the mobility portfolio scheme is a peer-to-peer ridematching module to find the best TOC modes in real time for each individual, using a dynamic programming method, and then learning-based optimization schemes for the travel choices each during different periods or phases of the portfolio period. Once the ridematching process is completed, we system participants' perception of travel time and cost, based on their matching experiences, are updated. Using these data, we execute a decision-making module to recommend a more attractive travel option to the users for their next trip.

The bundling mechanism in the mobility portfolio has a designated shared-mobility usage period and credits for each bundle option. Keeping these features in mind, we mathematically formulate the mobility portfolio problem aimed to find the combination of travel modes that lead to the maximum travel cost savings within the portfolio, for each individual. The objective function in the mobility portfolio problem is a nondifferentiable function. Therefore, we apply a heuristic algorithm, which in this case is a learning-based iterative method. The novel feature of our proposed learning method is that is has a periodic from that incorporates two different time periods simultaneously. The learning happens over travel experiences accumulated on the day of travel, and the same day corresponding to the previous time period. We update the expected travel time for the next day based on the Bayesian Inference model, and then use a modified ant colony optimization approach to consider the data collected at different iteration points. To prevent a situation in which the system participants use up their credit for a certain travel status before their trip is completed, we specify a rick value function. We also demonstrate the flexibility of this framework by incorporating different shared-mobility services such as a shared autonomous fleet vehicle service and a peer-to-peer carsharing service.

To measure the performance of the developed framework, we performed a simulation-based analysis on an Irvine area network with travel demand data from the California Statewide Transportation Demand model (CSTDM).

The results from the simulation, including shared autonomous fleet vehicles (SAFVs) operations, we demonstrate that the adopted two-stage learning mechanism helps system participants in finding a better travel solution for the next day or time period by allowing people to shift their travel statuses. From the results of the numerical experiments, we also find the impacts of not only the mobility portfolio scheme itself, but also the changes in mobility providers in the shared transportation systems. From an individual point of view, the mobility portfolio scheme results in cost savings. From a system perspective, operating the multimodal ridesharing system in conjunction with SAFVs results in VMT reduction. We also demonstrate the efficiency and flexibility of the TOC modes by illustrating shared travel movements and temporal ownership and expand the original problem to analyze peer-to-peer carsharing systems. Results also show the potential of buses acting as feeders to the next leg of users' trips. Overall, we can conclude that implementing the mobility portfolio schemes in shared transportation systems effectively improves performance at the individual and system level.

A mobility portfolio service provider would be interested in a system that maximizes the number of service users and lowers system-wide costs. Thus, we formulate a problem to maximize cost savings, which is solved using a novel graphical method that models the problem as a transshipment network. Numerical experiments have yielded valuable insights on the ridematching performance under various levels of supply and demands. For every ridematching problem instance, the graphical approach results in optimal cost saving solutions and a higher matching success rate, compared to the real-time ridematching approach. Furthermore, we find that the relaxed ridematching constraints, coupled with an appropriate rider-driver ratio, leads to fewer transfers.

We also performed a stand-alone demand-side study to analyze how people respond to a proposed multimodal shared transportation system, at the beginning of the research reported here. To capture the implicit determinants of individual preference on shared travel movements, we first select four attributes: number of transfers, travel time, travel cost and incentives, all of which are widely considered to impact people's travel choices on the shared transportation system. Then, we employ a choice-based conjoint analysis method and use a web-based survey platform to understand users' acceptance of probable shared travel movements in the system. The estimation reinforces the importance and viability of factor estimation modeling, and the significance of the number of transfers factor in how people choose to make their trips.

## 8.2 Future Research Areas

Modeling the shared travel movements with the mobility portfolio scheme is a relatively new area of research that can be extended in various directions.

One shortcoming in mobility portfolio frameworks is the strong assumption made on the subscribers' acceptance behavior, meaning 100% compliance once a travel status is provided to a user. Another assumption is that the mobility portfolio system users do not leave the system even when purchasing the portfolio offers no benefits to them. In the worst case, some people may not be matched at all and would have to drive themselves. This concern can be mitigated by building a demand forecasting model that combines the mobility portfolio scheme and the demand behavior model described in chapter 6. Sensitivity analysis can measure the performance of the mobility portfolio scheme in the model by changing cost saving incentive ratio, number of transfers, and desirable detouring time for riders. In addition, since the mobility portfolio framework arrives at a least cost solution, it is possible to test the impact of the different level of incentives needed for user retention. Since the mobility portfolio already considers vehicle costs in its formulation, future research can extend this formulation to include dynamic vehicle costs that depends on vehicle usage.

It would be beneficial to analyze how vehicle ownership impacts mobility portfolio subscriptions. In the context of COVID-19, data show a significant change in travel behavior, with many people are more likely to work from home, thereby resulting in lower vehicle usage. These circumstances may encourage people to not undertake the financial commitment of purchasing a vehicle especially when it is not being used for commuting. This behavioral shift incentivizes people to opt for flexible mobility portfolios, instead. On the contrary, due to COVID-19, people may feel safer using their own car. Therefore, more studies are required to accurately gauge user perception of ridesharing and vehicle ownership.

Furthermore, the mobility portfolio model can be extended by considering a chain of daily trip activities. The current model only considers a one-way trip, usually a work trip. In reality, travel mode and travel status are chosen depending on their activities. In addition, the mobility portfolio plan can be formulated as a family plan by allowing the exchanges in credits between family members.

From an operational perspective, we can develop different dispatching strategies for SAFVs to minimize waiting times or to maximize profits for SAFVs providers.

Shared mobility has already changed the transportation landscape in cites all over the world. Connected, electric, autonomous, and shared vehicles are expected to revolutionize multimodal shared transportation system even further. In the light of these transformations, the future directions of research that we outlined are essential in promoting better planning, engineering, and operations in urban and suburban and communities across the United States.

# Bibliography

## 1 Bibliography


Adomavicius, G. and A. Tuzhilin (2005). Toward the next generation of recommender systems: A survey of the state-of-the-art and possible extensions, *in IEEE Transactions on Knowledge and Data Engineering 17*(6), 734 – 749.

Agatz, N., A. Erera, M. Savelsbergh, and X. Wang (2009). Sustainable passenger transportation: Dynamic ride-sharing. *ERIM Report Series Reference No. ERS-2010-010-LIS.*

Agatz, N., A. L. Erera, M. W. Savelsbergh, and X. Wang (2011). Dynamic ride-sharing: A simulation study in metro Atlanta. *Transportation Research Part B: Methodological 45*(9), 1450 – 1464.

Agatz, N., A. Erera, M. Savelsbergh, and X. Wang (2012). Optimization for dynamic ride-Sharing: a Review. *European Journal of Operational Research 223*(2), 295 – 303.

Aissat, K. and S. Varone (2015). Real-time ride-sharing substitution service in multi-modal public transport using buckets, *Modelling, Computation and Optimization in Information Systems and Management Sciences 360*, 425–436.

An, S., D. Nam, and R. Jayakrishnan (2019). Impacts of integrating shared autonomous vehicles into a peer-to-peer ridesharing system. *Procedia Computer Science 151*, 511 – 518.

Aydin, O. F., I. Gokasar, and O. Kalan (2020). Matching algorithm for improving ridesharing by incorporating route splits and social factors. *PLoS ONE 15*(3) 1 – 23.

Ballús-Armet, I., S. A. Shaheen, K. Clonts, and D. Weinzimmer (2014). Peer-to-reer carsharing, exploring public perception and market characteristics the San Francisco Bay Area, California, *Transportation Research Record: Journal of the Transportation Research Board (2416)*, 27 – 36.

Berjani, B. and T. Strufe (2011). A recommendation system for spots in location-based online social networks, *In Proceedings of the 4th Workshop Social Network Systems 4*, 1 – 6.

Bilali, A., F. Dandl, U. Fastenrath, and K. Bogenberger (2019). Impact of service quality factors on ridesharing in urban areas. *In Proceedings of the 6th International Conference on Models and Technologies for Intelligent Transportation Systems (MT-ITS), Krakow, Poland, 2019*.

Brownstone, D., and T. F. Golob (1992). The effectiveness of ridesharing incentives: discrete-choice models of commuting in Southern California. *Regional Science and Urban Economics 22*(1), 5 – 24.

Bruglieri, M., F. Pezzella, and O. Pisacane (2016). Heuristic algorithms for the operator-based relocation problem in one-way electric carsharing systems, *Discrete Optimization 23*(4), 56 – 80.

Bruglieri, M., F. Pezzella, and O. Pisacane (2018a). A two-phase optimization method for a multi-objective vehicle relocation problem in electric carsharing systems, *Journal of Combinatorial Optimization 36*, 162 – 193.

Bruglieri, M., F. Pezzella, and O. Pisacane (2018b). An adaptive large neighborhood search for relocating vehicles in electric carsharing services, *Discrete Applied Mathematics 253*(30), 185 – 200.

Bsaybes, S., A. Quilliot, A. K. Wagler, and J. T. Wegener (2015). Two flow-based approaches for the static relocation problem in carsharing systems. ArXiv, abs/1511.02650.

Czioska, P., D. C. Mattfeld, and M. Sester (2017). GIS-based identification and assessment of suitable meeting point locations for ridesharing. *Transportation Research Procedia 22*, 314 – 324.

Chow, J. Y. J. and H. Liu (2012). Generalized profitable tour problems for online activity routing system, Transportation Research Record: *Journal of the Transportation Research Board (2284)*, 1 – 9.

Fagnant, D. J., K. M. Kockelman, and P. Bansal (2015). Operations of shared autonomous vehicle fleet for Austin, Texas, Market. *Transportation Research Record: Journal of the Transportation Research Board (2536)*, 98 – 106.

Fahnenschreiber, F., M. Gündling, H. Keyhani, and M. Schnee (2013). A multi-modal routing approach combining dynamic ridesharing and Public Transport, *Transportation Research Procedia 13*, 176 – 183.

Faroqi, H. and A. Sadeghi-Niaraki (2016). GIS-based ride-sharing and DRT in Tehran city, *Public Transportation 8*(2), 243 – 260.

Furuhata, M., M. Dessouky, F. Ordóñez, M. Brunet, X. Wang, and S. Koenig (2013). Ridesharing: the state-of-the-art and future directions, *Transportation Research Part B 57*, 28 – 46.

Ginavičienė, J. and I. Sprogytė (2020). Factors of service quality affecting services in Vilnius, Lithuania, Society. *SOCIETY. INTEGRATION, EDUCATION. Proceedings of the International Scientific Conference 6*, 615-624.

Glotz-Richter, M. (2012). Car-sharing – “Car-on-call” for reclaiming street space, *Procedia – Social and Behavioral Sciences 48*, 1451-1463.

Gruebele, P. (2008). Interactive system for real time dynamic multi-hop carpooling. *Global Transport Knowledge Partnership*, 2008.

Gucwa, M. (2014). The mobility and energy impacts of automated cars, *Ph.D. Dissertation at Stanford University*.

Gurumurthy, K. M. and K. M. Kockelman (2018). Analyzing the dynamic ridesharing potential for shared autonomous vehicle fleets using cell phone data from Orlando, Florida, *Computers, Environment and Urban Systems 71*, 177 – 185.

Gutowski, N., T. Amghar, O. Camp, and S. Hammoudi (2017). A framework for context-aware service recommendation for mobile users: A focus on mobility in smart cities, *From Data To Decision*. 2017.

Haaijer, M. E. (1999). Modeling conjoint choice experiments with the Probit model. *Ph.D. Dissertation at University of Groningen*.

Herbawi, W. and M. Weber (2012). A genetic and insertion heuristic algorithm for solving the dynamic ridematching problem with time windows. In *Proceedings of the 14th international conference on Genetic and evolutionary computation conference*, 385 – 392.

Herbawi, W. and M. Weber (2011a). Ant colony vs. genetic multi-objective route planning in dynamic multi-hop ridesharing. *In Tools with Artificial Intelligence (ICTAI), 2011 IEEE Conference*.

Herbawi, W. and M. Weber (2012b). Comparison of multi-objective evolutionary algorithm for solving the multiobjective route planning in dynamic multi-hop ridesharing. *In Proceedings of the 11th European conference on evolutionary computation in combinatorial optimization, Torino, Italy*, 84 – 95.

Herbawi, W., M. Knoll, M. Kaiser and W. Gruel (2016). An evolutionary algorithm for the vehicle relocation problem in free floating carsharing, *2016 IEEE Congress on Evolutionary Computation (CEC), Vancouver, Canada*, 2873 – 2879.

Ho, C.Q., D.A. Hensher, C. Mulley, and Y.Z. Wong (2018). Potential uptake and willingness-to-pay for Mobility as a Service (MaaS): A stated choice study. *Transportation Research Part A: Policy and Practice 117*, 302 – 318.

Ho, C.Q., C. Mulley, and D. A. Hensher (2020). Public preferences for mobility as a service: Insights from stated preference surveys. *Transportation Research Part A: Policy and Practice 131*, 70 – 90.

Ho, C.Q., D.A. Hensher, D. J. Reck, S. Lorimer, and I. Lu (2021a), MaaS bundle design and implementation: Lessons from the Sydney MaaS Trial, *Transportation Research Part A: Policy and Practice 149*, 339 – 376.

Ho, C.Q., D.A. Hensher, and D. J. Reck (2021b). Drivers of participant's choices of monthly mobility bundles: Key behavioral findings from the Sydney Mobility as a Service (MaaS) trial. *Transportation Research Part C: Emerging Technologies 124*, 102932.

Huang, K., G. H. A. Correia, and K. An (2018). Solving the station-based one-way carsharing network planning problem with relocations and non-linear demand, *Transportation Research Part C: Emerging Technologies 90*, 1 – 17.

Hyland, F. M. and H. S. Mahmassani (2018). Dynamic autonomous vehicle fleet operations: Optimization-based strategies to assign AVs to immediate traveler demand requests, *Transportation Research Part C: Emerging Technologies 92*, 278 – 297.

Jorge, D., G. H. A. Correia and C. Barnhart (2014). Comparing optimal relocation operations with simulated relocation policies in one-way carsharing systems. *IEEE Transactions on Intelligent Transportation Systems 15(4)*, 1667 – 1675.

Jayakrishnan, R., D. Nam, S. An (2019). Report: Efficient mobility portfolio schemes for integrated, intermodal, and incentivized shared transportation, *University of California, Irvine*, https: //sunghia.weebly.com/uploads/1/3/6/7/136775476/3is_project_final_report.pdf

Jha, M., S. Madanat, and S. Peeta (1998). Perception updating and day-to-day travel choice dynamics in traffic networks with information provision. *Transportation Research Part C: Emerging Technologies 6*(3), 189 – 212.

Kim, D., J. Ko, and Y. Park (2015). Factors affecting electric vehicle sharing program participants' attitudes about car ownership and program participation. *Transportation Research Part D: Transport and Environment 36*, 96 – 106.

Karniouchina, E. V, W. L. Moore, B. van der Rhee, and R. Verma (2009). Issues in the use of ratings-based versus choice-based conjoint analysis in operations management research. *European Journal of Operational Research 197*(1), 340 – 348.

Ko, J., D. Kim, D. Nam, and T. Lee (2017). Determining locations of charging stations for electric taxis using taxi operation data. *Transportation Planning and Technology 0*(4) 1 – 14.

Kofteci, S., M. Ergun, and H. S. Ay (2010). Modeling freight transportation preferences: conjoint analysis for Turkish Region. *Scientific Research and Essays 5*(15), 2016 – 2021.

Korea Railroad Research Institute (2016). Annual Report: Core technology development of subsonic capsule train. https://scienceon.kisti.re.kr/srch/selectPORSrchReport.do?cn= TRKO201900018038

Levandoski, J. J., M. Sarwat, A. Eldawy, and M. F. Mokbel, LARS: A location-aware recommender system, *2012 IEEE 28th International Conference on Data Engineering*, 450 – 461. IEEE, 2012

Li, L., W. Chu, J. Langford, and R. E. Schapire (2019). A contextual-bandit approach to personalized news article recommendation. *In Proceeding the 19th International Conference World Wide Web (WWW 2010), Raleigh, North Carolina*, 661 – 670.

Li, J. -P., G. -J. Horng, S. -T. Cheng and C. -F. Chen (2015). Intelligent ridesharing system for taxi to reduce cab fee, 2015 *IEEE 12th International Conference on Networking, Sensing and Control*, 468 – 473.

Li X., S. Hu, W. Fan, and K. Deng (2018). Modeling an enhanced ridesharing system with meet points and time windows. *PLoS ONE 13*(5).

Lin, J., S. Sasidharan, S. Ma, and O. Wolfson (2016). A model of multimodal ridesharing and its analysis, *In Proceedings of the 2016 17th IEEE International Conference on Mobile Data Management*, 164-173.

Liu, J., W. Deng, and B. Zhang (2011). Conjoint analysis based transit service quality research. *Journal of Transportation Systems Engineering and Information Technology 11*(4), 97 – 102.

Lloret-Batlle, R., N. Masoud, and D. Nam (2017). Peer-to-Peer ridesharing with ride-back on High-Occupancy-Vehicle lanes. *Transportation Research Record: Journal of the Transportation Research Board (2668)*, 21 – 28.

Nam, D., D. Yang, S. An, J. G. Yu, R. Jayakrishnan, and N. Masoud (2018). Designing a transit-feeder system using multiple sustainable modes: Peer-to-peer (p2p) ridesharing, bike sharing, and walking, *Transportation Research Record: Journal of the Transportation Research Board 2672*(8), 754 – 763.

Nourinejad, M., S. Zhu, S. Bahrami, and M. J. Roorda (2015). Vehicle relocation and staff rebalancing in one-way carsharing systems, *Transportation Research Part E: Logistics and Transportation Review 81*, 98 – 113.

Ma, S., Y. Zheong, and O. Wolfson (2015). Real-time city-scale taxi ridesharing, *IEEE transactions on knowledge and data engineering 27*(7), 1782 – 1795.

Ma, T. -Y., J. Y. J. Chow, and S. Rasulkhani (2018). An integrated dynamic ridesharing dispatch and idle vehicle repositioning strategy on a bimodal transport network, *In Proceedings of 7th Transportation Research Arena (TRA) 2018*.

Ma, T. -Y. (2017). On-demand dynamic Bi-/Multi-modal ride-sharing using optimal passenger-vehicle assignments, *In 2017 IEEE International Conference on Environment and Electrical Engineering and 2017 IEEE Industrial and Commercial Power Systems Europe (EEEIC/ICPS Europe)*, 1 – 5. IEEE Industrial Electronics Society.

Masoud, N., D. Nam, J. Yu, and R. Jayakrishnan. Promoting peer-to-peer ridesharing services as transit system feeders. *Transportation Research Record: Journal of the Transportation Research Board 2650*(1), 74 – 83.

Masoud, N., and R. Jayakrishnan (2017a). A real-time algorithm to solve the peer-to-peer ride-matching problem in a flexible ridesharing system. *Transportation Research Part B: Methodological 106*, 218 – 236.

Masoud, N., and R. Jayakrishnan (2017b). A decomposition algorithm to solve the multi-hop peer-to-peer ride-matching problem. *Transportation Research Part B: Methodological 99*, 1 – 29.

Moeckel, R., R. Fussell, and R. Donnelly (2013). Mode choice modeling for long-distance travel. *Transportation Letters 7*(1), 35 – 46.

Matyas, M., and M. Kamargianni, (2019). The potential of mobility as a service bundles as a mobility management tool. *Transportation 46*, 1951 – 1968.

Priatama, Y., N. Yusuf, and H. Burhan (2018). Mode choice between ridesourcing service and private vehicle (study case: DKI Jakarta), *AIP Conference Proceedings 2020* (1).

Rao, V. R. (2013). Applied conjoint analysis. *Springer Heidelberg New York Dordrecht London*, 2013.

Rudnicki, R., K. -H. Anders, and M. Sester (2008). Rendezvous-problem in local shared-ride trip planning. *International archives of Photogrammetry, Remote Sensing and Spatial Information Sciences 38*.

Segal, M., and K. M. Kockelman (2016). Design and implementation of a shared autonomous vehicle 1 system for Austin, Texas. *In Proceedings of the Transportation Research Board 95th Annual Meeting (No. 16-1837)*, January 2016, Washington, D.C.

Seok, H. E., S. J. Kim, J. H. Choi, and H. Kim. Consumer's welfare of O2O-based designated driver service. *Korea Association for Telecommunications Polices 23*(4), 1 – 28.

Stiglic M., N. Agatz, M. Savelsbergh, and M. Gradisar (2015). The benefits of meeting points in ride-sharing system. *Transportation Research Part B: Methodological 85*, 36 – 53.

Stiglic, M., N. Agatz, M. Savelsbergh, and M. Gradisar (2016). Making dynamic ridesharing work: the impact of driver and rider flexibility. *Transportation Research Part E: Logistics and Transportation Review 91*, 190 – 207.

Stiglic, M., N. Agatz, M. Savelsberghc, and M. Gradisara (2018). Enhancing urban mobility: Integrating ride-sharing and public transit, *Computers and Operations Research 90*, 12 – 21.

Shaheen, S. and A. Bansal (2015). Perceptions of peer-to-peer carsharing in the San Francisco Bay Area, CA, USA, *Institute of Transportation Engineers (ITE) Journal 85*(5), 39 – 42.

Shaheen, S., and N. Chan (2015). Mobility and the shared economy: impacts synopsis: http://innovativemobility.org/wp-content/uploads/2015/07/Innovative-Mobility-Industry-Outlook_SM-Spring-2015.pdf. Accessed: 2022-02-06.

Shaheen, S., A. Cohen, and M. Jaffee (2018a). Innovative mobility: carsharing outlook: https://escholarship.org/uc/item/1mw8n13h. Accessed: 2022-02-06.

Shaheen, S., M. Elliot, and A. Bansal (2018b). Report: Peer-to-peer (P2P) carsharing: understanding early markets, social dynamics, and behavioral impacts, *University of California, Berkeley*, https://escholarship.org/uc/item/7s8207tb/. Accessed: 2022-02-06.

Schoettle, B., and M. Sivak (2017). Technical Report: Potential impact of self-driving vehicles on household vehicle demand and usage, *University of Michigan Sustainable Worldwide Transportation (UMTRI-2015-3)*, http://www.driverlesstransportation.com/wp-content/uploads /2015/02/UMTRI-2015-3.pdf. Accessed: 2017-07-28.

Song, X. (2018). Personalization of future urban mobility, *Ph.D. Dissertation at Massachusetts Institute of Technology*.

Tebaldi, C., and M. West (1998). Bayesian inference on network traffic using link count data, *Journal of the American Statistical Association 93*(442), 557 – 573.

Varone, S., and K. Aissat (2015). Multi-modal transportation with public transport and ridesharing (Multi-modal transportation using a Path-based Method), *In Proceedings of the 17th international conference on enterprise information systems (ICEIS-2015)*, 479 – 486.

Wagner, S., C. Willing, T. Brandt, and D. Neumann (2015). Data analytics for location-based services: enabling user-based relocation of carsharing vehicles, *In Proceedings of the 36th international conference on information system (ICIS 2015)*.

Wang, H., M. Terrovitis and N. Mamoulis (2013). Location recommendation in location-based social networks using user check-in data, *In Proceeding of the 21st ACM SIGSPATIAL international conference advances in geographic information systems*, 2013, 374 – 383.

Wang, X. (2013). Optimizing ride matches for dynamic ridesharing systems, *Ph.D. Dissertation at Georgia Institute of Technology*.

Xing, X., T. Warden, T. Nicolai, O. Herzog (2009). SMIZE: A spontaneous ridesharing system for individual urban transit. *In German Conference on Multiagent System Technologies*, 165 – 176.

Xu, Z., C. Men, P. Li, B. Jin, G. Li, Y. Yang, C. Liu, B. Wang, and X. Qie (2020). When recommender systems meet fleet management: practical study in online driver repositioning system, *WWW '20: Proceedings of The Web Conference*, 2220 –2229.

Yang, J., X. Shi, M. Marchese, and Y. Liang (2008). An ant colony optimization method for generalized TSP problem, *Progress in Natural Science 18*(11), 1417 – 1422.

Ye, M., P. Yin, and W. C. Lee (2010). Location recommendation for location based social networks, *In Proceeding of the 18th SIGSPATIAL international conference advances in geographic information systems*, 458 – 461.

Yoon, G., J. Y. J. Chow, A. Dmitriyeva, and D. Fay (2020). Effect of routing constraints on learning efficiency of destination recommender systems in Mobility-on-Demand services, *IEEE Transactions on Intelligent Transportation Systems*, 2020.

Zhang, G., H. Zhang, L. Li, and C. Dai (2014). Agent-based Simulation and Optimization of Urban Transit System, *Transportation on Intelligent Transportation systems 15*(2), 589 – 596.

Zhang, W., S. Guhathakurta, J. Fang and G. Zhang (2015). The performance and benefits of a shared autonomous vehicles based dynamic ridesharing system: an agent-based simulation approach. *In Proceedings of the Transportation Research Board 94th Annual Meeting, January 2015, Washington, D.C.*

Zhao, Y., and K. M. Kockelman (2018). Anticipating the regional impacts of connected and automated vehicle travel in Austin, Texas, *Journal of Urban Planning and Development 144*(4).

Zhou, J., X. Lai, and J. Y. J. Chow (2019). Multi-armed bandit on-time arrival algorithms for sequential reliable route selection under uncertainty, *Transportation Research Record: Journal of the Transportation Research Board 2673*(10), 673 – 682.

Zhou, X., and J. Taylor (2014). DTALite: A queue-based mesoscopic traffic simulator for fast model evaluation and calibration, *Cogent Engineering 1*(1), 961345.